

Thank you for your helpful comments. In the text below, reviewer comments are indicated with colored background, our replies are in plain text and changes to the manuscript are put in italic.

Response to general comments

General comment 1

>> Future climate: The surface mass balance model was forced with climatic observations in the past, and with CMIP5 climate scenarios for the future (l. 410-419). However, some important information seems to be missing:

(i) Which climate models did you use (model name, institute, resolution, ...)? (ii) Did you applied a de-biasing procedure to accommodate the future climate projections with the past climatic dataset (e.g. Huss & Hock, 2015)? Such a procedure is often needed to avoid sudden changes in temperature/precipitation between the past climate dataset and the future climate projections. (iii) Why did you use a linear trend (l. 413-415) for the future temperature and precipitation and not the trend (and variability) proposed by the CMIP5 data? This virtually discards any CMIP5 information between now and the end of the century...

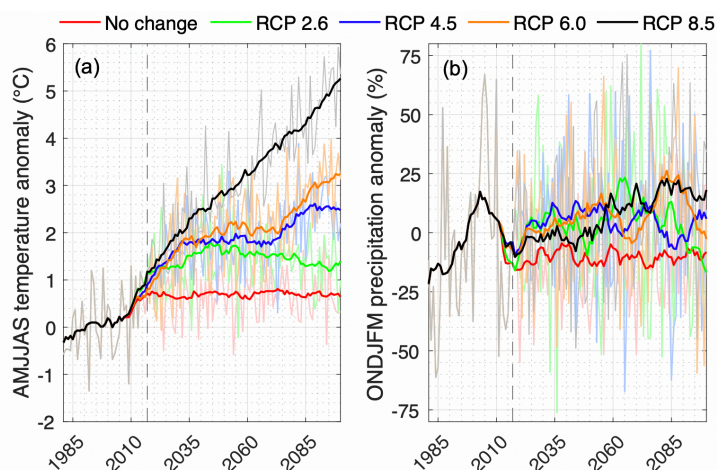
We acknowledge that our original approach to derive future climate projections used a simplified linear approximation for the 21th century based on average CMIP5 model output. We have now recreated the future climate forcing directly from available CMIP5 models for the grid cell closest to Djankuat Glacier. In this way we encompass the variability captured by the CMIP5 models. We also applied a de-biasing procedure to match the future climate forcing with the past, both concerning the trend and the variability. The following text is now used to describe the future climate forcing and replaces lines 411-419:

“Future projections of temperature and precipitation were obtained by a multi-model approach, using output from the Coupled Model Intercomparison Project Phase 5 (CMIP5) simulations (Taylor et al., 2012) for the grid cell closest to the Djankuat Glacier. Mean temperature and total precipitation amount at monthly resolution from 21 Global Circulation Models (GCMs) for the RCP 2.6, RCP 4.5, RCP 6.0 and RCP 8.5 scenarios were used, based upon their availability (Table 2 and 3). The data were downloaded for both historical runs (from 1981 AD) and for projections (until 2100 AD). Although the choice of ensemble member can largely influence the eventual results (e.g. Huss and Hock, 2015), we solely focus on the first realization, i.e. ensemble member r1i1p1. Absolute data were at first scaled to anomalies with respect to the 1981–2010 reference values for each respective model, so that additive (temperature) and multiplicative (precipitation) biases could be removed when matching to the past forcing. For each RCP, the monthly temperature and precipitation data were then averaged over all models, resulting in a multi-model mean time series. To account for year-to-year variability, the CMIP5 data were at last rescaled with respect to the standard deviation of the overlapping period for the observed Terskol data (e.g. Huss and Hock, 2015; Zekollari et al., 2019). As with the past simulations, the observed 3-hourly Terskol data sequence was finally used to downscale the monthly data to the temporal resolution that suits the mass balance model.

All scenarios exhibit a further increase of the temperature, which is most pronounced in the summer season. Projected precipitation, on the other hand, shows slightly decreasing values at annual resolution, but shows a tendency for a drier summer half year (April to September, AMJJAS) and a wetter winter half year (October to March, ONDJFM). By 2071–2100 AD, the mean AMJJAS temperature (total ONDJFM precipitation) anomalies with respect to the 1981–2010 period are +1.4°C (+0.1 %), +2.3°C (+3.7 %), +2.7°C, (+11.2 %) and +4.5°C (+11.7 %) for the RCP 2.6, RCP 4.5, RCP 6.0 and RCP 8.5 scenarios respectively (Fig. 10a and b). Additionally, also a future projection is made under a no change scenario, in which the last observed 10-year climatic interval (2009–2018 AD) is repeated with respect to its mean

(corresponding to a AMJJAS mean temperature and a total ONDJFM precipitation amount of 9.2°C and 373.3 mm yr⁻¹ w.e. respectively).”

A figure in which these results are summarized is added as Figure 10 in the updated manuscript, and replaces Table 2 of the original manuscript:



New Figure 10 in the updated manuscript. Projected future (a) AMJJAS temperature and (b) ONDJFM precipitation changes for Terskol, as compared to the 1981–2010 reference, for different RCP scenarios until 2100 AD. Thin colored lines represent annual values, thicker lines represent 15-yr moving means. The dashed vertical line represents the present (i.e. 2017, the most recent year of glaciological observations).

A new Table 3 was added to the updated manuscript, indicating which climate models were selected to reconstruct the future forcing:

New Table 3 in the updated paper. CMIP5 climate models used to reconstruct the future forcing (2019–2100 AD).

Model	Spatial resolution	RCP 2.6	RCP 4.5	RCP 6.0	RCP 8.5
BCC-CSM1-1-M	2.81°×2.81°	X	X	X	
INMCM4	1.50°×2.00°		X		X
ACCESS1-3	1.25°×1.88°	X	X		X
CNRM-CM5	1.41°×1.41°	X	X		X
IPSL-CM5A-LR	1.90°×3.75°		X	X	X
IPSL-CM5B-LR	1.90°×3.75°	X	X		X
MPI-ESM-MR	1.88°×1.88°	X	X		X
GFDL-ESM2G	2.00°×2.00°	X	X	X	X
GISS-E2-R	2.00°×2.50°		X	X	X
HadGEM2-CC	1.25°×1.88°		X		X
ACCESS1-0	1.25°×1.88°		X		X
BCC-CSM1-1	2.81°×2.81°	X	X	X	X
BNU-ESM	2.81°×2.81°	X	X		X
IPSL-CM5A-MR	1.25°×2.50°	X	X	X	X
MPI-ESM-LR	1.88°×1.88°	X	X		X
NorESM1-M	1.88°×1.88°	X	X	X	X
CMCC-CMS	3.75°×3.75°		X		X
GFDL-CM3	2.00°×2.50°	X	X		X
GFDL-ESM2M	2.00°×2.50°	X	X	X	X
GISS-E2-R-CC	2.00°×2.50°		X		X
HadGEM2-ES	1.25°×1.88°	X	X	X	

A small section was added related to the application of the most extreme scenario (Line 449):

“The averaging of the future climatic data implies a reduction of spread. When, for example, the model was forced with the highest warming scenario of all CMIP5 models (i.e. the RCP 8.5 scenario of the GFDL-CM3 model, with mean AMJJAS temperature increase of +7.9°C by 2071–2100 AD), the glacier will cease to exist by 2086 AD.”

The resulting projections of future glacier geometry are included in the comment to “Fig. 12” below.

General comment 2

>> Mass balance perturbation: In the manuscript, a mass balance perturbation is used as a tuning factor, so that model results agree with observations (l. 330, 390, 493, fig. 9 and fig. 11). However, how this perturbation factor is calculated and applied is not well explained. Here additional information are absolutely needed so that the reader can understand what this factor is and how it is meant.

The mass balance perturbation ΔB_a , used in the dynamic calibration procedure, was not explicitly calculated but was instead derived by a trial and error procedure. In this regard, the values for ΔB_a were iteratively adjusted to calibrate historic length variations of the glacier. These artificial mass balance perturbations were therefore superimposed on the mass balance profile that was simulated with the climatic input, until modelled and observed historic length coincided. The process is now clarified in the updated paper by explicitly stating how the procedure was applied (Lines 389-392 of the original paper):

“...applied by incorporating artificial mass balance perturbations (ΔB_a) into the model. This factor was not explicitly calculated but was instead derived and adjusted iteratively by a trial and error procedure. The obtained perturbations were then superimposed on the mass balance profile that was simulated with the climatic input, until the reconstructed glacier length sufficiently matched with the observed values (e.g. Oerlemans, 1997; Zekollari et al., 2014):

$$B_a = B_{a(SMB)} + \Delta B_a,$$

Here, $B_{a(SMB)}$ is the mass balance simulated with the climatic datasets and ΔB_a is the artificial mass balance perturbation that was applied in the dynamic calibration procedure.”

For more information, we refer to general comment 2 of RC 3.

General comment 3

>> Model sensitivity: l. 330-338 show a sensitivity analysis. However, also here many important informations are missing. (i) Are these experiments done starting by a glacier steady state? If yes, during which time period? (ii) Your results show how much the glacier length changes for each degree ($^{\circ}\text{C}$) of warming, using the unit ‘ $\text{m}/^{\circ}\text{C}$ ’, (line 335). Over what temperature-range can the glacier response be expected to be linear? It seems easy to imagine that the topography of the glacier and its bedrock play a role, since they are not homogeneous and thus influence the glacier response depending on the glacier’s position?

(i) All sensitivity experiments were conducted with respect to a steady state glacier with present-day length (i.e. a length of 3260 meter). We clarified this in the paper, and Lines 330-331 now read:

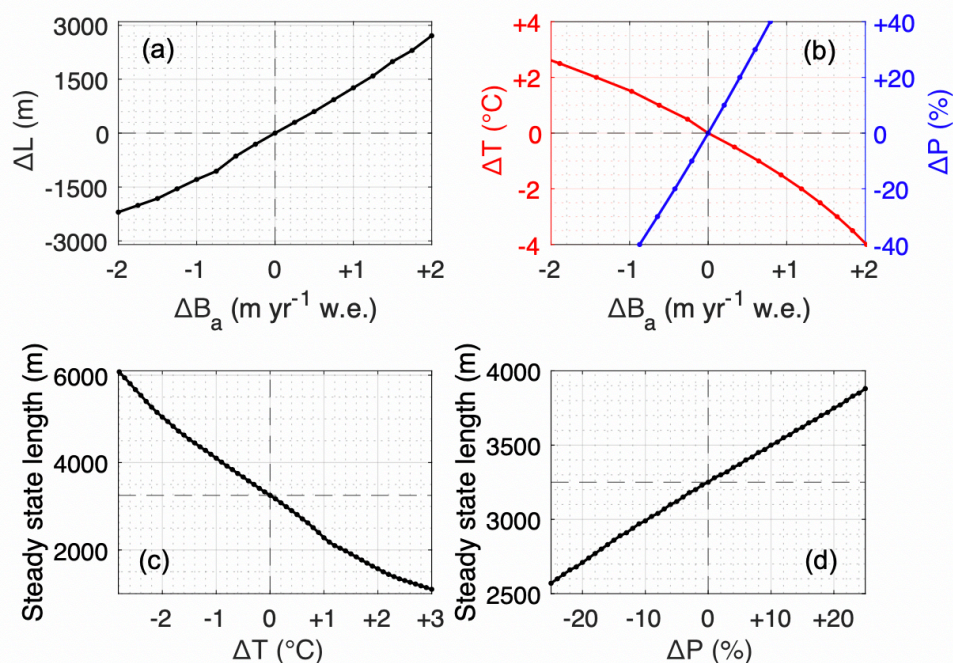
“Some basic sensitivity tests were conducted with the flow model, which all initially started from a steady state glacier with present-day geometry. Perturbed mass balance profiles (ΔB_a , in steps of 0.25 m yr^{-1} w.e.) were then used as forcing to the model, until a new steady state was reached. As such, a relationship with a slight deviation from linear was found between the steady state length and ΔB_a , exhibiting a value for $\partial L / \partial B_a$ of ca. 1100 and 1355 $\text{m} (\text{m yr}^{-1} \text{ w.e.})^{-1}$ for negative and positive perturbations respectively (Fig. 7a).”

(ii) We acknowledge that glacier geometry plays a decisive role in determining the climate sensitivity ($\text{m}/^{\circ}\text{C}$) of the glacier. In this regard, sensitivity to temperature changes shows a linear behavior ($815 \text{ m}/^{\circ}\text{C}$) for temperature perturbations between -1.4 and $+0.7^{\circ}\text{C}$ (with respect to the 1967/68–2006/07 reference climate). Outside this range, the climate sensitivity slightly deviates from that linear trend, see Fig. 7c below. As suggested, the bed topography is key to explain this

behavior, as the glacier front is located on significantly steeper terrain for higher temperatures. Clarification has also been added to the text, as Lines 334-335 now read:

“To assess the climate and glacier sensitivity for equilibrium, mass balance profiles were furthermore altered by temperature and precipitation perturbations within the -3 to +3°C and -25 % to +25 % range respectively (as compared to the 1967/68–2006/07 reference values). Sensitivity of steady state length to temperature changes ($\partial L/\partial T_{air}$) shows a linear behavior ($815 \text{ m}^\circ\text{C}^{-1}$) for perturbations between -1.4 and +0.7°C, but is modelled to vary between 400 and 1400 $\text{m}^\circ\text{C}^{-1}$ when assessed over the entire range (Fig. 7c). The glacier sensitivity depends largely upon geometry and increases (decreases) for more negative (positive) mass balance perturbations, predominantly due to the flatter (steeper) terrain. The sensitivity also peaks around a temperature perturbation of +1°C, i.e. when the glacier front is positioned at the transition between the broad accumulation area and the narrower snout (ca. $x = 2300 \text{ m}$ on the flow line). Also the non-linear nature of the temperature-mass balance relationship (Fig. 7b) triggers a deviation from linear behavior. Consequently, the change in forcing needed for a retreat from 2 to 1 km is nearly twice as large as for a retreat from 4 to 3 km. For precipitation the sensitivity is more or less constant for a value of $250 \text{ m } 10\%^{-1}$ (Fig. 7d).”

We present the new Fig. 7 as a replacement to the old Fig. 7-9 (in Sect. 4 of the original paper):



“New Figure 7 in the updated manuscript. Sensitivity of the Djankuat Glacier showing (a) sensitivity of the glacier steady state length to mass balance perturbations (ΔB_a), (b) sensitivity of the mass balance to temperature (ΔT) and precipitation (ΔP) changes for a fixed present-day glacier geometry, (c) sensitivity of the steady state glacier length to temperature changes, and (d) the same for precipitation changes. All perturbations are with respect to the 1967/68–2006/07 AD reference climate (2.5°C and 980.7 mm yr^{-1} w.e.), and with respect to a steady state glacier with present-day length (3260 meter).”

Line-by-line comments

>> **Line 14:** Better to say already in the abstract which future climate data you used.

Agreed. This was added:

“Future projections using CMIP5 temperature and precipitation data exhibit...”

>> Line 24-25: This sentence needs some references.

We have included some references to these sentences:

“... changing climate (e.g. Shannon et al., 2019; Zekollari et al., 2019; Hock et al., 2019).”

>> Line 40: Change ‘.’ to ‘,’.

Done.

>> Line 44-45: Are you referring to the whole Caucasian region?

Yes, the reference is updated, and it is stated explicitly that this encompasses the whole region:

“...debris coverage has expanded at a rate of ca. +0.22 % yr⁻¹ between 1986 and 2014 when the entire Caucasus region is considered (Tielidze et al. 2020).”

>> Line 65: you cannot use one glacier as representative for a whole area (Huss, 2008). However, at lines 78-79 it becomes clearer what you meant. So, please reformulate.

To avoid confusion, it is clarified in the updated manuscript:

“... the behavior of the Djankuat Glacier as a WGMS reference glacier for the Caucasus ...”

>> Line 89: Give a number for ‘higher elevations’

It was added to the updated text:

“... higher elevations (> 3600 meter) and the...”

>> Line 101: (i) it is not clear which mean annual temperature you are referring to (mean temperature of the 1981-2010 period?) (ii) it is not clear what ‘here’ is referring to.

(i) We refer to average annual temperatures. (ii) The word ‘here’ refers to both the Terskol and Mestia meteo stations. This is now clarified in the updated manuscript:

“The average annual mean temperatures in Terskol and Mestia are 2.8°C and 6.0°C respectively during the 1981–2010 reference period. For the summer half-year from April to September (AMJJAS), the corresponding mean temperatures are 8.7°C and 12.0°C.”

Likewise, for precipitation:

“At Terskol and Mestia, the average total precipitation amounts equal 1001.1 and 1035.1 mm yr⁻¹ w.e. respectively for the 1981–2010 climate. During the accumulation season (October to March, ONDJFM), the corresponding precipitation values are 418.4 and 490.0 mm yr⁻¹ w.e. respectively.”

>> Line 106: (i) you mentioned two places and then you say that you used only one automatic weather station (AWS). Did you used the same AWS in the two places? (ii) ‘was installed’ → can you add from when to when? This information is especially important if you used only one AWS for two places.

(i) We used data from 2 AWSs (one in the Adylsu Valley near the LIA extent of the glacier, AWS 1, and one in the glacier ablation zone, AWS 2). We used data from AWS 1 for precipitation comparisons between Terskol and the Adylsu Valley, and data from AWS 2 to derive transmissivity, temperature lapse rates, albedo, and shortwave, longwave and turbulent fluxes. We now specifically refer to each AWS when data are discussed in the text. For Line 147:

“Hence, a direct comparison of measured air temperatures between AWS 2 on Djankuat and the Terskol weather station was found...”

For Line 150:

“In this study, a value for f_e of 1.5 between Terskol and the Adylsu Valley was found after a comparison of precipitation amounts from AWS 1 in the glacier valley.”

For Line 179:

“Measurements of the incoming solar radiation from the AWS 2 were used to derive atmospheric transmissivity...”

For Line 185:

“The ice albedo α_{ice} can, according to raw data from the AWS 2, vary between 0.15 and 0.40 depending...”

And Line 191:

“Here, these fluxes, as derived from AWS 2, are added up and plotted analyzed against air temperature following the method...”

The location of AWS 1 and 2 were added to Figure 1 of the original manuscript. (ii) These AWSs were only operational during the summer months (June to September) between 2007 and 2017. This was clarified manuscript as follows:

“In 2007, two automatic weather stations (AWS) were additionally installed, one in the Adylsu Valley at ca. 2640 m elevation (AWS 1 in Fig. 1) and one in the ablation zone of the glacier at ca. 2960 m on a sparsely debris-covered ice surface (AWS 2 in Fig. 1). During the summer seasons (June to September) of 2007–2017, a wide range of additional meteorological variables have therefore been acquired by AWS 1 and 2 (air temperature, dew point temperature, incoming and outgoing shortwave/longwave radiation, relative humidity, wind speed and direction, air pressure and for AWS 1 also precipitation amounts) (Rets et al., 2019). The AWSs did not operate outside the JJAS period.”

>> Line 114: Maybe add ‘glacier’ before ‘top’, so that it becomes 100% clear.

Done.

>> Line 117-119: Sorry, I cannot follow this sentence. Can you maybe reformulate it?

The main point here is that we want to make our 1D flow line representative for the 3D glacier to not misestimate the rate of glacier shrinkage. To make this clearer, it was reformulated as:

“To avoid creating a bias in the rate of glacier evolution, the representativeness of the glacier cross-section along the flow line was further determined...”

>> Line 121 (eq1): The way Eq. 1 is cast looks somewhat unusual to me. Can you add a reference where the derivation can be looked up? Or add the derivation in the manuscript?

The continuity equation in this form was discussed and derived by Oerlemans (2001).

>> Line 134: Spell out ‘FTCS’.

Done and added to the text:

“... FTCS (forward in time, centered in space) numerical scheme...”

>> Line 141: Remove 'specific', since it is the glacier wide balance here.

The terminology in the literature is not consistent in this aspect. We choose to leave it like this.

>> Line 145: Is there one value of ACC for the whole glacier, is it evaluated along the central flowline, or is there some sort of spatial grid playing a role?

It was derived for every point along the flow line. This was clarified in the text:

"Accumulation for each point along the flow line is only dependent..."

>> Line 149: (Oct-Mar) add the day, or whether the beginning/end of the month are meant.

Done. The text was updated to:

"Due to lack of AWS data outside of the JJAS period, a temperature lapse rate of $-0.0049^{\circ}\text{C m}^{-1}$ was used for the winter half-year (1 Oct – 31 Mar), in accordance..."

>> Line 154: Add link to table 1 already after 'gamma_p'

Done.

>> Line 144-159: Not super clear to me, especially how exactly all these factors are derived.

Precipitation between the Adylsu Valley and Terskol was scaled using a factor f_e . For the precipitation gradient, we did not have reliable data to extrapolate the precipitation from the Adylsu Valley over the entire glacier. We therefore used the accumulation profile to tune the precipitation gradient. The derivation of the parameters has now been described more extensively in the revised manuscript. Firstly, it is clarified where the factor f_e comes from (See also comment Line 106):

"In this study, a value for f_e of 1.5 between Terskol and the Adylsu Valley was found after a comparison of precipitation amounts with AWS 1 in the glacier valley."

Secondly, it was explicitly stated that the precipitation gradient γ_p is used as a tuning parameter:

"... by making use of a vertical precipitation gradient γ_p , of which the latter is used as a tuning parameter due to a lack of data (see Sect. 3.1)."

Thirdly, with respect to f_{red} , for which a description was already present in the text, some additional info was included into the revised manuscript as follows:

"Here, a topographic characteristic is used to parameterize snow addition or removal from the glacier surface. It was quantified by dividing the linear accumulation profile (without the redistribution factor) with the observed profile and correlating these anomalies to the laterally averaged surface slope s along the flow line (e.g. Huss et al., 2009). As such, a polynomial fit was found. For slopes steeper than the threshold, removal of snow can hence occur, and is assumed to be proportional to the surface slope itself."

>> Line 167: And alpha? Add that alpha is the albedo.

Done.

>> Line 180: About which 'tilt' are you speaking? Is the AWS station tilted?

The tilt of surface slope is not relevant to measure incoming solar radiation. This was adjusted:

"To derive atmospheric transmissivity, measurements of the incoming solar radiation from AWS 2 were used."

>> Line 189: ‘more or less’ - please use a synonym.

This is changed to:

“... are approximately equally important...”

>> Line 189: ‘Table 1’ - It took me quite a lot to find values that you were referring to. Can't it simply be added to the text?

We opted to put less values in the text to not oversaturate the text with numbers. Therefore, we synthesized most values in one single table.

>> Line 192: ‘plotted’ – Is this the correct word? With ‘plotted’ I expect a Figure...

To avoid confusion, the choice of words was adjusted. In the text, this was modified as follows:

“... fluxes, as derived from AWS 2, are added up and analyzed against air temperature...”

>> Line 200-205: Is the implicit assumption that C_{debris} is homogeneous within the entire glacier body? Since that's unlikely to be true, the assumption should at least be discussed.

This assumption had to be made due to lack of abundant information for this parameter. A short section is added to the revised manuscript to discuss the assumption:

“Here, a constant value for C_{debris} in space and time is assumed. The emphasis of this work is to investigate the effect of supraglacial debris on melt patterns and glacier geometry. Encompassing englacial debris pathways or the spatial distribution of englacial debris concentration would add more detail than warranted by the lack of reliable data.”

In this regard, another change was made in Sect. 7 of the original manuscript. Here, we constrained the up-glacier position of the debris input locations x_{debris} to a maximum position of $x_{debris} = x_{ELA}$, where ELA is the equilibrium line altitude. This was addressed as (Line 454):

“... is initiated from $x_{debris} = x_{ELA}$, at $t_{debris} = 2035$ with a magnitude of $F_{debris}^{input} = 1.5 \text{ m yr}^{-1}$. For x_{ELA} , we calculated the average position of the ELA during a window of ± 15 years surrounding t_{debris} in the ‘no additional debris scenario’ (Sect. 6.1), which hence varies for each climatic scenario. We therefore choose to not initiate debris fluxes from positions above the ELA, due to the neglect of englacial pathways in our debris model (see Sect. 2.5).”

“... the debris input location x_{debris} was changed to 80%, 60% and 40% of the distance between x_{ELA} and x_L (further downstream), ...”

>> Line 208: ‘at 1680 m from the highest point’ where is this point? Maybe show in Fig.1.

The reader can locate this point on the map by identifying the margin of the up-glacier debris extent in Figure 1. The following text was added to the manuscript:

“... 1680 m from the highest point (just below the ELA, at 88% of the distance between the terminus x_L and the ELA x_{ELA}), since it is...”

>> Line 209-211: the choice of stopping the debris input flux at a given glacier width sounds rather arbitrary. Also the fact that the debris input location x_{debris} is fixed in time (and not moving) causes some doubts. Both points seem to merit some discussion.

We link connectivity issues between the topographic debris source and the main glacier body to this assumption. Hence, by that time, the glacier has shrunk too much to ensure that debris fluxes reach the glacier surface. This was added accordingly to the text (Line 212):

“Connectivity issues between the topographic source and the main glacier are forwarded as the main reason to justify this modification of the Anderson and Anderson (2016) model. Hence,

by that time, the glacier shrunk too much to ensure that debris fluxes could still reach its surface.”

With regards to the debris input location, we attribute a lack of direct observations regarding past or future (static or moving) topographic debris sources to this assumption. However, an archived (rather unclear) satellite image of the Djankuat glacier in Pasthukov (2011) seems to point out that there has been only minor up-glacier migration of debris on the main glacier body since the 1970s. This led us to believe that our assumption of a static debris source could indirectly be justified. It was added the following discussion (Line 209):

“It was chosen to keep the debris input location at a fixed position due to a lack of direct observations regarding past or future (static or moving) topographic debris sources. However, a comparison of present-day satellite imagery with those from the 1970s (Pasthukov, 2011) seems to point out that the debris patches exhibit only minor up-glacier migration of debris on the main glacier tributary and the debris-covered orographically left part of the snout (when seen from the downstream direction), hence indirectly justifying the assumption.”

>> Line 215 (eq 13): The variable ‘ t_{debris} ’ is not introduced.

It is now indicated explicitly what the term means (Line 208 in the original manuscript):

“Hence, t_{debris} is the time at which the topographic debris source firstly starts to release its mass flux towards the glacier surface.”

>> Line 225: Can you give some more details about the relationship which was found?

This relationship can be seen in Eq. 15 and Fig. 5d of the paper. It incorporates an exponential decay of the fractional area along the flow line. We added this to the text:

“...parameterized based upon the distance from the terminus D_T , for which an exponential relationship was found from observations...”

>> Line 228: How is the debris-area growth factor G_A ‘updated yearly’? One should be pointed at eq. 17 at this stage.

Done. We added a reference to eq. 17: *“(see Eq. 17 in Sect. 3.2).”*

>> Line 234: you took into account the melting reduction effect of debris, but what about the melting enhancement effect of thin debris (e.g. Østrem, 1959)? Add discussion about this.

With respect to the inclusion of the melt-enhancing effect for thin debris, studies performed on Djankuat Glacier point to a low value of the critical thickness (0.03 m by Lambrecht et al., 2011 and 0.07 m by Bozhinskiy et al., 1986). The areal fraction of debris cover on the Djankuat Glacier that holds such thin thickness values is very small, so we believe that the ablation enhancement effect of debris plays a very minor role on Djankuat Glacier. Therefore, the inclusion of this factor was not included in the parameterization. The following section was added to the updated manuscript for justification (Line 224):

“The melt enhancement that may occur for a very thin debris cover was not implemented. Values in the literature of the critical debris thickness for the Djankuat Glacier vary from 0.03 m (Lambrecht et al., 2011) to 0.07 m (Bozhinskiy et al., 1986). The areal fraction of Djankuat Glacier that holds these thin thickness values is very small (Popovnin et al., 2015) and are therefore not believed to have a significant influence on the ablation of Djankuat Glacier.”

>> Line 247, 251, 254: ‘this time period’ – maybe re-state the time period. Use same unit.

We changed *“this time period”* to *“the 1967/68–2006/07 period”*. Consistency in the units was achieved by changing them to *“ $m\ yr^{-1}$ w.e. m^{-1} ”*.

>> Line 258: What's the meaning of 'between 0.18 and +/- 0.6 m'.

The \pm means "approximately", and the text was adjusted accordingly'.

>> Line 261: 'second a' to 'a second'

Done.

>> Line 267: Can you give numbers about the 'snow redistribution by wind/avalanche'?

In the upper part (> 3600 meter), the local mass balance of the glacier is reduced by ca. 76%. The following was added to the text (Line 94):

"Moreover, the mass balance profile in these upper areas is significantly distorted (by ca. -76%) by snow redistribution processes (Pastukhov, 2011)."

>> Line 270-273: Did you validate the model with the same data which were used also to calibrate the model? If not, specify which data you used. If yes, isn't there a different, independent dataset which can be used for model validation?

There are very few or no independent data to validate the model results. In the revised manuscript this was acknowledged by reformulating the text in several places, e.g. Line 308 (Sect. 3.3):

"However, as with the mass balance and debris cover model, there are no, or only few, independent data to validate our model results with a sufficient degree of certainty."

For Line 394-395, Sect. 5.2, the word 'validation' was removed:

"It can thus be stated that the calibrated mass balance model performs well when forced with the observed Terskol climatic data, and that credibility can be assigned to the dynamic calibration procedure."

The same was done for the statement in the conclusion (Line 495, Sect. 8):

"... no artificial mass balance perturbations were needed, ensuring proper model calibration and credibility."

>> Line 280: I don't understand what t_{debris} exactly is (cf. l. 215).

See comment Line 215 above.

>> Line 297: 'the bed was slightly adjusted' – how? Can you give some more details?

This was clarified in the text by adding the following:

"Additionally, the bed width for the assumed trapezoidal-shaped cross section was slightly adjusted to ensure that the parameterization fits the observed area-elevation distribution for a total surface area of 2.688 km²."

>> Line 326: Is the volume change a yearly volume change? If yes correct the unit.

Yes, "annual" was added.

>> Line 331: Please correct the unit/make it consistent with the rest of the manuscript.

Not sure what is unclear here.

>> Line 332: Can you add a reference or details about the 'e-folding length response time'?

The following was added for clarification:

"The e-folding length response time (i.e. the time needed to achieve $(1 - e^{-1})$ or ~63% of the total length change) of D_{jankuat} is in the order of ..."

>> Line 334-335: Well, I imagine that these numbers depend a lot on the topography (see general comments)?

See general comment 3.

>> Line 330-338: the sensitivity experiments need some more details on how they are done (see general comments).

See general comment 3.

>> Line 356-357: ‘an acceptable accuracy’ – please give a number.

The integrated mass balance of the glacier in steady state exhibits a value of $0 \pm 0.006 \text{ m yr}^{-1}$ w.e., which was added to the text in the following way:

“...integrated surface mass balance over the entire glacier approaches zero to within an acceptable accuracy of 0.006 m yr^{-1} w.e. and by...”

>> Line 381-387: In my opinion, all these sentences can be reduced into one or two.

The subsection was shortened to:

“Especially during the last few decades, an accelerated warming trend has occurred, as the latest 10-year climatic interval exhibits a mean annual temperature anomaly of $+0.5^{\circ}\text{C}$ compared to the 1981–2010 mean. This makes it the warmest period in the reconstructed time series. For temperature, a clear sequence of colder and warmer intervals can be seen. Changes in precipitation show a sequence of drier and wetter periods (Fig. 8).”

>> Line 390-395: How is this mass balance perturbation obtained (see main comments)?

See general comment 2.

>> Line 411-413, 413-415, 417: Can you give some more details about these data? Did you use global circulation models (GCMs) or regional climate models (RCMs)? Which model did you use (all GCMs and RCMs have specific names, realizations, institutions...). Why did you use a linear temperature and precipitation evolution? Why not using the transient evolutions of the climate models? Moreover: did you apply a de-biasing approach between past dataset and the future climate projections? (see main comments). ‘ $+7.1^{\circ}\text{C}$ ’ compared to when? Is this number a temperature difference between two periods or a temperature mean? If it is a temperature mean, please report also the value of the first period, or the difference.

See general comment 1.

>> Line 445-456: Are these values arbitrary? That seems fine but if they are, better add a sentence explaining why these values are taken and from where.

These values are indeed arbitrary. It was added after Line 459 of the original manuscript:

“It must be noted that the values of these parameters are arbitrary, as the exact location, time and magnitude of future debris sources cannot be predicted. By assessing multiple possible values for each of these parameters, we encompass various potential future scenarios in order to account for the high uncertainty regarding these parameters.”

>> Line 503: ‘-80%’ – of area? Of volume? Or of length?

The following was changed (with a slight deviation due to the new future climatic datasets):

“... most drastically (ca. -93 % of its current surface area) under the RCP 8.5 scenario...”

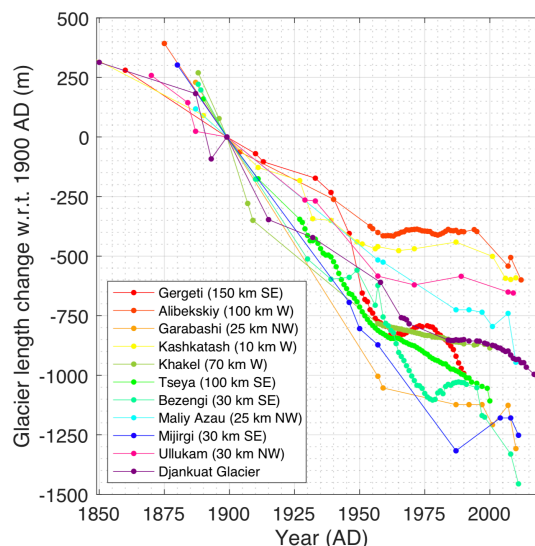
Comments to figures and tables

>> Fig. 1: The scale bar is bizarre. Why not 0, 0.25, 0.5, 1 km instead of 0.5, 0.25, 0, 0.5 km?

We don't think the scale bar in this form is confusing.

>> Fig. 2: Would be nice to have a little map showing where these other glaciers are, or at least their distance to Djankuat Glacier.

The distances and direction to Djankuat Glacier are added to the updated Figure 2. Balance years are changed to calendar years and all length changes are now relative to 1900 AD:



“New Figure 2 in the updated manuscript. Historic length variations of the Djankuat Glacier compared to other glaciers in the Caucasus (Solomina et al., 2016; WGMS, 2018). Approximate distances and direction to the Djankuat Glacier are indicated.”

>> Fig. 4: (i) I may have missed it, but what is causing the modelled MB gradient to ‘flip’ at the highest elevations (>3550 m) in Fig. 4a? (ii) Also the units are different than in main text.

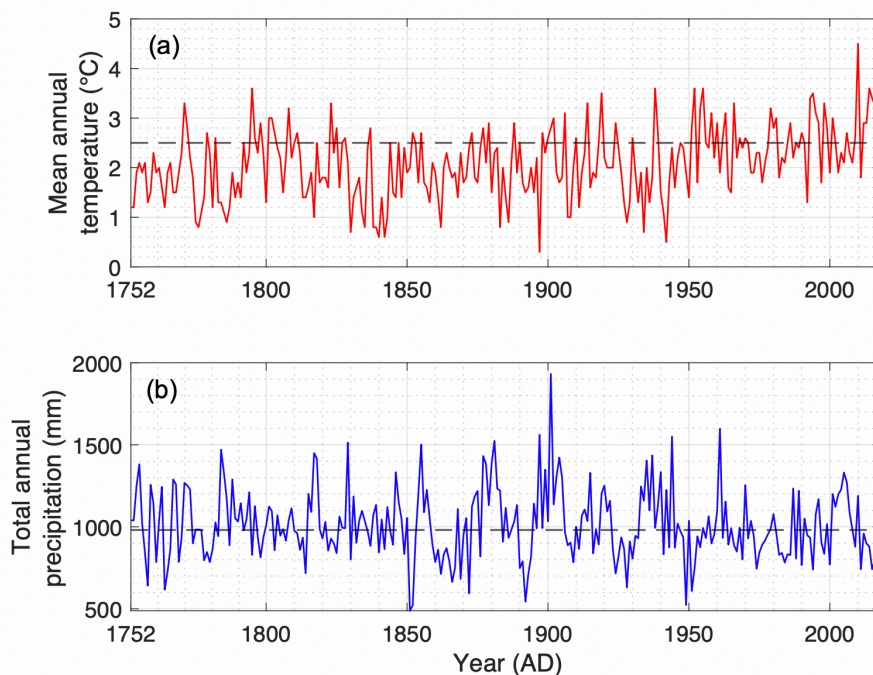
(i) This is due to snow redistribution due to avalanches/wind redistribution in the steep upper part of the glacier (Lines 154-159 in the original manuscript). See comment to Line 267 above.
 (ii) All mass balance terms are expressed in m w.e. yr⁻¹.

>> Fig. 5: (i) Would be interesting to see longer-term evolution of these values as well. (ii) What’s causing the sharp bend around 1985? Is it the switch to very negative MBs

(i) An additional figure with the further evolution of the debris layer was not added to the manuscript in order to not overload the paper. The effect of additional debris sources can however be inferred from Fig. 14 in the original paper. (ii) The bend around the 1980s is when the debris that had been deposited at $x_{debris} = 1680$ meter since $t_{debris} = 1958$, has reached the glacier terminus due to advection.

>> Fig. 10: (i) add labels for temperature and precipitation, (ii) say what “w.r.t.” is and (iii) say what the black line is.

Labels were added, “w.r.t.” has been deleted and the data have been converted from balance years to calendar years:



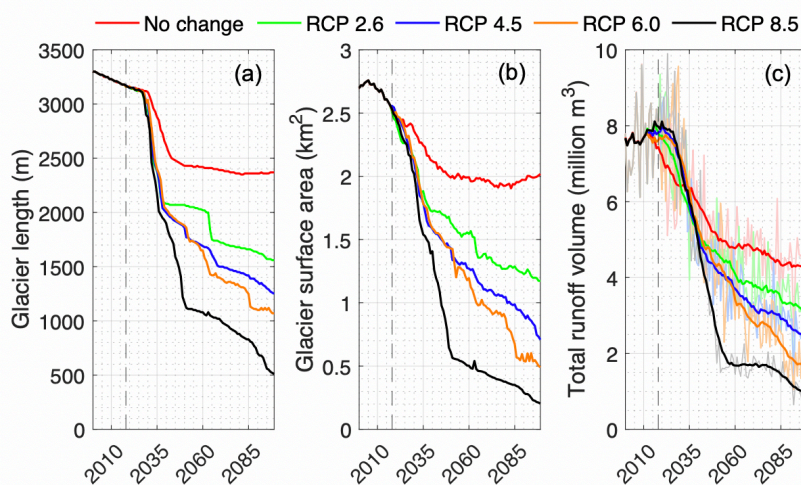
“New Figure 8 in the updated manuscript. Reconstructed and observed evolution of (a) mean annual temperature and (b) total precipitation for Terskol weather station, based upon proxy data (tree ring reconstructions) and measurements from nearby weather stations (Mestia, Pyatigorsk and Mineralnye Vody). The dashed horizontal line represents the 1981–2010 annual reference values (2.6 °C and 1001.1 mm w.e. yr⁻¹). We refer to the text and Table 2 for more details.”

>> Fig. 11: What is the black line?

This is the 15-yr moving average. This is now clarified in the figure caption.

>> Fig. 12: Can the volume be plotted as well? That seems an important quantity.

We have opted to not overload the picture with an additional volume projection. Rather we chose to merge total annual runoff volumes (old Fig. 13) into the figure of the future projections, in the light of future water resource management. The results of the new future projections are represented in the following updated Figure 11:



“New Figure 11 in the updated paper. Modelled (a) glacier length, (b) glacier surface area, and (c) total annual runoff volume of the Djankuat Glacier for different RCP scenarios until 2100 AD. In (c), the thin lines represent annual values, while the thicker lines represent 15-yr moving average. The dashed vertical line denotes the present (i.e. 2017, the most recent year of glaciological observations).”

>> Fig. 13: (i) unit in the y-axis (/year?), (ii) say in the caption what ‘present’ is for this study.

This figure has been deleted and incorporated in the updated Figure 11 (see comment above).

>> Fig. 14: Why are the impacts visible only after ca. 2050?

The following statement is added to the manuscript:

“It is worth mentioning that the effects on glacier length are not immediate, as it takes some time for the debris to be advected to the terminus.”

>> General comment about figures: The ‘YYYY/YY’ format is distracting. Better use ‘YYYY’

Done for all figures that require annual labels on the x-axis.

>> Table 1: Can you explain what the ‘-’ means?

The – means that there is no constant value for this parameter. We have added this as:

“Table 1. Variables, constants and their units. The – denotes a variable or a dimensionless quantity.”

New references added:

Huss, M. & Hock, R: A new model for global glacier change and sea-level rise. *Frontiers in Earth Science* 3, 2015.

Hock, R., Rasul, G., Adler, C., Cáceres, B., Gruber, S., Hirabayashi, Y., Jackson, M., Kääb, A., Kang, S., Kutuzov, S., Milner, A., Molau, U., Morin, S., Orlove, B., and Steltzer, H.: High Mountain Areas. In: IPCC Special Report on the Ocean and Cryosphere in a Changing Climate [Pörtner, H.-O., Roberts, DC., Masson-Delmotte, V., Zhai, P., Tignor, M., Poloczanska, E., Mintenbeck, K., Alegría, A., Nicolai, M., Okem, A., Petzold, J., Rama, B., Weyer, N. M. (eds.)]. In press, 2019.

Shannon, S., Smith, R., Wiltshire, A., Payne, T., Huss, M., Betts, R., Caesar, J., Koutroulis, A., Jones, D., and Harrison, S.: Global glacier volume projections under high-end climate change scenarios, *The Cryosphere*, 13, 325–350, doi: <https://doi.org/10.5194/tc-13-325-2019>, 2019.

Taylor, K. E., Stouffer, R. J., and Meehl, G. A.: An overview of CMIP5 and the experiment design, *Bull. Am. Meteorol. Soc.*, 93, 485–498, doi: [10.1175/BAMS-D-11-00094.1](https://doi.org/10.1175/BAMS-D-11-00094.1), 2012.

Zekollari, H., Huss, M., and Farinotti, D.: Modelling the future evolution of glaciers in the European Alps under the EURO-CORDEX RCM ensemble, *The Cryosphere*, 13, 1125–1146, doi: <https://doi.org/10.5194/tc-13-1125-2019>, 2019.

Thank you for your detailed and helpful comments and suggestions. In the text below, reviewer comments are indicated with colored background, our replies are in plain text and our changes to the manuscript are put in italic.

Response to major comments

Major comment 1

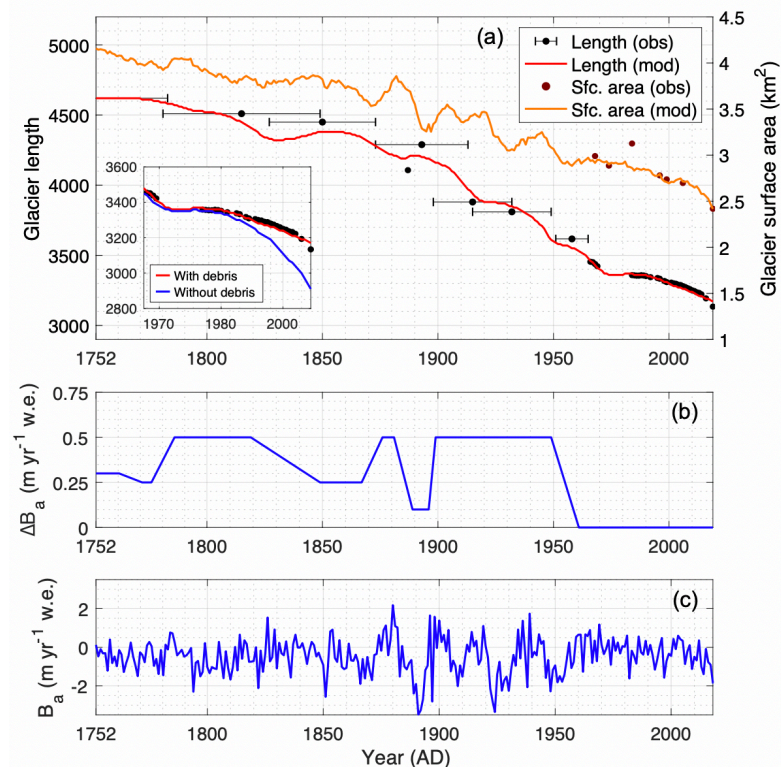
>> Evaluation of glacier change in terms of terminus position and glacier area: We know that debris-covered glaciers have a different response to climate warming based on remote sensing observations and numerical modelling, which shows that they lose the majority of mass by surface lowering rather than terminus recession. Therefore, the metrics that are useful for clean-ice glaciers are poor indicators of the behaviour of a debris-covered glacier. My main concern with the study is that the debris model is unnecessary given the characteristics of Djankaut Glacier (e.g. large areas of visible clean ice on the tongue, steep slope below the ELA, high velocities, large changes in length and area over several decades, short response time) and introduces a bias to the results. It would be valuable to demonstrate the difference between simulations with and without the debris-cover model to evaluate its impact on glacier change and if the observed change can be replicated without this additional calculation. It appears that the info is contained in Fig. 14, which shows future glacier evolution under different climatic forcings, but is not discussed in the text and the figure is difficult to interpret; it appears that the debris has no impact on glacier length change until the second half of the century.

Indeed, our experiments brought to light that an extensive debris cover on Djankuat Glacier is a more recent phenomenon, largely linked to glacier retreat exposing debris sources, however that was not made very explicit in the manuscript. On the other hand, debris cover becomes an important characteristic of the glacier in the future. In that sense, we disagree with the reviewer that the debris cover is unnecessary to study the future behavior of Djankuat Glacier. We have more explicitly addressed this issue by including the results of an additional experiment without debris cover. Both model runs with and without debris cover exhibit very similar results prior to the observational period. As shown in the new inset in Fig. 9 below, debris played only a minor role prior to ca. 1980 AD, with length differences of only 20 to 40 meter. By 2009/10 AD, however, the length difference between both runs is already modelled to be 160 meter. This is also evident from observations, where one can clearly see that the debris-free section of the snout has retreated faster than the debris-covered section. In the manuscript, the following additional explanation was therefore added (Line 409):

A historic model run conducted with a 100 % clean-ice glacier, shown as an inset in Fig. 9a, revealed that debris played only a minor role prior to ca. 1980 AD, with length differences of only 20 to 40 meter. By 2009/10 AD, however, the modelled length difference between a debris-free and debris-covered glacier already increased to 160 meter.”

And (Line 451):

“Despite present-day areas of visible clean ice on the tongue, a steep slope below the ELA, relatively high ice velocities, and a short response time, also observations show that the supraglacial debris cover on the Djankuat Glacier has significantly affected glacier geometry during the last several decades, as evident from the differential retreat of the snout (Fig. 1).



Updated Figure 9. Historic variations of (a) the modelled and observed glacier length of the Djankuat Glacier since 1752/53 AD until 2017 AD, (b) additional mass balance perturbations ΔB_a and (c) reconstructed time series of the total annual mass balance B_a of the Djankuat Glacier with changing geometry. Observed length variations are derived from lichenometric dating of moraines in the valley, historic documents, and/or field measurements and/or recent satellite imagery (Boyarsky, 1978; Zolotarev, 1998; Petrakov et al., 2012; WGMS, 2018). An additional model run for a 100% clean ice glacier was conducted is shown in the inset in panel a.

We have furthermore expanded the discussion of Figure 14 to underline that supraglacial debris cover is of large importance for the future evolution of the glacier:

The figure shows the impact of debris input location x_{debris} , the time of release of the debris source from the surrounding topography t_{debris} , and debris flux magnitude F_{debris} (rows) on the future length extension of the Djankuat Glacier under different climatic scenarios (columns). The black lines indicate the scenario where no additional debris source is released in the future. The other lines are for experiments that include an additional future debris source from the surrounding topography for varying values of the earlier mentioned debris-related parameters. It is clear that the addition of an increasingly widespread debris cover dampens glacier retreat. It should be noted that the effects on glacier length are not immediate, as it takes some time for the debris to be advected to the terminus after its initiation at time t_{debris} .

Major comment 2

>> Value of sub-debris melt calculation: In relation to my point above, I have two concerns about the debris-cover model; (a) the gradient of the exponential function used to scale sub-debris melt is steep using $H^*_{debris} = 1.15$ m (see review Fig. 1), and (b) the thickness of debris on the glacier is similar to the critical thickness observed on debris-covered glaciers elsewhere and therefore likely to both enhance and reduce ablation across the tongue. The glacier model accounts for the impact of supraglacial debris by reducing mass balance, a valid assumption

beneath debris that is thicker than a critical thickness of about 0.1–0.2 m. An exponential function is used to reduce ablation with debris thickness. However, images of the present day glacier including Fig. 1 and data presented in the manuscript (Fig. 5a) illustrate that the debris thickness at the terminus is ~1.0 m in 2010 and was <0.5 m before 1990. As debris thickness decreases rapidly upglacier (Fig. 5c), is the same scaling is assumed then most of the debris layer was <0.25 m thick before 1990 and therefore close to the critical thickness. For such thin and discontinuous debris layers, there is likely to be little reduction in ablation due to insulation by the debris layer (the exponential function used here will only reduce sub-debris melt by <20% compared from the clean-ice value – see review Fig. 1) and instead an enhancement of ablation due to the reduction in albedo of debris-covered ice compared to clean-ice surfaces. The model does include an albedo term but does not use this to adjust for the impact of debris on ablation.

We understand the reviewers' concern related to the decay of the exponential curve for H^* debris and acknowledge that the value found for Djankuat Glacier deviates somewhat compared to earlier research for other glaciers. As pointed out in Anderson and Anderson (2016) and Lambrecht et al. (2011), the value for H^* debris depends, amongst other factors, on the thermal conductivity of the debris material, the debris cover porosity and is also influenced by the debris layer water saturation. Values for these factors seem somewhat out of range for the Djankuat Glacier and explain the deviating value of the H^* debris parameter (Anderson and Anderson, 2016; Lambrecht et al., 2011; Bozhinskiy et al., 1986). The following section was added to the manuscript for clarification (Sect. 3.1, Line 262):

“A value of 1.15 meter was found for H^ debris. The gradient of the exponential decay is somewhat out of range with respect to earlier studies for other glaciers (e.g. Anderson and Anderson, 2016). Explanations for this high value of H^* debris can be found in the relatively high thermal conductivity of the granite-type debris cover on the glacier ($2.8 \text{ W m}^{-1} \text{ }^\circ\text{C}^{-1}$) and the high debris cover porosity (0.43 in the case of Djankuat Glacier, Bozhinskiy et al., 1986). Also the relatively low water saturation, as mentioned by Lambrecht et al. (2011), suggests that heat conduction towards the debris-ice interface seems to occur quite easily on the Djankuat Glacier.”*

With respect to the inclusion of the melt-enhancing effect for thin debris, studies performed on Djankuat Glacier point to a lower value of the critical thickness than mentioned by the reviewer (0.03 m by Lambrecht et al., 2011 and 0.07 m by Bozhinskiy et al., 1986). The areal fraction of debris cover on the Djankuat Glacier that holds such thin thickness values is very small, so we believe that the ablation enhancement effect of thin debris plays a very minor role on Djankuat Glacier. Therefore, this factor was not included in the parameterization. The following section was added to the revised manuscript for justification (Line 224):

“The melt enhancement that may occur for a very thin debris cover was not implemented. Values in the literature of the critical debris thickness for the Djankuat Glacier vary from 0.03 m (Lambrecht et al., 2011) to 0.07 m (Bozhinskiy et al., 1986). The areal fraction of Djankuat Glacier that holds these thin thickness values is very small (Popovnin et al., 2015) and are therefore not believed to have a significant influence on the ablation of Djankuat Glacier.”

The following limitations were furthermore added for completion, after Line 228:

“The debris model also neglects other processes that may potentially play a role in the spatial and temporal distribution of debris, such as the formation and thickening of medial moraines, ice cliffs and surface ponds (Anderson and Anderson, 2016).”

Major comment 3

>> Evolution of the debris layer: As observed in Fig. 5, the debris layer has thickened by a factor of 2–3 over the last 20 years. Djankaut Glacier is steep, fast-flowing and thinly debris-

covered over a section of its ablation area, and based on this geometry and the presence of large ice-marginal moraines it seems likely that during the LIA and subsequently, the glacier exported the majority of its debris to its margins rather than developing a supraglacial layer. Therefore, the assumption in the spin up simulation that the glacier is debris covered (Section 5.1) may not hold. However, from Fig. 14 it appears that the debris layer has no impact on glacier change until about 1970 CE.

We agree that the increasingly widespread supraglacial debris cover on Djankuat Glacier is a more recent phenomenon, largely related to exposure of debris sources due to glacier retreat and climate warming. We furthermore refer to the new Fig. 9a in general comment 1 to demonstrate that the debris cover only became important during the last several decades, and has had little influence prior to ca. 1980 AD. However, there is also an indirect evidence for the presence of at least some supraglacial debris in the historic period, shown by e.g. the presence of end moraines in the valley (Fig. 1), and a photograph taken around 1930 AD that shows some debris patches on the snout (Aleynikov et al., 2002). It is furthermore unclear to us how we could have initialized the glacier model at the LIA without debris cover. The following section was therefore added to the manuscript to discuss this issue (in Sect. 5.1):

“As can be deduced from the large lateral moraines in the Adylsu Valley (Fig. 1) and fast-flowing nature of the paleo-glacier tongue in the valley (up to 100 m yr^{-1} around 1752 AD, Fig. 6d), Djankuat Glacier used to export most of its debris to the margins rapidly in the historic period, rather than developing a supraglacial debris cover. Furthermore, debris sources from surrounding topography were likely less widespread in the historic period because the slopes were covered by the glacier itself and were more stable in a colder climate. For this reason, supraglacial debris is believed to have been much less widespread prior to the observational period of 1967/68 AD, implying that the glacier was not very much influenced by debris cover in the historic period. However, there is also indirect evidence for at least some supraglacial debris in the historic period from the presence of end moraines in the valley (Fig. 1) and a photograph taken around 1930 showing some debris patches on the snout (Aleynikov et al., 2002). It would be furthermore unrealistic to only introduce a debris cover in the model once the model approaches the start of the observations. This would contradict the presence of moraines and the observation that there already was an expanding debris cover during the first data collection in 1967/68 AD (Popovnin et al., 2015). Because there is no direct evidence for the origin of the debris cover, it was chosen to include melt-out processes in the model from the initialization onwards.”

As a minor point, Fig. 14 (now Fig. 12) only showed results after 2009, so we are a bit puzzled how reviewer 2 came to the conclusion that the debris layer has no impact until about 1970 CE.

Major comment 4

>> Lack of discussion: The manuscript organisation is somewhat unconventional. After the Introduction, Methods and Model Description, there are four Results sections (not named as such) followed by the Conclusions. There is very limited discussion of the context of results and their interpretation, and no dedicated section for this.

We organized the manuscript in such a way that discussion items are merged into the result sections, so that all information related to one specific subject appears sequentially in a chronological, continuous text. This way of structuring was preferred, rather than jumping from one section to another. However, also in response to the other reviewers, the discussion was expanded in several places. This included additional discussion on model validation versus model calibration, justification of assumptions in the debris cover model, and the effect of debris on future glacier evolution.

Response to minor comments

>> Line 13: “retreat” see major comment 1 about terminus recession versus surface lowering.

To elaborate more on the thinning out of debris-covered glaciers, we added (Line 51):

“If a thick supraglacial debris cover is present over a large portion of a glacier’s ablation zone, surface melting and terminal retreat can be drastically suppressed, even under a warming climate (e.g. Scherler et al., 2011; Benn et al., 2012). In such cases, debris-covered glaciers are shown to lose mass by lowering the surface in their ablation zone (downwasting), rather than by terminus retreat (e.g. Hambrey et al., 2008; Rowan et al., 2015).”

>> Line 15-16: The change in glacier length and area stated here are not meaningful unless the initial length and area are also given, or these are stated as % change.

Done. This was rectified in the text:

“... have decreased by 1.4 km (- 29.5 %) and 1.6 km² (-35.2 %) respectively...”

>> Line 24-25: Vague statement.

We have included some references to these sentences:

“... changing climate (e.g. Shannon et al., 2019; Zekollari et al., 2019; Hock et al., 2019).”

>> Line 39: Use of “significantly” should be reserved to its precise statistical meaning, whereas here it is used for emphasis and could be replaced with “dramatically” or in this sentence the meaning would be the same if this word was removed.

The word ‘significantly’ was removed and replaced by ‘drastically’.

>> Line 45-47: What is the glacierised area and debris-covered area in the Caucasus in km²? This is needed to indicate the context suggested in this statement.

The total glaciated area is stated in Line 30 (691.5 ± 29.0 km² in 1986, 590.0 ± 25.8 km² in 2014). The manuscript mentioned on Line 46 that 26.2% of that glacierized area is debris covered, referring to Scherler et al. (2018). Hence, the debris-covered area is ca. 155 ± 6.7 km² for present-day conditions. This number is now added:

“...be 26.2 % at for present-day conditions (ca. 155 ± 6.7 km²), hence enabling...”

>> Line 53: Citations to previous modelling studies of debris-covered glaciers. Please note that Rowan et al. (2015) did not use a simple parameterisation of the impact of debris on mass balance as stated here, but instead made a dynamic simulation of the feedbacks between ice flow, debris transport and mass balance using a higher-order ice flow model. The statement ending in line 64 is therefore incorrect, as previous studies have taken this approach. A citation to Wirbel et al. (2017) should also be included.

This has been rectified in the text, thanks for pointing this out. The sentence was changed to:

“The pronounced effect of debris should not be ignored in numerical models to determine the future evolution of mountain glaciers, yet only few studies have included this complex process in time-dependent models (e.g. Juvet et al., 2011; Rowan et al., 2015; Huss and Fischer, 2016; Kienholz et al., 2017; Rezepkin and Popovnin, 2018; Wirbel et al., 2018).”

>> Line 73: State glacier area here.

Done.

>> Line 96-98: Use metres for debris thickness values here to be consistent with the rest of the text.

Done.

>> Line 101: “Mean annual air temperature”, and “+” is not needed before the values.

Changed.

>> Line 110: Explain what you mean by “1.5D” or stick with “1D” to indicate a flow line calculation. L112. Do you mean 2D rather than “3D”, i.e. a matrix calculation?

The model only uses ice and debris flow in 1 dimension, namely along the x-axis. However, the remaining glacier area was also implicitly taken into account by using the width in the continuity equation. To avoid confusion, it was changed to “*numerical flow line model*”.

>> Line 224: Give value for H^* debris, from Table 1, the value used after tuning was 1.15 m, which results in the steep curve mentioned in Major Comment 1. Also it is not clear as written here how this model compared to that presented in Anderson and Anderson (2016) as mentioned in the Introduction, which used a hyperbolic rather than exponential function to scale sub-debris melt; $h^*/(h^*+h_{\text{debris}})$ their Eq. 3 with h^* of 0.065 m.

See major comment 2.

>> Line 258, 260: Unclear as written. What is the meaning of “±” before the values given for H^* debris? Do these values range from –0.6 to 0.6 m?

The ± means “*approximately*”, and the text was adjusted accordingly’.

>> Line 259: One of the key references for a previous application of this model to Djankaut Glacier is Rybak et al. (2018), which is cited to justify parameter choices and to give detail about the model. However, this document is difficult to locate and appears to only be available in Russian. I was not able to use this reference to collect information about the model. At Line 259 the citation here is incorrect, as “Rybak (2018)” is not in the reference list.

We acknowledge that both Russian papers are hard to find and not easy to understand, and have therefore decided to remove these from the manuscript.

>> Line 363: All the models have different time steps; 3-hourly for the mass balance model, ~4 hourly for the ice flow model and ~4 days for the debris transport model. How are the integrated, and what impact do these time steps have on the result when the response time is ~30 years?

The time steps for the ice flow and debris models were chosen for reasons of numerical stability to satisfy the CFL criterion for diffusion and advection problems. The timestep of 3 hours for the mass balance model is required to capture the daily cycle and because the weather data were not available at shorter intervals. The mass balance is calculated for a full balance year, changing year per year. The choice of these time steps has a negligible impact on the results given the length response time of ca. 31 years.

>> Line 455-459: What evidence is there for the choice of debris input parameters?

These values represent a range of possible future scenarios informed by the past, as the location, release and magnitude of future debris sources can of course not be predicted. We added the following text after Line 459 for clarification:

“It must be noted that the values for these parameters represent a range of possible future scenarios, as the exact location, time and magnitude of future debris sources cannot be predicted.”

>> **Line 490:** Incorrect statement, see comment on line 53 above.

Agreed. Changed to:

“... not yet integrated in numerical flow line models.”

>> **Line 508-518:** Here and elsewhere, although the written text is generally clear and free of typographic errors, the writing style is rather vague and qualitative, using large lists of variables/controls without indicating their importance, and the meaning can be difficult to follow. The manuscript would benefit from editing to enable clearer, more precise statements to present the study and its results.

Noted.

>> **Model code:** The code and data used are described as available on request from the author. I believe the Cryosphere now requires these to be open access in a repository.

To comply with TC's data policy, we now make the model code publicly available via GitHub/Zenodo. The model code that served for this research can be found and downloaded from: https://github.com/yoniv1/Djankuat_glacier_model. The code placed here is a 1D coupled ice flow-debris cover model. It uses bedrock geometry together with a parameterized mass balance profile to calculate the ice thickness evolution on a grid with spatial resolution dx for the Djankuat Glacier, and also takes into account an evolving supraglacial debris cover until a steady state situation has been reached. Our code availability statement now reads:

“Code availability. Code availability. The coupled ice flow-supraglacial debris cover model for the Djankuat Glacier used in this research was written in MATLAB_R2019a. It can be downloaded from the GitHub repository at: https://github.com/yoniv1/Djankuat_glacier_model, doi: <https://doi.org/10.5281/zenodo.3934612>.”

Newly added references

Aleynikov, A. A., Zolotaryov, Ye. A., Voytkovskiy, K. F., and Popovnin, V.V.: Indirect Estimation of the Djankuat Glacier Volume Based on Surface Topography, *Hydrology Research*, 33 (1), 95–110, doi:10.2166/nh.2002.0006, 2002.

Benn, D. I., Bolch, T., Hands, K., Gulley, J., Luckman, A., Nicholson, L. I., Quincey, D., Thompson, S., Toumi, R., and Wiseman, S.: Response of debris-covered glaciers in the Mount Everest region to recent warming, and implications for outburst flood hazards, *Earth Sci. Rev.*, 114, 156–174, doi:10.1016/j.earscirev.2012.03.008, 2012.

Hambrey, M., Quincey, D., Glasser, N. F., Reynolds, J. M., Richardson, S. J., and Clemmens, S.: Sedimentological, geomorphological and dynamic context of debris-mantled glaciers, Mount Everest (Sagarmatha) region, Nepal, *Quaternary Sci. Rev.*, 27, 2341–2360, 2008.

Hock, R., Rasul, G., Adler, C., Cáceres, B., Gruber, S., Hirabayashi, Y., Jackson, M., Kääb, A., Kang, S., Kutuzov, S., Milner, A., Molau, U., Morin, S., Orlove, B., and Steltzer, H.: High Mountain Areas. In: IPCC Special Report on the Ocean and Cryosphere in a Changing Climate [Pörtner, H.-O., Roberts, DC., Masson-Delmotte, V., Zhai, P., Tignor, M., Poloczanska, E., Mintenbeck, K., Alegría, A., Nicolai, M., Okem, A., Petzold, J., Rama, B., Weyer, N. M. (eds.)]. In press, 2019.

Scherler, D., Bookhagen, B., and Strecker, M. R.: Spatially variable response of Himalayan glaciers to climate change affected by debris cover, *Nat. Geosci.*, 4, 156–159, 2011.

Shannon, S., Smith, R., Wiltshire, A., Payne, T., Huss, M., Betts, R., Caesar, J., Koutroulis, A., Jones, D., and Harrison, S.: Global glacier volume projections under high-end climate change scenarios, *The Cryosphere*, 13, 325–350, doi: <https://doi.org/10.5194/tc-13-325-2019>, 2019.

Wirbel, A., Jarosch, A. H. and Nicholson, L.: Modelling debris transport within glaciers by advection in a full-Stokes ice flow model, *The Cryosphere*, 12, 189-204, <https://doi.org/10.5194/tc-12-189-2018>, 2018.

Zekollari, H., Huss, M., and Farinotti, D.: Modelling the future evolution of glaciers in the European Alps under the EURO-CORDEX RCM ensemble, *The Cryosphere*, 13, 1125–1146, doi: <https://doi.org/10.5194/tc-13-1125-2019>, 2019.

Thank you for your detailed and helpful comments and suggestions. In the text below, reviewer comments are indicated with colored background, our replies are in plain text and our changes to the manuscript are put in italic.

Response to general comments

General comment 1

>> **Model validation**: at several places in the manuscript, the authors say that the model was validated, for example: “It can thus be stated that the model performs well and underwent a successful validation to within acceptable accuracy”. I argue that a model is validated when its capacity to reproduce the “unseen” is assessed (past and future evolution, or unobserved variables). A model is useful when model predictions are associated with an uncertainty estimate. As it is now, the model has a very large number of free parameters which are calibrated to match observations almost perfectly. Per design, the study does not allow validation with independent or out-of-sample data (e.g. cross-validation). I don’t think that it is possible to change this aspect of the study at this stage, but I would like to see the problem of model uncertainty and over-calibration discussed in the manuscript, and the statement that the model has been successfully “validated” should be changed to “calibrated”. I think that the consequences of parameter equifinality are most likely to be seen in the sensitivity experiments of the debris cover parameterization and the future projections.

It is correct that there are very few or no independent data to validate the model results and we agree that ‘validation’ is not the appropriate choice of word in this regard. In the revised manuscript this was acknowledged by reformulating the text in several places, basically substituting ‘validation’ by ‘calibration’ (e.g. Line 308, Sect. 3.3):

“However, as with the mass balance and debris cover model, there are no, or only few, independent data to validate our model results with a sufficient degree of certainty.”

For Line 394 (Sect. 5.2), we removed the word ‘validated’:

“It can thus be stated that the calibrated mass balance model performs well when forced with the observed Terskol climatic data, and that credibility can be assigned to the dynamic calibration procedure.”

The same was done for the statement in the conclusion (Line 495, Sect. 8):

“... no artificial mass balance perturbations were needed, ensuring proper model calibration and credibility.”

Furthermore, a small section was introduced related to over-calibration. Apart from a small areal fraction in the highest altitudinal zones (> 3600 meter), where data availability is limited and snow redistribution processes create complex patterns, we think that our calibration dataset is sufficiently long (39 years) to assume that the environmental conditions within the calibration window have some validity for past and future conditions (Sect. 3.1, Line 273):

“The calibration dataset for the mass balance model is quite long (39 years from 1967/68 to 2006/07 AD), making it credible to assume that the parameters calibrated to this period have some validity for past and future conditions as well. Apart from the high-elevation areas (> 3600 meter), where data availability is limited and snow redistribution processes create complex conditions, it can be expected that the environmental setting within the calibration window also holds for periods prior to and after the observational period. However, it must be noted that the areal fraction of this high-altitudinal zone is limited (ca. 3% of the glacier area in 2009/10 AD).”

General comment 2

>> Added value of the past simulations: the model is dynamically tuned to fit observed length changes, with a time varying bias parameter. I am aware that this has been done before (and will be done in the future), but I have to ask: in the end, what is the added value of such a simulation? What do we learn from it, that we didn't already know from length change observations alone? What are the implications of the dynamic parameterization for the future projections?

The dynamic calibration procedure is needed to account for imperfections in the model and the climate forcing datasets, which are generally larger for more distant time periods. Because the glacier is currently still responding to past changes of climate, geometry and dynamics, these imperfections would produce a current glacier state that deviates from the observed one, and this deviation would be carried forward in any projection. The positive aspect of our dynamic calibration is that mass balance corrections were only required for the period before 1967 AD, so that (keeping in mind the e-folding length response time of ca. 31 years) future projections have largely 'forgotten' the older artificial mass balance corrections. We further refer to general comment 2 of the Loris Compagno review (RC 1) and its responses. For clarification, the following was added to the text (Line 395):

“Such a procedure is needed to counteract imperfections in the flow model, mass balance model and the climate forcing. The added value of this procedure is to ensure a current glacier state that matches the observed one, as the glacier is still responding to changes in past climate, geometry and dynamics.”

And:

“It furthermore implies that future projections are no longer influenced by the corresponding artificial mass balance corrections, keeping in mind an e-folding length response time of ca. 31 years for the Djankuat Glacier.”

General comment 3

>> Debris cover parameterization: in my opinion, the true added value of this study lies in the coupling of a debris parameterization with the flowline model. I think it would add great value to the manuscript to extend the sensitivity analyses to the past glacier simulation as well (which, as it stands, is of very limited usefulness). How is the past glacier evolution changed by the inclusion of debris cover? In order not to make this paper even longer, I would suggest to remove Fig. 7 to 9, which are quite qualitative.

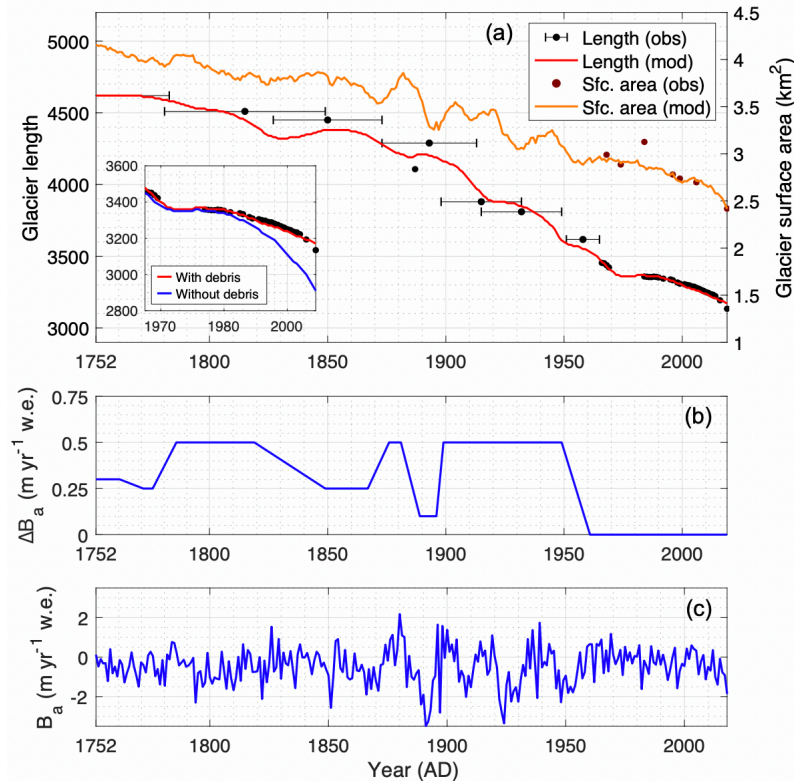
We believe that the extensive debris cover on Djankuat Glacier is a more recent phenomenon, largely linked to glacier retreat exposing debris sources. We therefore assume that the glacier was not very much influenced by debris cover prior to the observational period (1967/68 AD). In that sense, an experiment related to historic debris characteristics was carried out by executing a model run for the historic period, both with and without the debris parametrization. Both model runs exhibited very similar results prior to the observational period. As shown in the new inset in Fig. 9 below, debris played only a minor role prior to ca. 1980 AD, with length differences of only 20 to 40 meter. In this regard, the following was added to the paper (in Sect. 5.1):

“As can be deduced from the large lateral moraines in the Adylsu Valley (Fig. 1) and fast-flowing nature of the paleo-glacier tongue in the valley (up to 100 m yr^{-1} around 1752 AD, Fig. 6d), Djankuat Glacier used to export most of its debris to the margins rapidly in the historic period, rather than developing a supraglacial debris cover. Furthermore, debris sources from surrounding topography were likely less widespread in the historic period because the slopes were covered by the glacier itself and were more stable in a colder climate. For this reason, supraglacial debris

is believed to have been much less widespread prior to the observational period of 1967/68 AD, implying that the glacier was not very much influenced by debris cover in the historic period.”

And (Line 409):

“A historic model run conducted with a 100 % clean-ice glacier, shown as an inset in Fig. 9a, revealed that debris played only a minor role prior to ca. 1980 AD, with length differences of only 20 to 40 meter. By 2009/10 AD, however, the modelled length difference between a debris-free and debris-covered glacier increased to 160 meter”



Updated Figure 9. Historic variations of (a) the modelled and observed glacier length of the Djankuat Glacier since 1752/53 AD until 2017 AD, (b) additional mass balance perturbations ΔB_a used in the dynamic calibration procedure and (c) reconstructed time series of the total annual mass balance B_a of the Djankuat Glacier with changing geometry. Observed length variations are derived from lichenometric dating of moraines in the valley, historic documents, field measurements and recent satellite imagery (Boyarsky, 1978; Zolotarev, 1998; Petrakov et al., 2012; WGMS, 2018). An additional model run for a 100% clean ice glacier is shown in the inset in panel a.

To limit paper length, we removed Figs. 7 to 9 of the original paper and replaced it with a single all-encompassing figure regarding glacier sensitivity (see also our response to general comment 3 of reviewer RC 1).

General comment 4

>> **Code and data availability:** you write: “the refined debris cover implementation can be used for comparable glacier models in future research”. I agree! But it would be considerably more useful if the code and data used in this study would be made freely available under a proper software license and in a public repository. Platforms like zenodo.org will preserve the version

of the model as it is at the time of this publication. And it will create a DOI to make it citable for future research. See TC’s data policy: https://www.the-cryosphere.net/about/data_policy.html

You are right. To comply with TC’s data policy, we now make the model code publicly available via GitHub/Zenodo. The model code that served for this research can be found and downloaded from: https://github.com/yoniv1/Djankuat_glacier_model. The code placed here is a 1D coupled ice flow-debris cover model. It uses bedrock geometry together with a parameterized mass balance profile to calculate the ice thickness evolution on a grid with spatial resolution dx for the Djankuat Glacier, and also takes into account an evolving supraglacial debris cover until a steady state situation has been reached. Our code availability statement now reads:

“Code availability. The coupled ice flow-supraglacial debris cover model for the Djankuat Glacier used in this research was written in MATLAB_R2019a. It can be downloaded from the GitHub repository at: https://github.com/yoniv1/Djankuat_glacier_model, doi: <https://doi.org/10.5281/zenodo.3934612>.”

Specific comments

>> Abstract L10: I would prefer not to use the term "1.5D". I never understood what the "0.5" is referring to: the widths? The vertically integrated velocity? Should a 2D SIA model then be called a 2.5D model? I think that a “SIA flowline model” is explicit enough.

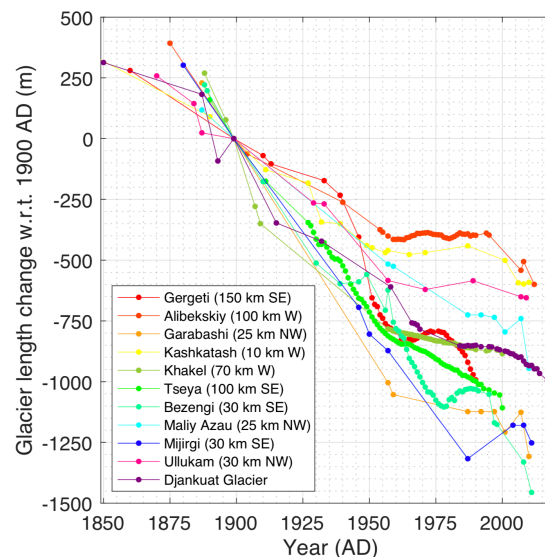
We have replaced the term ‘1.5D’ in the original manuscript and now call the model ‘flow line model’ in the new text, so that its 1-dimensional nature can be derived explicitly from its name.

>> Figure 1: If possible, indicate the location of AWS Adylsu Valley

Done.

>> Figure 2: It is misleading to compare length changes like this, because they all have a different zero baseline. It would be better to plot them as relative length change since year X.

The figure was updated, where distances and direction to Djankuat Glacier are added. Balance years are changed to calendar years and all length changes are now relative to 1900 AD:



“New Figure 2 in the updated manuscript. Historic length variations of the Djankuat Glacier compared to other glaciers in the Caucasus (Solomina et al., 2016; WGMS, 2018). Approximate distances and direction to the Djankuat Glacier are indicated.”

>> Figure 6a and chapter 5.1: Could you elaborate on why the 1752 steady-state glacier has a longer and thicker tongue while the ice thickness above 3000 m a.s.l. is more or less equal to the 2009 glacier?

This is a well-known characteristic of glacier retreat. Retreating glaciers thin their ablation areas with little effect above the equilibrium line, which is well reproduced by the model.

>> Figure 10 and 11c: I assume the black lines are rolling means. Please specify years.

These are 15-yr moving means. This was added to the figure caption.

>> Line 106: Please specify which data period and parameters are available at these stations.

We used data from 2 AWSs (one in the Adylsu Valley near the LIA extent of the glacier, AWS 1, and one in the glacier ablation zone, AWS 2). We used data from AWS 1 for precipitation comparisons between Terskol and the Adylsu Valley, and data from AWS 2 to derive transmissivity, temperature lapse rates, albedo, and shortwave, longwave and turbulent fluxes. These AWSs were only operational during the summer months (June to September) between 2007 and 2017. This was clarified manuscript as follows:

“In 2007, two automatic weather stations (AWS) were additionally installed, one in the Adylsu Valley at ca. 2640 m elevation (AWS 1 in Fig. 1) and one in the ablation zone of the glacier at ca. 2960 m on a sparsely debris-covered ice surface (AWS 2 in Fig. 1). During the summer seasons (June to September) of 2007–2017, a wide range of additional meteorological variables have therefore been acquired by AWS 1 and 2 (air temperature, dew point temperature, incoming and outgoing shortwave/longwave radiation, relative humidity, wind speed and direction, air pressure and for AWS 1 also precipitation amounts) (Rets et al., 2019). The AWSs did not operate outside the JJAS period.”

The location of AWS 1 and 2 were added to Figure 1 of the original manuscript.

>> Line 134: The time step is fixed at 0.0005 years. Did any stability considerations or tests go into this choice?

The following was added to the updated manuscript (Line 135):

“...with Δt of 0.0005 years, as determined by the CFL-condition for diffusion problems”.

And Line 221:

“...with $\Delta t = 0.01$ years, in accordance with the CFL-condition for advection problems”.

>> Line 147, 179, 183: Which time period was used?

We used the data from the AWSs, which were only operational during the summer seasons of 2007-2017. We refer to comment Line 106 above.

>> Line 149: Was the winter temperature lapse rate solely chosen based on the reported ELA temperature by WGMS (2018) or was AWS data used as well?

The AWSs were not operational outside the June to September window. This was clarified:

“Due to lack of AWS data outside of the June to September period, a temperature lapse rate of $-0.0049^{\circ}\text{C m}^{-1}$ was used for the winter half-year (1 Oct – 31 Mar), in accordance...”

>> Line 150, 179, 191: It is often not clear if data from the AWS Djankuat or the AWS Adylsu Valley is used.

We used data from AWS 1 for precipitation comparisons, and data from AWS 2 to derive transmissivity, temperature lapse rates, albedo, and shortwave, longwave and turbulent fluxes. We specifically referred to each respective AWS when data are discussed in the text. For Line 147:

“Hence, a direct comparison of measured air temperatures between AWS 2 on Djankuat and the Terskol weather station was found...”

For Line 150:

“In this study, a value for f_e of 1.5 between Terskol and the Adylsu Valley was found after a comparison of precipitation amounts from AWS 1 in the glacier valley.”

For Line 179:

“Measurements of the incoming solar radiation from the AWS 2 were used to derive atmospheric transmissivity...”

For Line 185:

“The ice albedo α_{ice} can, according to raw data from the AWS 2, vary between 0.15 and 0.40 depending...”

And Line 191:

“Here, these fluxes, as derived from AWS 2, are added up and plotted analyzed against air temperature following the method...”

>> **Line 150, 250:** Is the precipitation scaled to match one of these AWS? If yes which one?

Precipitation between the Adylsu Valley and Terskol was scaled using a factor f_e , using AWS 1. For the precipitation gradient, we did not have reliable data to extrapolate the precipitation from the Adylsu Valley over the entire glacier. We therefore used the accumulation profile to tune the precipitation gradient. It is clarified where the factor f_e comes from:

“In this study, a value for f_e of 1.5 between Terskol and the Adylsu Valley was found after a comparison of precipitation amounts with AWS 1 in the glacier valley.”

Secondly, it was explicitly stated that the precipitation gradient γ_p is used as a tuning parameter:

“... by making use of a vertical precipitation gradient γ_p , of which the latter is used as a tuning parameter due to a lack of data (see Sect. 3.1).”

>> **Line 162 (Eq. 7):** It might be worth noting that this melt term is only one part of the total runoff of the mass-balance model and that the rest is derived in the next chapter.

Done:

“It must be noted that the melt term M is only one part of the total runoff RO of the mass balance model (see Sect. 2.5).”

>> **Line 187:** Can you please specify how the fractional cloud cover is parametrized?

It was done using a linear relationship between the cloud cover and net longwave radiation. The following was added:

“These were derived from an approximately linear relationship between the cloud cover and the net longwave radiation balance (Voloshina, 2002), of which the latter was measured by AWS 2 on the glacier surface.”

>> **Line 192:** From that sentence I would expect a Figure similar to Figure A1 of Giesen and Oerlemans (2010).

To avoid confusion, the choice of words was adjusted. In the text, this was modified as follows:

“... fluxes, as derived from AWS 2, are added up and analyzed against air temperature...”

>> Line 369: “At first, data from the pre-observational period ...”

Done. We changed “for” to “from”.

>> Line 370: Terskol time period is already specified in Table 2.

The text “(1977–2013 with a data gap between 1990–1997)” was deleted.

>> Line 373: How was the available data repeated into the past? By just copying the entire time period? Shuffling of individual days/months/years? Were any sensitivity tests made in that regard?

As mentioned in the manuscript, the data sequence for Terskol over which measurements with a 3-hourly interval are available (1977–2013 with a data gap between 1990–1997) was repeated into the past and future in order to maintain intra-daily and intra-annual variability in the data. These 30-year sequences were copied / pasted until the entire time series had been covered. Afterwards, they were adjusted for the monthly temperature and precipitation data that were obtained with the climatic reconstruction and future projections. We did not carry out a sensitivity analysis as we think the data sequence is long enough to encompass inter- and intra-yearly variability.

>> Line 374: Terskol time period is already specified in Table 2 and line 370.

The text “(1977–2013 with a data gap between 1990–1997)” was deleted.

>> Line 378-388: This paragraph (and also L 396-400) with the listing of different dates and periods is a bit cumbersome to read. Maybe it would be better to indicate these periods in the anyway mentioned Fig. 10 and be more concise in the text.

The subsection was shortened to:

“Especially during the last few decades, an accelerated warming trend has occurred, as the latest 10-year climatic interval exhibits a mean annual temperature anomaly of +0.5°C compared to the 1981–2010 mean. This makes it the warmest period in the reconstructed time series. For temperature, a clear sequence of colder and warmer intervals can be seen. Changes in precipitation show a sequence of drier and wetter periods (Fig. 8).”

>> Line 393-395 (and 494-495): The mass-balance and debris cover models were calibrated for the period 1967-2007 with the use of multiple tuning parameters to fit the observed surface mass-balance. The fact that no further dynamic calibration via mass-balance perturbations was necessary for this period cannot lead to conclusions about the model performance and accuracy.

See general comment 1.

>> Future glacier evolution: Like other reviewers, I do not understand how the GCM climate is used in this study. Why is the linear change necessary, why not applying the GCMs delta T and delta P directly?

We have now recreated the future climate forcing directly from available CMIP5 models for the grid cell closest to Djankuat Glacier. We therefore used a multi-model mean approach using 21 Global Circulation Models. We also applied a de-biasing procedure to match the future climate

RC 3 – Fabien Maussion (rebuttal by Verhaegen et al. – tc-2019-312)

forcing with the past, both concerning the trend and the variability. See general comment 1 from RC 1.

Modelling the evolution of Djankuat Glacier, North Caucasus, from 1752 until 2100 AD

Yoni Verhaegen¹, Philippe Huybrechts¹, Oleg Rybak^{1,2,3} and Victor V. Popovnin⁴

¹Earth System Science and Department of Geography, Vrije Universiteit Brussel, Pleinlaan 2, B-1050 Brussels, Belgium

5 ²Water Problems Institute, Russian Academy of Sciences, Gubkina Str. 3, 119333 Moscow, Russia

³~~FRC Subtropical Centre of RAS, Theatralnaya Str., 8-a, 354000 Sochi, Russia~~ [FRC SSC RAS, Theatralnaya Str., 8-a, 354000, Sochi, Russia](#)

⁴Department of Geography, Lomonosov Moscow State University, 1 Leninskie Gory, 119991 Moscow, Russia

Correspondence to: Yoni Verhaegen (yoni.verhaegen@vub.be)

10 **Abstract.** We use a numerical ~~1.5D~~ [flow line](#) model to simulate the behaviour of the Djankuat Glacier, a WGMS reference glacier situated in the North Caucasus (Republic of Kabardino-Balkaria, Russian Federation), in response to past, present and future climate conditions (1752–2100 AD). The model consists of a coupled ice flow–mass balance model that also takes into account the evolution of a supraglacial debris cover. After simulation of the past retreat by applying a dynamic calibration procedure, the model was forced with ~~climatic~~ data for the future period under different scenarios regarding

15 temperature, precipitation and debris input. The main results show that the glacier length and surface area have decreased by 1.4 km ([-29.5 %](#)) and 1.6 km² ([-35.2 %](#)) respectively between the initial state in 1752 AD and present-day conditions. Some minor stabilization and/or readvancements of the glacier have occurred, but the general trend shows an almost continuous retreat since the 1850s. Future projections [using CMIP5 temperature and precipitation data](#) exhibit a further decline of the glacier. Under constant present-day climate conditions, its length and surface area will further shrink by ca. ~~50-30 %~~ by 2100

20 AD. However, even under the most extreme RCP 8.5 scenario, the glacier will not have disappeared completely [by the end of the modelling period](#). The presence of an increasingly widespread supraglacial debris cover is shown to significantly delay glacier retreat, depending on the interaction between the prevailing climatic conditions, the debris input location, the debris mass flux magnitude and the time of release of debris sources from the surrounding topography.

25 1 Introduction

Recently, a lot of attention has been given to modelling mountain glaciers, in particular due to their worldwide observed shrinkage and important role within the current changing climate ([e.g. Shannon et al., 2019; Zekollari et al., 2019; Hock et al., 2019](#)). The observed warming trend is a significant matter of concern to scientists and all other people (in)directly involved in the behaviour of these glacial systems, as projected scenarios point towards an even further increase of the global

30 mean temperature in the future, especially if no efficient mitigation strategies are implemented (Vaughan et al., 2013; [Rasul](#)

and Molden, 2019; Hock et al., 2019). Being consistent with this global trend, the accelerated retreat of Caucasian glaciers during the last several decades has been clearly noticed (e.g. Shahgedanova et al., 2014; Zemp et al., 2015; Tielidze, 2016). Accordingly, total glaciated area has decreased from 691.5 ± 29.0 km² to 590.0 ± 25.8 km² (-0.52 % yr⁻¹) in the period between 1986 and 2014 (Tielidze et al., ~~2017~~2020). Further degradation of Caucasian glaciers may affect the supply of water used for drinking, irrigation and hydroelectric energy generation, whereas it may also pose a threat for downstream communities via flooding, glacier collapses, avalanches, debris flows and glacial lake outbursts (e.g. Volodicheva, 2002; Ahouissoussi et al., 2014; Taillant, 2015; Chernomorets et al., 2018). Furthermore, the presence of glaciers in the Caucasus can be considered important for paleoclimatic research, tourism, cultural heritage and biodiversity (e.g. Popovnin, 1999; Shahgedanova et al., 2005; Hagg et al., 2010; Makowska et al., 2016; Tielidze and Wheate, 2018; Rets et al., 2019). Despite these rising concerns, however, modelling of Caucasian glaciers is scarce and has only been attempted in a few studies (e.g. Rybak and Rybak, 2018; Rybak et al., 2018; Rezepkin and Popovnin, 2018; Belozarov et al., 2020).

In a warming climate, debris coverage onto the glacier's surface is believed to increase significantly drastically due to the build-up of more englacial melt-out material, lower flow velocities and increased slope instability, hence favouring which favour the occurrence of rock slides and mass movements from the surrounding topography (Østrem, 1959; Kirkbride, 2000; Stokes et al., 2007; Jouvét et al., 2011; Carenzo et al., 2016). During the last decades, a sharp increase of debris-covered glacier surfaces has been observed over the Caucasus region, owing to the combined effects of steep terrain, a wet climate, small average glacier size, large lateral moraines and the presence of local easily erodible sedimentary rock outcrops. ~~Owing to the additional effects of steep terrain, a wet climate, small average glacier size, large lateral moraines and the presence of local easily erodible sedimentary rock outcrops, a sharp increase of debris covered glacier surfaces has been observed over the Caucasus region.~~ Accordingly, debris coverage has expanded at a rate of ca. ~~+0.220.32~~ % yr⁻¹ between 1986 and 2014 when the entire Caucasus region is considered (Tielidze et al., ~~2020~~2017). Scherler et al. (2018) estimates the supraglacial debris cover on Caucasian glaciers to be 26.2 % (ca. 155 ± 6.7 km²) at present-day, hence enabling the area to hold the world's most abundant share of debris-covered glacier surfaces in relative terms. Evidently, the presence of such supraglacial debris can influence the evolution of mountain glaciers in a variety of ways, depending on its thickness, properties and spatial/temporal distribution (Nicholson and Benn, 2006; Anderson and Anderson, 2016). Apart from a slight melt enhancement for a very thin debris layer ~~More specifically~~, thick debris has been shown to reduce runoff volumes and reverse mass balance gradients due to its melt-reducing effect (e.g. Østrem, 1959; Bozhinskiy et al., 1986; Anderson and Anderson, 2016). If a thick supraglacial debris cover is present over a large portion of a glacier's ablation zone, surface melting and terminal retreat can be drastically suppressed, even under a warming climate (e.g. Scherler et al., 2011; Benn et al., 2012). In such cases, debris-covered glaciers are shown to lose mass by lowering the surface in their ablation zone (downwasting), rather than by terminus retreat (e.g. Hambrey et al., 2008; Rowan et al., 2015). The pronounced effect of debris should therefore not be ignored in numerical experiments to determine the future evolution of mountain glaciers, ~~but, yet~~ only few studies have included this complex process in time-dependent models, ~~merely using only simple parameterizations~~ (e.g.

Jouvet et al., 2011; Rowan et al., 2015; Huss and Fischer, 2016; Kienholz et al., 2017; Rezepkin and Popovnin, 2018; [Wirbel et al., 2018](#)).

In this paper, we focus on modelling the Djankuat Glacier (North Caucasus, Russian Federation), [a WGMS \(World Glacier Monitoring Service\) reference glacier](#) which has a broad observational network in both space and time. However, despite abundant field data availability and increasing interest concerning [its](#) future behaviour, the Djankuat Glacier has not yet been modelled extensively. ~~We accordingly present here, for the first time,~~ [Here we present](#) a 1.5D-numerical flow line model ~~for this glacier~~ to simulate its response to past, present and future climatic change. The calculations relate to ice dynamics, supraglacial debris cover evolution and annual surface mass balances. More specifically, the objectives of this study are to construct and calibrate a coupled ice flow–mass balance–supraglacial debris cover model for the Djankuat Glacier, to reconstruct its front variations and mass balance series since 1752 AD, and to simulate the response to future climate change under different scenarios until 2100 AD. In particular, we adapt a ~~more sophisticated and physically~~ [physically](#)-based debris model from Anderson and Anderson (2016) to ~~look at~~ [investigate](#) the impact of supraglacial debris cover on the glacier's evolution, which has not been previously applied in time-dependent ~~glacier modelling~~ [numerical flow line models](#). The results can hence be used to more accurately assess the behaviour of the Djankuat Glacier as ~~representative a~~ [WGMS reference glacier](#) for the Caucasus area, including the potential side effects of its evolution such as the regulation of water resources. Furthermore, the refined debris cover implementation can be used for comparable glacier models in future research.

2 Location, data and models

2.1 The Djankuat Glacier

The Djankuat Glacier [43°12' N, 42°46' E] is a northwest-facing and partly debris-covered temperate valley glacier that is situated on the northern slope of the Main Caucasus Ridge near the border of the Russian Federation ~~and with~~ Georgia, which is the most heavily glaciated area of the Northern Caucasus Mountains. As of 2009/10 AD, the glacier ~~occupies~~ [occupied](#) a total surface area of 2.688 km², of which the majority is situated at higher elevations (Fig. 3). ~~It~~ [The glacier](#) consists of four major ice flows and ~~currently has had~~ a length of 3.26 km when taken from its highest point on the south face of the Djantugan peak (Fig. 1). [However, by 2017 AD, satellite imagery revealed that the glacier area had further decreased to 2.418 km² \(Rets et al., 2019\), while the glacier length shortened to a value of 3.12 km.](#) ~~A~~ [Furthermore, a](#) unique characteristic of the glacier is the origin of its main ice flux on ~~a~~ [the](#) divergent and vast Djantugan firn plateau south of the main ridge, of which the contributing area to the glacier changes regularly ([Aleynikov et al., 2002a](#)).

The Djankuat Glacier has been monitored thoroughly since glaciological measurements began in the 1960s, resulting in an abundant amount of field data ~~and hence,~~ enabling this glacier as an ideal candidate for modelling studies (e.g. Popovnin, 1999; Aleynikov et al., 2002b; Popovnin and Naruse, 2005; Lavrentiev et al., 2014; WGMS, 2018; Rets et al., 2019).

95 Consequently, the Djankuat Glacier has been selected by the WGMS as a reference glacier for the Caucasus region, hence defining its behaviour as representative for other ~~glaciated areas~~glaciers across ~~the entire Caucasus region~~this area. As such, a comparison with glacier length variations in the Caucasus since the 19th century AD shows that the Djankuat Glacier genuinely reflects the general trend in the broader area, as can be seen in Fig. 2 (e.g. Kotlyakov et al., 1991; Solomina et al., 2016; WGMS, 2018).

100 2.2 Field data

The start of the standard monitoring program on the Djankuat Glacier dates back to ~~the~~ 1967/68 AD ~~season~~ and includes measurements concerning geometry, supraglacial debris cover and (local) annual surface mass balance. Additionally, ice velocity measurements ~~were performed~~ ~~occurred~~ during the summer seasons of ~~the late 1990s~~ 1994–2001 ~~and are~~ based upon both direct (theodolite surveys of stakes) and indirect (stereophotogrammetrical) measurements, of which the resulting maps are reported in Aleynikov et al. (1999) and Pastukhov (2011). Glacier-wide ice thickness maps have also been constructed by Lavrentiev et al. (2014), using ground-based radio-echo measurements. However, direct and reliable observations lack at the higher elevations (~~> 3600 m~~) and the Djantugan Plateau ~~due to difficult accessibility~~, ~~where~~ ~~In these areas~~ ~~Here~~, ice thickness values have been derived indirectly using surface velocity and slope (Aleynikov et al., 2002b; Pastukhov, 2011). ~~As of 2009/10 AD, the glacier occupies a total surface area of 2.688 km², of which the majority is situated at higher elevations (Fig. 3).~~ The current ice thickness ~~goes~~ ~~has been found to go~~ up to ca. 100 m in the central part of the main glacier body, and to more than 200 m at the Djantugan Plateau. ~~Moreover,~~ ~~the~~ ~~Furthermore,~~ ~~the~~ glacier's cumulative surface mass balance during the 1967/68–2016/17 period ~~exhibits~~ ~~exhibited~~ a strongly negative value of -14.33 m w.e., ~~with a mean equilibrium line altitude (ELA) of 3213 m~~ (WGMS, 2018). ~~Moreover, the mass balance profile in these upper areas is significantly modified (at 3600 m by ca. -76 % of the value that the local specific mass balance would have if it were extrapolated according to the mass balance gradient found below) by snow redistribution processes (Pastukhov, 2011).~~

Both glacier-averaged debris thickness (from 0.28 m in 1983 to 0.54 m in 2010) and total debris-covered area (from ca. 0.10 km² or 3.5 % in 1968 to ca. 0.34 km² or 12.7 % ~~of the glacier~~ in 2010 AD) have increased largely. However, at the debris-covered left side of the snout (~~when seen in the downstream direction~~), debris thickness increased exponentially over the years, resulting in mean values of ~~100 cm~~ ~~1 m~~ at the glacier front in 2010, compared to ~~29 cm~~ ~~0.29 m~~ in 1983 and ~~45 cm~~ ~~0.45 m~~ in 1994 AD (Popovnin et al., 2015). ~~Recent observations have shown the importance of the debris cover on the Djankuat Glacier, as the debris-covered left side of the front clearly retreated slower than the less affected right part. As of 2010 AD, the length difference between both sides was ca. 180 m (Fig. 1) but this has increased to ca. 250 m by 2017 AD (Rets et al., 2019).~~

The climate around the glacier can be inferred from nearby weather stations, such as Terskol (elevation 2141 m, approx. 20 km northwest of the glacier) and Mestia (approx. 16 km southwest from Djankuat Glacier, in Georgia, at 1441 m elevation), see Fig. 1 ~~and Table 2~~. ~~The average mean~~ ~~Mean~~ annual temperatures ~~here~~ ~~in Terskol and Mestia~~ are +2.8 °C and +6.0 °C

respectively for the 1981–2010 ~~reference period~~ climate. For the summer half-year from April to September (AMJJAS), the corresponding mean temperatures are 8.7 °C and 12.0 °C. ~~Especially since the early 1990s, mean annual temperatures in the area have been increasing, resulting in record high values.~~ Precipitation, on the other hand, is rather complex in the region due to variations of atmospheric circulation patterns, orographic uplift and convective precipitation in the summer season (Boyersky, 1978; Shahgedanova et al., 2007; Hagg et al., 2010; Popovnin and Pylayeva, 2015; ~~Rybak et al., 2018~~). At Terskol and Mestia, total annual precipitation amounts equal ~~1001.1~~ 945.5 and 1035.1 mm yr⁻¹ respectively for the 1981–2010 climate. During the accumulation season (October to March, ONDJFM), the corresponding precipitation values are 418.4 and 490.0 mm yr⁻¹ w.e. respectively. ~~In the Adylsu Valley (ca. 2650 m elevation) and in the ablation zone of the glacier (ca. 2960 m elevation), an automatic weather station (AWS) was installed, measuring a wide range of meteorological variables (air temperature, incoming and outgoing shortwave/longwave radiation, relative humidity and wind speed).~~ In 2007, two automatic weather stations (AWS) were additionally installed, one in the Adylsu Valley at ca. 2640 m elevation (AWS 1 in Fig. 1) and one in the ablation zone of the glacier at ca. 2960 m on a sparsely debris-covered ice surface (AWS 2 in Fig. 1). During the summer seasons (June to September, JJAS) of 2007–2017, a wide range of additional meteorological variables have therefore been acquired by both AWSs (air temperature, dew point temperature, incoming and outgoing shortwave/longwave radiation, relative humidity, wind speed and direction, air pressure and for AWS 1 also precipitation amounts). The AWSs did, however, not operate outside the JJAS period (Rets et al., 2019).

2.3 Ice dynamic model

The ice dynamic model is implemented as a ~~1D (-1.5D)~~ numerical flow line model, in which the prognostic continuity equation for ice thickness change is solved. We choose to only model ice flow along a central axis in the x-direction and not upgrade the model to 3D due to the abundant amount of experiments that were conducted. However, the y-dimension is implicitly taken into account due to inclusion of glacier width along this central axis. ~~As such, one~~ One central flow line is considered ~~in the area~~ with a total length of 5 km, ~~that flows~~ stretching from the glacier top near the Djantugan peak down to the current snout and further into the Adylsu Valley (Fig. 1). The flow line is constructed perpendicular to the surface elevation isolines, generally close to the location where the cross-sectional ice thickness and ice velocity are maximal as determined from ice thickness and surface velocity maps. ~~The flow line was chosen so that it is representative for the Djankuat Glacier as a whole and incorporates the highest point of the glacier near the Djantugan peak. It remains perpendicular to the surface elevation isolines, while sources of lateral drag near the margins have a negligible influence on the movement of ice due to its central position. The representativeness was further determined by ice thickness maps, where the flow line crosses representative areas of thick ice, and dynamical maps, where ice velocities are large along the major central axis of the glacier.~~ The model treats ice flow as a non-linear diffusion problem in a vertically integrated approach (e.g. Oerlemans, 2001):

$$\begin{aligned}\frac{\partial H}{\partial t} &= -\frac{1}{W_{sfc}} \left(\frac{\partial F_{ice}}{\partial x} \right) + b_a \\ &= -\frac{1}{W_0 + \mu H} \left[\frac{\partial}{\partial x} \left(\left[(W_0 + \frac{1}{2} \mu H) (\rho_i g H)^3 (f_d H^2 + f_s) \left(\frac{\partial h}{\partial x} \right)^2 \right] \frac{\partial h}{\partial x} \right) \right] + b_a\end{aligned}\quad (1)$$

160 where H is the ice thickness, t the time, μ the slope of the lateral valley walls, W_0 the glacier bed width, W_{sfc} the glacier surface width, F_{ice} the ice volume flux, x the horizontal distance, b_a the local annual surface mass balance, ρ_i the ice density, g the gravitational acceleration, f_d the flow parameter related to internal deformation, f_s the flow parameter related to basal sliding and h the surface elevation. The vertically integrated velocity is calculated by assuming that the 1D Shallow Ice Approximation is applicable to derive driving stresses on a xz plane and that ice is treated as a homogenous, 165 incompressible and isothermal non-Newtonian fluid in Glen's flow law. For basal sliding, a simplified Weertman-type flow law is used where the basal water pressure is proportional to the ice thickness and the basal shear stress equals the driving stress (e.g. Oerlemans, 1992; Oerlemans, 2001; Leclercq et al. 2012):

$$\bar{u} = \bar{u}_d + u_s = \left(-\rho_i g H \frac{\partial h}{\partial x} \right)^3 \left(f_d H + \frac{f_s}{H} \right)\quad (2)$$

Here, \bar{u} is the vertically averaged horizontal velocity, ~~while and~~ \bar{u}_d and u_s are the velocity components related to internal 170 deformation and basal sliding respectively. Equation (1) is then solved on a staggered grid with a spatial resolution Δx of 10 m ~~starting from zero ice thickness m, while the integration~~ Integration over time is achieved with a forward in time, centered in space (FTCS) numerical scheme using a time step Δt of 0.0005 years, as determined by the CFL-condition for diffusion problems.

2.4 Mass balance model

175 The mass balance model is based upon the ~~trade-off~~ difference between accumulation ACC and runoff RO over the balance year (1 October – 30 September), so that the ~~temporal change of the~~ local surface mass balance b_a is defined as:

$$\frac{\partial b_a}{\partial t} = \int_{yr} (ACC - RO) * dt \quad ~~ACC - RO~~\quad (3)$$

Mean specific (total) mass balances B_a were then derived by integrating b_a over the entire glacier surface.

$$B_a = \frac{1}{A} \int_A b_a dA \quad (4)$$

180 ~~where A is the surface area of the glacier.~~ Accumulation for each point along the flow line is only dependent on the part of the total precipitation that is solid (P_{solid}), which only takes place if precipitation occurs below a certain threshold temperature T_{tresh} :

$$ACC = P_{solid} = \begin{cases} ([P_{Terskol} * f_e] * P_{scale\ ratio}) * f_{red} & \text{if } T_{air} < T_{tresh} \\ 0 & \text{if } T_{air} \geq T_{tresh} \end{cases}\quad (54)$$

185 Air temperatures T_{air} from Terskol weather station were interpolated to any surface elevation height on the Djankuat Glacier
 by applying vertical temperature lapse rates γ_T (Table 1). ~~Hence, a~~ direct comparison of measured air temperatures
 between AWS 2 on Djankuat and the Terskol weather station was found to exhibit a strong correlation ($R^2 = 0.81$),
 generating a summer season ~~-~~lapse rate of $-0.0067 \text{ }^\circ\text{C m}^{-1}$ between 2007–2017 AD. Due to lack of AWS data outside of the
JJAS period, a temperature lapse rate of $-0.0049^\circ\text{C m}^{-1}$ was used for the winter half-year (ONDJFM), in accordance ~~For~~
~~winter season (Oct–Mar), $-0.0049 \text{ }^\circ\text{C m}^{-1}$ was used in accordance~~ with a mean annual ELA temperature of $-3.75 \text{ }^\circ\text{C}$ for
 190 Djankuat Glacier (WGMS, 2018). The term $P_{Terskol} * f_e$ represents the precipitation in the Adylsu Valley, calculated by
 multiplying the precipitation in Terskol with a horizontal precipitation enhancement factor f_e to account for horizontal
 precipitation variations. In this study, a value for f_e of 1.5 between Terskol and the Adylsu Valley was found after a
comparison of precipitation amounts from AWS 1 in the glacier valley. The factor $P_{ratioscale}$ is used to scale ~~precipitation~~
~~obtained precipitation amounts~~ to the entire glacier from ~~the elevation of~~ the Adylsu Valley to any surface elevation h , by
 195 making use of a vertical precipitation gradient γ_P , where the latter is used as a tuning parameter due to a lack of data (see
Sect. 3.1):

$$P_{ratioscale} = \left(\frac{P_{Terskol} * f_e + (\gamma_P * \Delta h)}{P_{Terskol} * f_e} \right) \quad (5)$$

At last, the factor f_{red} represents a snow redistribution factor which corrects the solid precipitation for redistribution by wind
 and/or avalanches. ~~It was parameterized by dividing the linear accumulation profile with the observed profile and correlating~~
~~these anomalies to the laterally averaged surface slope s along the flow line (e.g. Huss et al., 2009):~~ Here, a topographic
 200 characteristic is used to parameterize snow addition or removal from the glacier surface. It was quantified by dividing the
linear accumulation profile (without the redistribution factor) with the observed profile and correlating these anomalies to the
laterally averaged surface slope s along the flow line (e.g. Huss et al., 2009). As such, a polynomial fit was found. For slopes
steeper than the threshold, removal of snow can occur, and is assumed to be influenced by the surface slope itself:

$$f_{red} = \begin{cases} 1.2 & \text{if } s < s_{crit} \\ -0.0017s^2 + 0.0535s + 0.9041 & \text{if } s \geq s_{crit} \end{cases} \quad (6)$$

205 The critical slope s_{crit} ~~hereby~~ distinguishes between slopes s that either favour snow addition or snow removal (Table 1).
 We do acknowledge that the f_{red} parameterization is solely used for curve fitting of the accumulation profile.

Melt production M , on the other hand, only takes place when the net energy flux per unit area at the surface Ψ_0 is positive
 (e.g. Oerlemans, 2001; Nemec et al., 2009):

$$M = \max\left(0, \frac{\Psi_0}{\rho_w L_m}\right) \quad (7)$$

210 where ρ_w is the water density and L_m the latent heat of fusion. As discussed further in section 2.5, the melt term M is further
modified by the debris cover to obtain the total runoff RO .

As discussed further in section 2.5, the melt term M is further modified by the debris cover and meltwater retention in the snowpack to obtain the total runoff RO . The net energy flux is parameterized as (Oerlemans, 2001; Giesen and Oerlemans, 2010; Leclercq et al., 2012):

$$215 \quad \Psi_0 = \begin{cases} S_{\downarrow}(1 - \alpha)\tau + c_0 & \text{if } T_{air} < T_{break} \\ S_{\downarrow}(1 - \alpha)\tau + c_0 + c_1 T_{air} & \text{if } T_{air} \geq T_{break} \end{cases} \quad (8)$$

Here, τ is the atmospheric transmissivity, α is the surface albedo, while c_0 and c_1 are constants to describe the air temperature-dependent fluxes (i.e. the net longwave, latent heat and sensible heat fluxes). Hence, for air temperatures below the threshold T_{break} , Ψ_0 has a constant value. For higher temperatures, however, Ψ_0 increases linearly with T_{air} , where the rate of increase is determined by c_1 (Giesen and Oerlemans, 2012). The downward incoming solar radiation at the surface S_{\downarrow}

220 incident on an inclined surface with a certain surface slope and aspect, is hereby calculated as (e.g. Oerlemans, 2001):

$$S_{\downarrow} = \begin{cases} S_{\downarrow(TOA)}(f_{dir} \cos(\theta) + f_{dif} \cos(\theta_z)) & \text{if } \theta_e > 0^\circ \text{ \& } \theta < 90^\circ \\ S_{\downarrow(TOA)}(f_{dif} \cos(\theta_z)) & \text{if } \theta_e > 0^\circ \text{ \& } \theta \geq 90^\circ \\ 0 & \text{i. } f \theta_e \leq 0^\circ \end{cases} \quad (9)$$

~~As such where~~, $S_{\downarrow(TOA)}$ is the incoming instantaneous extraterrestrial shortwave radiation on a horizontal plane at the top of the atmosphere, θ_e and θ_z are the solar elevation and zenith angle calculated using basic astronomical formulas (e.g. Allen et al., 2006; Duffie and Beckman, 2006), and θ is the angle of incidence, ~~which are all taking into account the surface slope calculated using basic astronomical formulas (e.g. Iqbal, 1983; Allen et al., 2006; Duffie and Beckman, 2006) respectively,~~

225 ~~and θ is the angle of incidence, which are all calculated using basic astronomical formulas (e.g. Iqbal, 1983; Allen et al., 2006; Duffie and Beckman, 2006).~~ Furthermore, f_{dir} and f_{dif} are the fraction of direct and diffuse solar radiation, which are derived from parameterizations used by Oerlemans (1992, 2001, 2010) and Voloshina (2002) that use the fractional cloud cover f_{cl} :

$$\begin{cases} f_{dir} = 0.1 + 0.80(1 - f_{cl}) \\ f_{dif} = 0.9 - 0.80(1 - f_{cl}) \end{cases} \quad (10)$$

At last, surface albedo α is parameterized as (e.g. Oerlemans and Knap, 1998; Nemeč et al., 2009):

$$\alpha = \alpha_{snow} + (\alpha_{ice} - \alpha_{snow}) \exp\left(\frac{-d_{snow}^*}{d_{snow}^*}\right) \quad (11)$$

where α_{snow} is the snow albedo, α_{ice} the ice albedo and d_{snow}^* a characteristic snow depth.

235 Measurements of the incoming solar radiation from the AWS 2 were used to derive atmospheric transmissivity, ~~which were at first corrected for the tilt at the AWS location (i.e. a slope of 4°).~~ These data were ~~then~~ therefore compared to the theoretical maximum incoming solar radiation at the top of the atmosphere, calculated with standard astronomical formulas (e.g. Iqbal, 1983; Allen et al., 2006; Duffie and Beckman, 2006). Consequently, the overall atmospheric transmissivity τ in

the summer season over the Djankuat Glacier could be deduced as an average of 0.53 (Table 1). The ice albedo α_{ice} can, according to raw data from the AWS 2, vary between 0.15 and 0.40 depending on the presence of water, moraine cover and other impurities and has an average value of 0.22, corresponding to moderately debris-loaded ice. Sparse snow-covered conditions during the ablation season causes α_{snow} to increase to the 0.40–0.90 range (mean 0.79). Next, values for f_{air} and f_{air} are derived from the parameterization of the fractional cloud cover f_{cl} over the Djankuat Glacier, ~~using the relationship between cloud cover and measured net longwave radiation in the Western Caucasus as found by Voloshina (2002).~~ using an approximately linear relationship between the cloud cover and the net longwave radiation balance (Voloshina, 2002), of which the latter was derived from measurements by AWS 2 on the glacier surface. The analysis points out that direct and diffuse solar radiation are ~~more or less~~ approximately equally important for the glacier (Table 1). The constants c_0 , c_1 and T_{break} , describing the air-temperature dependent fluxes and their relationship with the air temperature T_{air} itself, are at last derived from measurements of ~~the~~ AWS 2 of the net longwave radiation, as well as from a parameterization of the sensible and latent heat fluxes via Kuzmin’s method (Kuzmin, 1961; Toropov et al., 2017). Here, these fluxes are added up and ~~plotted~~ analyzed against air temperature following the method of Giesen and Oerlemans (2010) and Leclercq et al. (2012), as can be seen from Eq. (8).

2.5 Debris cover model

The supraglacial debris cover on the Djankuat Glacier was parameterized in order to account for the effects of melt reduction under debris-covered ice. The debris thickness was approached with a steady deposit model adopted from Anderson and Anderson (2016), where debris input onto the glacier is generated from a fixed point on the flow line. In the model, debris thickness then changes according to either melt-out from debris-loaded ice (first term), the downstream advection of supraglacial debris (second term) and the input or removal of supraglacial debris on the glacier surface (third term):

$$\frac{\partial H_{debris}}{\partial t} = - \left(\frac{C_{debris}(\min(0, b_a))}{(1 - \phi_{debris}) \rho_{debris}} \right) - \left(\frac{\partial(u_{sfc} H_{debris})}{\partial x} \right) + I_{debris} \quad (12)$$

Here, H_{debris} is the debris thickness, t the time, C_{debris} the englacial debris concentration, ϕ_{debris} the debris cover porosity, ρ_{debris} the debris rock density, b_a the specific surface mass balance, u_{sfc} the glacier surface velocity and I_{debris} the input or removal of debris from the glacier surface. The advection equation is solved using a first order upwind scheme with $\Delta t = 0.01$ years, in accordance with the CFL-condition for advection problems. In the model, the factors ϕ_{debris} and ρ_{debris} are constants in space and time and taken at 0.43 and 2600 kg m⁻³ respectively (Bozhinskiy et al., 1986). For C_{debris} , we use a value of 1.05 kg m⁻³, referring to a bulk debris concentration inside the ice of 0.12 % ~~to the value of 0.12 %~~ as found by the same authors for the Djankuat Glacier in the 1980s (Table 1). Also here, a constant value in space and time is assumed. Incorporating englacial debris pathways or the spatial distribution of englacial debris concentration would add more detail than warranted by the lack of reliable data regarding this value.

At ~~Next, at~~ the debris input location x_{debris} , a steady debris flux per unit area F_{debris}^{input} transmits material from the surrounding topography to the glacier by means of a debris deposition rate (m yr⁻¹), starting from ~~the time of release of the debris source~~ t_{debris} onwards. Here, t_{debris} is defined as the time at which the topographic debris source firstly starts to release its mass flux towards the glacier surface. We set the debris input location x_{debris} at 1680 m from the highest point (just below the ELA, at 88% of the distance between the terminus x_L and the ELA x_{ELA}), since it is the furthest point up-glacier for which observed debris thickness values are reported in Popovnin et al. (2015). It was chosen to keep the debris input location at a fixed position due to the general absence of direct observations regarding past (static or moving) topographic debris sources. However, a comparison of present-day satellite imagery with those from the 1970s (Pastukov, 2011) points out that the debris patches exhibited only minor up-glacier migration on the main glacier tributary and the debris-covered part of the snout, lending some support to this assumption.

To avoid the buildup of unrealistically high debris thickness in low flow velocity zones in the future ~~period~~, we furthermore choose to let the debris mass flux stop when the surface width at point x_{debris} has reached a value lower than 90 % ($t_{wsfc-10\%}$) of its original value at time t_{debris} . This is considered a reasonable value, as the current observed debris-covered area is ca. 10 % at this specific point (Fig. 3). Connectivity issues between the topographic source and the main glacier are forwarded as the main reason to justify this modification of the Anderson and Anderson (2016) model. Consequently, by then the glacier has laterally shrunk too much to ensure that debris fluxes could still reach its surface. ~~proper connectivity between the debris source and the glacier surface.~~ At the terminus (the last non-zero ice thickness grid point), debris is removed into the foreland by a debris flux per unit area $F_{debris}^{x=L}$ (Anderson and Anderson, 2016):

$$I_{debris} = \begin{cases} F_{debris}^{input} & \text{if } x = x_{debris} \text{ \& } t_{debris} \leq t < t_{wsfc-10\%} \\ -F_{debris}^{x=L} = c_L H_{debris}^{x=L} & \text{if } x = x_L \\ F_{debris}^{x=L+1} = F_{debris}^{x=L(orig)} - F_{debris}^{x=L} & \text{if } x = x_{L+1} \\ 0 & \text{else} \end{cases} \quad (13)$$

where x_L is the terminus position and c_L is a constant describing the strength of debris removal from the terminus into the foreland, for which we used the same value as suggested in Anderson and Anderson (2016), i.e. $c_L = 1$ (Table 1). As such, what is deposited in the foreland by $F_{debris}^{x=L+1}$ is the difference between the original debris flux on point $x = x_L$ (i.e. without the parameterization) minus the actual debris flux obtained with the parameterization. Eventually, the debris-related melt reduction factor f_{debris} is taken as (e.g. Vacco et al., 2010; Huss and Fischer, 2016):

$$f_{debris} = \exp\left(\frac{-H_{debris}}{H_{debris}^*}\right) \quad (14)$$

Here, H_{debris}^* is a characteristic debris thickness (i.e. the debris thickness at which the melt rate is e^{-1} or $\sim 37\%$ of the clean ice melt rate). It must be noted that the melt enhancement that may occur for a very thin debris cover was not implemented in the debris model. However, values in literature of the debris thickness for which a maximum amount of melt enhancement occurs on the Djankuat Glacier vary 0.02 m to 0.07 m (Bozhinskiy et al., 1986; Popovnin and Rozova, 2002; Lambrecht et

al., 2011), and the areal fraction of Djankuat Glacier that holds these thin thickness values is very small (Popovnin and Rozova, 2002; Popovnin et al., 2015). It is therefore not believed to have a significant influence on the ablation of Djankuat Glacier.

Next, the fractional debris covered area along the flow line is parameterized based upon the distance from the terminus D_T , for which [an exponential](#) relationship was found from observations that can, of course, not exceed 1:

$$\frac{A_{debris}}{A} = \min(G_A \exp(-0.01612 * D_T - 0.01720), 1) \quad (15)$$

Here, G_A is a yearly updated growth factor that controls the expansion of the debris covered area (see Eq. 17 in Sect. 3.2). It is furthermore worth noting that the debris model also neglects other processes that may potentially play a role in the spatial and temporal distribution of debris, such as the formation and thickening of medial moraines, ice cliffs and surface ponds (Anderson and Anderson, 2016).

As such, in the case that snow is present at the glacier surface, runoff is calculated as the meltwater outflow from a saturated snowpack W_{snow} , following the principles applied in Schaepli and Huss (2011). On the other hand, in case of snow-free conditions, runoff is affected by the presence of a debris cover on the glacier ice (e.g. Lambrecht et al., 2011):

$$RO = \begin{cases} W_{snow} = \max(0, w_{snow} - \eta_s d_{snow}) & \text{if } d_{snow} > 0 \\ M_{ice} = M \left(\frac{A - A_{debris}}{A} \right) + M \left(\frac{A_{debris}}{A} \right) f_{debris} & \text{if } d_{snow} = 0 \end{cases} \quad (16)$$

where M is the melt production (see Sect. 2.4), W_{snow} is the water outflow from the saturated snowpack, w_{snow} the liquid snow store, η_s the water holding capacity of the snowpack, f_{debris} the melt-reduction factor from debris, A_{debris} the debris covered area and d_{snow} the snow depth.

3 Model setup and calibration

3.1 Mass balance model

We used the 1967/68–2006/07 period to calibrate the mass balance model, as this time frame holds both specific (elevation-dependent) and mean specific (glacier-wide) surface mass balance measurements (WGMS, 2018). Accordingly, 3-hourly temperature and precipitation data of the corresponding period were used from the Terskol weather station. For geometric data that serve as input for solar geometry calculations, we use laterally averaged values for slope and aspect, calculated by averaging all intra-glacier values along a line perpendicular to the flow line. Surface elevations were directly extracted from a DEM for 2009/10 AD conditions. We hereby take into account the same spatial spacing of 10 m that is used in the flow model. Afterwards, geometric input data were smoothed using a window size of ± 100 m around every grid point. Calibration of the mass balance model further assumes the geometry (slope, aspect, glacier length and surface area) to be fixed over [the 1967/68–2006/07 period](#) ~~this time period~~, whereas in fact length and surface area decreased by 113 m and 0.346 km² respectively.

For the accumulation part, the ~~precipitation enhancement factor f_e and the vertical precipitation gradient γ_p were~~ used as a tuning parameters by fitting the accumulation profile of the glacier. In literature, ~~horizontal precipitation enhancement factors varying between 1.2 and 1.7 have been proposed between Terskol and the Adylsu Valley to account for horizontal precipitation variation in the area, whereas several values for this vertical precipitation gradients parameter~~ have been proposed as well, varying between 0.0005 and 0.0046 m yr⁻¹ w.e. m⁻¹ (e.g. Boyarsky, 1978; Hagg et al., 2010; Giesen and Oerlemans, 2012; WGMS, 2018; ~~Rybak et al., 2018~~). To ensure successful calibration, a ~~precipitation enhancement factor of 1.5 between Terskol and the Adylsu Valley was found to be sufficient, whereas a~~ precipitation gradient of 0.0023 m w.e. yr⁻¹ w.e. m⁻¹ was derived to extract these data over the entire glacier surface. At last, the snow redistribution factor f_{red} was used for curve fitting of the accumulation profile, as discussed before.

Concerning ablation, three variables were chosen as tuning parameters. Due to lack of field data concerning the water holding capacity of snow η_s , it was used to calibrate the ablation in the accumulation area. Additionally, the intercept of the air temperature-dependent fluxes c_0 was chosen as a second tuning parameter due to the lack of reliable and/or sufficient data below T_{break} during the observational period (Table 1). For the factor H_{debris}^* , which controls the strength of the melt-reducing effect of debris, ~~several values between 0.18 and ± 0.60 m have already been proposed for Djankuat Glacier (e.g. Bozhinskiy et al., 1986; Popovnin and Rozova, 2002; Lambrecht et al., 2011).~~ ~~According to Rybak (2018), on the other hand, melt reduction factors f_{debris} around 0.35–0.45 are modelled near the terminus, implying a value for H_{debris}^* of ca. 0.95–1.25 m.~~ Due to the large uncertainty regarding this factor, it was used as a third tuning parameter, this time for the lower elevation areas. Here, a value of 1.15 m was found to exhibit the best fit with the observations. We acknowledge that this value implies that the gradient of the exponential decay in Eq. 14 is somewhat out of range with respect to earlier studies for other glaciers (e.g. Anderson and Anderson, 2016). This rather atypical value can however be linked to the relatively high thermal conductivity of the granite-type debris cover on the glacier (2.8 W m⁻¹ °C⁻¹) and the high debris cover porosity (0.43 for Djankuat Glacier, Bozhinskiy et al., 1986). Also the relatively low water saturation and large particle size, as suggested by Lambrecht et al. (2011), may imply that heat conduction towards the debris-ice interface seems to occur efficiently on the Djankuat Glacier. ~~Additionally, the intercept of the air temperature-dependent fluxes c_0 was chosen as a second a tuning parameter due to the lack of reliable and/or sufficient data below T_{break} during the observational period (Table 1).~~

With the calibrated surface energy balance model, the multiyear mean mass balance profile of the Djankuat Glacier during the 1967/68–2006/07 period is successfully reproduced, as the calculated mass balance vs. elevation profile matches nicely with ~~its observed counterpart~~ the observations (Fig. 4). This profile ~~nicely~~ reflects the ~~determinative~~ determining processes affecting the Djankuat Glacier's mass balance: in the higher elevations, snow redistribution by wind/avalanches and meltwater retention are important factors, whereas in the lower areas, the presence of a supraglacial debris cover reduces the glacier's runoff volume significantly and hence dampens the mass balance gradient. Modelled mean specific balances of the Djankuat Glacier show a moderate agreement with observed values since 1967/68 AD ($R^2 = 0.52$). The RMSE of the

360 individual local annual mass balances and the multiyear mean mass balance-elevation profile was reduced to 0.61 m ~~w.e.~~yr⁻¹
w.e. m⁻¹ (R² = 0.91) and 0.18 m ~~w.e.~~yr⁻¹ w.e. m⁻¹ (R² = 0.99) respectively (Fig. 4).

365 As a remark, it must be noted that the calibration dataset for the mass balance model is quite long (39 years from 1967/68 to 2006/07 AD), making it credible to assume that the parameters calibrated to this period have some validity for past and future conditions as well. Apart from the high-elevation areas, where data availability is limited and snow redistribution processes create complex conditions (> 3600 m, of which the areal fraction is only ca. 3 % of the glacier area in 2010 AD), it can be expected that the environmental setting within the calibration window also holds for periods prior to and after the observational period. It must furthermore be noted that there are only few independent data to validate our model results with a sufficient degree of certainty.

3.2 Debris cover model

370 For the debris model calibration, we matched the temporal evolution of the average debris thickness at the front (i.e. the first 30 grid points) as well as the debris covered area, using t_{debris} , F_{debris}^{input} and G_A as tuning parameters. Values for the observed debris cover at different elevation bands from the survey year 1968 AD (only for debris area) as well as for 1983, 1994 and 2010 AD (for both debris area and thickness) are ~~therefore~~ available from Popovnin et al. (2015). Moreover, to obtain more detailed information concerning the current debris covered area on a spatial scale, the debris cover extent was manually
375 digitized based on satellite imagery of the year 2010 (see Fig. 1).

Accordingly, the observed debris thickness evolution was found to be best reproduced by setting t_{debris} to 1958 and F_{debris}^{input} to 1.60 m yr⁻¹ (Table 1). At last, a power relation (R² = 0.85) was found between the growth factor G_A and the modelled mean debris thickness at the glacier front as obtained in the previous step:

$$G_A = 1.17048 * (H_{debris}^{front})^{0.62047} \quad (17)$$

380 Where H_{debris}^{front} is the modelled debris thickness at the front (i.e. the first 30 grid points) as obtained before. As such, the RMSE between modelled and observed values between 1967/68 and 2009/10 AD was reduced to 0.07 m (R² = 0.83) for debris thickness at the front and 0.9 % (R² = 0.95) for the fractional debris-covered area respectively (Fig. 5).

3.3 Ice dynamics model

385 To calibrate the flow model, it was initially run from zero ice thickness until a steady state situation was reached, which is achieved when the glacier has less than 0.002 % change in its total volume per year. The steady state situation of the ice flow model was then tested by comparing the ice flux with the integrated upstream mass balance, by ensuring that the integrated surface mass balance over the entire glacier approaches 0 to within an acceptable accuracy (0.006 m yr⁻¹ w.e.), and by calculating the volume change with time. As expected for the model setup, all results exhibited an appropriate steady state situation for the glacier. The parameters ~~To calibrate the flow model, the parameters~~ f_a and f_s were adopted to minimize the

390 RMSE between observed and modelled ice thickness for 2009/10 AD conditions, ~~hereby~~ assuming a steady state. Geometric
input data for the flow model were ~~therefore~~ extracted from a DEM for 2009/10 AD conditions. Hence, bedrock elevation
was derived in combination with ice thickness maps from Pastukhov (2011) and Lavrentiev et al. (2014). ~~Surface-Glacier~~
~~surface~~ width was extracted by measuring the intra-glacier distance of 10-m spaced lines perpendicular to the orientation of
the flow line. After extracting the lateral valley slopes, the width at the bed was calculated, ~~where~~ assuming a trapezoidal
395 valley shape ~~was assumed~~ (e.g. Oerlemans, 1992; Gantayat et al., 2017). All data were finally joined to the closest point on
the flow line for every 10 m and smoothed with a window of ± 100 m around every grid point. For the Djankuat Glacier, the
best fit was found for $f_d = 6.5 \times 10^{-17} \text{ Pa}^{-3} \text{ yr}^{-1}$ and $f_s = 3.25 \times 10^{-13} \text{ Pa}^{-3} \text{ m}^2 \text{ yr}^{-1}$ (Table 1). Additionally, the bed width for
the assumed trapezoidal-shaped cross section was slightly adjusted to ensure that the parameterization fits the observed area-
elevation distribution for a total surface area of 2.688 km². ~~the area-elevation distribution and the total surface area of 2.688~~
400 ~~km² fit well with observed values.~~ The full set of parameter values used in the model is given in Table 1.

The flow model for the Djankuat Glacier was able to produce a steady state glacier profile with a length of 3.26 km after 200
years (Fig. 6). The model approaches the observed ice thickness as it minimizes the RMSE to 14.27 m ($R^2 = 0.90$). Despite
minimized RMSE, the mismatch near the snout and steep slopes near the Djantugan peak increase the error of the model.
However, it is argued that a significant part of the error reflects either the current non-steady state situation of the glacier and
405 the presence of a supraglacial debris cover at the front, or the lack of reliable and direct ice thickness observations at the
highest elevations of the glacier. As with the mass balance and debris cover model, there are no, or only few, independent
data to validate our model results with a sufficient degree of certainty.

Modelled current surface velocity for the Djankuat Glacier goes up to 79.7 m yr⁻¹ near the ice falls of the Djantugan Plateau
and also peak in the middle section of the glacier, which fits well with observations of maximum velocities in the 60–80 m
410 yr⁻¹ range (Aleynikov et al., 1999; Pastukhov, 2011). Moreover, the modelled deformational and basal sliding components
comprise respectively 45 % and 55 % of the vertically averaged ice flow velocity along the flow line.

4 Basic sensitivity experiments

With the calibrated submodels, some basic sensitivity tests were conducted with the flow model which all initially started
from a steady state glacier resembling the present-day geometry. Perturbed mass balance profiles (in steps of 0.25 m yr⁻¹
415 w.e.) were subsequently used as forcing into the flow model, until a new steady state was reached. As such, a relationship
with a slight deviation from linear was found between the steady state length and the mass balance perturbations, exhibiting
a value for of ca. 1100 and 1355 m (m yr⁻¹ w.e.)⁻¹ for negative and positive perturbations respectively (Fig. 7a). On the other
hand, the e-folding length response time (i.e. the time needed to achieve $1 - e^{-1}$ or ~63% of the total length change) of
Djankuat is in the order of 31 ± 3 years. Additional sensitivity experiments ~~with show that~~ the mass balance model show that
420 ~~of~~ the Djankuat Glacier, when its 2010 AD geometry and other parameters are considered fixed, is quite sensitive to both
temperature ($-0.70 \text{ m yr}^{-1} \text{ w.e. } ^\circ\text{C}^{-1}$) and precipitation changes ($+0.20 \text{ m yr}^{-1} \text{ w.e. } 10 \text{ \%}^{-1}$). As such, a 1 °C annual

temperature change for the Djankuat Glacier is only compensated when the precipitation change is in the order of ca. 35 %, ~~although mass~~ Mass balance sensitivity to temperature changes shows a non-linear ~~behaviour~~ behavior, whereas the relationship is linear for precipitation changes (Fig. 7b). ~~Also mass balance sensitivity to atmospheric transmissivity and albedo (combined for snow and ice) is large, as these values are calculated to $-0.25 \text{ m yr}^{-1} \text{ w.e. } (0.05)^{-1}$ and $+0.57 \text{ m yr}^{-1} \text{ w.e. } (0.05)^{-1}$ respectively. The latter shows a slightly non-linear trend, where sensitivity changes more drastically for negative mass balances compared to positive values. Forcing the flow model with a mass balance profile in the case of debris free conditions shows that the steady state glacier length would be 310 m (ca. 10 %) smaller than current values, at 2940 m.~~

~~Epecially in the 2700–2800 m ASL zone, reduction of runoff related to supraglacial debris increased significantly, as annual values rise from ca. 3 % reduction before the 1970s to ca. 40 % by 2009/10 AD. By 2010 AD, the debris-related melt reduction factor f_{debris} has decreased towards ca. 0.45 in this area, while fractional debris covered area increased to nearly 100 %. In the 2800–2900 m ASL zone, runoff reduction increased from ca. 1 % to ca. 17 %, while in the 2900–3000 m ASL zone values increased from ca. 0.5 % to 7 % reduction during that same period. The glacier-wide runoff was not affected significantly before the 1970s ($< 1 \%$) but was reduced by ca. 9 % around 2009/10 AD geometry (glacier-wide annual runoff volume decreases from ca. 3.81 to ca. 3.42 million m^3 around 2009/10 AD) when compared to debris free conditions with identical glacier. As such, the presence of supraglacial debris causes the local mass balance of the Djankuat Glacier to be ca. 23 %, 9 % and 4 % higher, on average over the calibration period, in the 2700–2800, 2800–2900 and 2900–3000 m ASL zones respectively. The effect is, however, not significantly pronounced further up glacier.~~

~~Response times seems to be slightly shorter for negative perturbations, which can be related to the steeper upslope terrain, increasing mass balance gradient in a warming climate and a smaller glacier size (Oerlemans, 2001). Sensitivity of steady state glacier length to temperature changes is modelled to be $815 \text{ m } ^\circ\text{C}^{-1}$, while for precipitation the corresponding value is $250 \text{ m } 10 \%^{-1}$. For atmospheric transmissivity and surface albedo, the steady state length sensitivity comprises values of $300 \text{ m } (0.05)^{-1}$ and $650 \text{ m } (0.05)^{-1}$.~~

To assess the climate and glacier sensitivity for equilibrium conditions, mass balance profiles were furthermore altered by temperature and precipitation perturbations within the -3 to $+3 \text{ } ^\circ\text{C}$ and -25% to $+25 \%$ range respectively (as compared to the 1967/68–2006/07 AD reference values). Sensitivity of steady state length to temperature changes was found to exhibit a linear behaviour ($815 \text{ m } ^\circ\text{C}^{-1}$) for perturbations between -1.4 and $+0.7 \text{ } ^\circ\text{C}$, but is modelled to vary between 400 and $1400 \text{ m } ^\circ\text{C}^{-1}$ when assessed over the entire range (Fig. 7c). The glacier sensitivity depends largely upon geometry and increases (decreases) for more negative (positive) mass balance perturbations, predominantly due to the flatter (steeper) terrain. The sensitivity also peaks around a temperature perturbation of $+1 \text{ } ^\circ\text{C}$, i.e. when the glacier front is positioned at the transition between the broad accumulation area and the narrower snout (ca. $x = 2300 \text{ m}$ on the flow line). Also, the non-linear nature of the temperature-mass balance relationship (Fig. 7b) triggers a deviation from linear behaviour. Consequently, the change in forcing needed for a retreat from 2 to 1 km is nearly twice as large as for a retreat from 4 to 3 km. For precipitation the sensitivity is more or less constant for a value of $250 \text{ m } 10 \%^{-1}$ (Fig. 7d). A temperature increase of $+3.4 \text{ } ^\circ\text{C}$

455 compared to the 1967/68–2006/07 [AD](#) Terskol mean of +2.5 °C is sufficient to cause a total drawdown of the glacier, as the last ice on the Djantugan Plateau melts away 470 years after the induced perturbation.

5 Past reconstruction of the Djankuat Glacier

5.1 LIA extent of the glacier

460 All three submodels (ice flow, mass balance and debris cover) are finally coupled to determine the past and future evolution of the Djankuat Glacier. Here, the mass balance model and debris cover model calculate annual surface mass balance profiles, which are then used as input for the continuity equation in the ice flow model ~~but converted~~[after conversion](#) to ice equivalents. Glacier length L is ~~hereby~~ calculated by ~~counting-multiplying up all~~[the number of](#) non-zero ice thickness grid points ~~multiplied~~ by Δx . L is thus not necessarily equal to the glacier terminus position, [as the glacier may disintegrate in several sections during retreat](#). As a first step, the model is initialized with a spin up run in which a steady state glacier, as 465 well as a steady state debris cover, are produced for the balance year 1752/53 AD. Although we have no clear indication to suspect steady state behaviour at this time due to lack of reliable [data on](#) debris cover, mass balance and length change, it was imposed to start the simulations without unwanted ~~transient model drift~~[behavior](#) at the initial stage.

~~Hence, we choose~~[We chose](#) to let the glacier grow until the length indicated by the end moraine of the 19th century (4.62 km), ~~which has been~~[as](#) determined by lichenometric dating in the paleovalley (Boyarsky, 1978; Zolotarev, 1998; Petrakov et al., 2012), ~~see-cf.~~ Fig. 1. To obtain a steady state glacier [with the ice flow model](#), the multiyear mean mass balance profile for the 1967/68–2006/07 [AD](#) climate had to be ~~perturbated~~[increased with](#) ~~by~~ an additional ~~AB~~[mass balance perturbation](#) of +1.12 m yr⁻¹ w.e., corresponding to an ELA lowering of 113 m. The steady state situation ~~of the model~~ was then tested [and verified as before \(Sect 2.3\)](#). ~~by comparing the ice flux with the integrated upstream mass balance, by ensuring that the integrated surface mass balance over the entire glacier approaches 0 to within an acceptable accuracy 0.006 m yr⁻¹ w.e., and by calculating the volume change with time. As expected for the model setup, all results exhibited an appropriate steady state situation for the glacier.~~ It can be noted that modelled ice thickness around the maximum extent of the glacier in the considered model period went up to 173.4 m in the valley. Additionally, surface velocities were as high as 101.7 m yr⁻¹ near the ice falls of the Djantugan Plateau and up to 98.1 m yr⁻¹ in the valley downstream (Fig. 6d).

[We furthermore chose to include a supraglacial debris cover in the initialization procedure. A](#) However, ~~as can be deduced from the large lateral moraines in the Adylsu Valley (Fig. 1), the Djankuat Glacier used to export most of its debris to the margins rapidly in the historic period, rather than developing a supraglacial debris cover. Furthermore, debris sources from surrounding topography and melt-out processes were likely less widespread in the historic period because the colder climate (i.e. the current exposed slopes were covered by the glacier itself and were more stable). Also, the fast-flowing nature of the paleo-glacier tongue in the valley (up to 100 m yr⁻¹ around 1752 AD, Fig. 6d) disfavors the accumulation of thick debris on~~ 485 [the glacier surface. For this reason, supraglacial debris is believed to have been much less widespread prior to the observational period of 1967/68 AD, implying that the glacier was not very much influenced by debris cover in the historic](#)

period. ~~However~~ Nevertheless, there is also indirect evidence for at least some supraglacial debris in the historic period from the presence of moraines in the valley (Fig. 1) and a photograph taken around 1930 showing some debris patches on the snout (Aleynikov et al., 2002b). It would be furthermore unrealistic to only introduce a debris cover in the model once the model approaches the start of the observations. This would contradict the presence of moraines and the observation that there already was an expanding debris cover during the first data collection in 1967/68 AD (Popovnin et al., 2015). Because there is no direct evidence for the origin of the debris cover, it was chosen to include melt-out processes in the model initialization, which implies that debris mass fluxes from surrounding topography are not incorporated in the initialization procedure (i.e. $F_{debris}^{input} = 0 \text{ m yr}^{-1}$ and $C_{debris} = 1.05 \text{ kg m}^{-3}$). With these values, the LIA steady state debris cover had a thickness of 0.64 m at the front and occupied a fractional area of ca. 8 % (ca. 0.331 km² of the 1752 AD glacier).

~~It can be noted that modelled ice thickness around the maximum extent of the glacier in the considered model period went up to 173.4 m in the valley. Additionally, surface velocities were as high as 101.7 m yr⁻¹ near the ice falls of the Djantugan Plateau and up to 98.1 m yr⁻¹ in the valley downstream (Fig. 6d).~~

5.2 Evolution of the glacier from 1752 AD to present

To force the model in the historic period, climatic data at 3-hourly intervals were ~~are~~ needed. Historic climatic datasets for Terskol weather station were therefore constructed using a multiproxy approach, ~~hence including using~~ information from various weather stations in the area, ~~including such as~~ Mestia, Pyatigorsk 365 (approximately 100 km northeast from the glacier at 512 m elevation) and Mineralnye Vody (approximately 115 km northeast from the glacier at 321 m elevation). Additionally, historic data from the CRUTEM4 and CRU TS datasets, as well as from tree ring reconstructions for the broader Caucasus area, were used for the remaining uncovered data gaps since 1752 AD (D'Arrigo et al., 2001; Toucham et al., 2003; Akkemik et al., 2005; Akkemik and Aras, 2005; Griggs et al., 2007; Köse et al., 2011; Jones et al., 2012; Harris et al., 2014; Holobacă et al., 2015; Martin-Benito et al., 2016; Dolgova, 2016). ~~At first, data from for from the pre-observational period outside the Terskol time series (1977–2013 with a data gap between 1990–1997) were averaged on a yearly basis over all the available datasets, both for precipitation and temperature. Next, mean monthly temperatures and precipitation amounts were derived by matching the mean and standard deviation of the overlapping parts of the obtained dataset with those from Terskol weather station (Table 2). Data from the pre-observational period outside the Terskol time series were therefore averaged over all the available datasets to create a multiproxy mean time series, for which mean monthly temperatures and total precipitation amounts were derived by matching the mean (corrected additively for temperature and multiplicatively for precipitation) and standard deviation of the overlapping part in the observed Terskol dataset (Table 2, e.g. Huss and Hock, 2015; Zekollari et al., 2019).~~ To obtain a record with a 3-hourly temporal resolution, the data sequence for Terskol over which measurements with a 3-hourly interval are available (~~1977–2013 with a data gap between 1990–1997~~) is repeated into the past and future in order to maintain intra-daily and intra-annual variability in the data. These data were afterwards corrected for the monthly mean temperature and precipitation amounts obtained in the

previous step (Table 2). The reconstruction of temperature and precipitation clearly indicates a shift in the climatic conditions after 1752 AD. ~~Especially during the last two decades, an accelerated warming trend has occurred, as temperatures have been increasing at an unprecedented rate. For temperature, a clear sequence of colder and warmer intervals can be seen, as clearly colder periods in the dataset are noticeable around the 1770–80s, 1830–40s, 1860s, 1880s, late 1890s into the early 1900s, late 1910s, early 1930s, early 1940s and during the 1970–80s AD. Warmer intervals, on the other hand, have occurred during the 1750–60s, 1790–1800s, 1820s, 1850s, 1870s, early 1890s, 1920s, late 1930s, 1950–60s and during the last two decades. The latest 30-year mean climatic interval of 1988–2017 exhibits a mean annual temperature anomaly of +0.72 °C compared to the 1961–1990 mean, making it the warmest period in the whole time series. Wetter periods have occurred during the early 1850s, 1870–80s, late 1890s into the early 1900s, late 1910s and early 1920s, late 1930s into early 1940s and early 2000s. Drier periods were present during the 1860s, early 1890s, late 1900s into the early 1910s, late 1920s, late 1940s and 1990s (Fig. 10).~~ Especially during the last few decades, an accelerated warming trend has occurred, as the latest 10-year climatic interval exhibits a mean annual temperature anomaly of +0.5°C compared to the 1981–2010 mean. This makes it the warmest period in the reconstructed time series. For temperature, a clear sequence of colder and warmer intervals can be seen. Changes in precipitation show a sequence of drier and wetter periods (Fig. 8).

After using the steady state glacier of 1752/53 AD as an initial input feature for the time-dependent model, dynamic calibration is applied by ~~iteratively adding additional mass balance perturbations to the obtained mass balance profile that was simulated with the climatic input, until the reconstructed glacier length matched with the observed values over the years (e.g. Oerlemans, 1997; Zekollari et al., 2014).~~ incorporating artificial mass balance perturbations (Δb_a) into the model. This factor was not explicitly calculated but was instead derived and adjusted iteratively by a trial and error procedure. The obtained perturbations were then superimposed on the mass balance profile that was simulated with the climatic input, until the reconstructed glacier length sufficiently matched with the observed values (e.g. Oerlemans, 1997; Zekollari et al., 2014):

$$b_{a(x,t)} = b_{a(x,t)}^{SMB} + \Delta b_{(t)} \quad (18)$$

Here, $b_{a(x,t)}^{SMB}$ is the local surface mass balance simulated with the climatic datasets and $\Delta b_{(t)}$ is the artificial mass balance perturbation that was applied in the dynamic calibration procedure. Such a procedure is needed to counteract imperfections in the flow model, mass balance model and the climate forcing. The added value of this procedure is to ensure a current glacier state that matches the observed one, as the glacier is still responding to changes in past climate, geometry and dynamics. The ~~dynamic calibration~~ procedure required a maximum additional mass balance perturbation of +0.5 m w.e.-yr⁻¹ w.e. but which varies over time (Fig. 9b). Nevertheless, since the balance year 1967/68 AD, i.e. the year from which the mass balance model was calibrated, no additional perturbations were needed. It can thus be stated that the model performs well when forced with the observed Terskol climatic data, and that credibility can be assigned to the dynamic calibration procedure. ~~and underwent a successful validation to within acceptable accuracy.~~ It furthermore implies that future projections are no longer influenced by the corresponding artificial mass balance corrections, keeping in mind an e-folding length response time of ca. 31 years for the Djankuat Glacier (see Sect. 4).

The resulting mass balance series shows clear peaks around the 1870–80s, early 1900s, late 1910s, 1940s, 1970s and early 2000s AD, hereby coinciding with slightly colder and/or wetter periods in the climatic datasets (Fig. 449c). Clear minima in the mass balance series can be noted in the 1860s, 1890s, early 1910s, 1920s, late 1940s and in the 21st century, which agrees fairly well with earlier mass balance reconstructions of Djankuat (Dyurgerov and Popovnin, 1988; Fyodorov and Zalikhanov, 2018) and Garabashi glaciers on the Elbrus massif (Rototaeva et al., 2003; Dolgova et al., 2013). As the Djankuat Glacier reacted to these climatic perturbations, an almost continuous retreat since the 1850s AD ~~has been pursued~~had occurred, exhibiting some minor readvances or steady states as well. As was already discussed earlier, the past behaviour of the Djankuat Glacier is in line with the general observed trend for other Caucasian glaciers (Fig. 2). During the last several decades, however, the addition of a thickening layer of supraglacial debris on the snout aided to temporarily postpone rapid retreat and more or less maintain steady state conditions. Still, the glacier has lost a total length of 1.39 km at present-day compared to the start of the reconstruction in 1752 AD (-29.4 %). The reconstruction also shows that the total glacier area around 1752 AD ~~was about 54 % larger~~by 35.2 % when compared to the 2009/10 AD situation, ~~with~~ (an area of 4.147 against 2.688 km², see Figs. 6 and 449a). Moreover, evolution of glacier surface area matches nicely with observed values except for the outlier around 1983, which has to do with a migrating ice divide on the Djantugan Plateau (Fig. 449a).

A historic model run conducted with a 100 % clean-ice glacier, shown as an inset in Fig. 9a, revealed that debris played only a minor role prior to ca. 1980 AD, with length differences of only 20 to 40 m. By 2010 AD, however, the modelled length difference between a debris-free and debris-covered glacier already increased to 160 m (Fig. 9a).

6 Future glacier evolution to 2100 AD

6.1 Response to future climate forcing

~~Future projections of temperature and precipitation (2019–2100 AD) were obtained by using output of the CMIP5 simulations for the country of Georgia under 4 different RCP scenarios (Alder and Hostetler, 2013). Hence, to force the model into the future, we use the RCP 2.6, RCP 4.5, RCP 6.0 and RCP 8.5 scenarios. As such, mean temperature and precipitation were changed linearly on a yearly basis, until the 2071–2095 AD mean values matched the CMIP5 simulation output for the different scenarios. All scenarios exhibit a further increase of the mean annual temperature, as well as a decreasing precipitation amount compared to the reference climate (Table 3). The most extreme changes, however, exist in the RCP 8.5 scenario, as Terskol mean annual temperatures increase to +7.1 °C by 2071–2095 AD. Additionally, also a future projection will be made under a no change scenario, in which the current climate (2007–2016 AD) is repeated with respect to its mean until 2100 AD.~~

Future projections of temperature and precipitation were obtained by a multi-model approach, using output from the Coupled Model Intercomparison Project Phase 5 (CMIP5) simulations (Taylor et al., 2012) for the grid cell closest to the Djankuat Glacier. Mean temperature and total precipitation amount at monthly resolution from 21 Global Circulation Models (GCMs) for the RCP 2.6, RCP 4.5, RCP 6.0 and RCP 8.5 scenarios were used, based upon their availability (Table 2 and 3). The data

were downloaded for both historical runs (from 1981 AD) and for projections (until 2100 AD). Although the choice of ensemble member can largely influence the eventual results (e.g. Huss and Hock, 2015), we solely focus on the first realization, i.e. ensemble member r1i1p1. As with the historic climate datasets, climate data were scaled to match the mean and standard deviation of the Terskol meteorological station. Absolute GCM data were therefore at first scaled to anomalies with respect to the 1981–2010 reference values for each respective model, so that additive (temperature) and multiplicative (precipitation) biases could be removed when matching to the past forcing. For each RCP, the monthly temperature and precipitation data were then averaged over all models, resulting in a multi-model mean time series. To account for year-to-year variability, the CMIP5 data were at last rescaled with respect to the standard deviation of the overlapping period for the observed Terskol data (e.g. Huss and Hock, 2015; Zekollari et al., 2019). As with the past, the observed 3-hourly Terskol data sequence was finally used to downscale the monthly data to the temporal resolution that suits the mass balance model.

Concerning debris cover evolution, the debris input location x_{debris} and flux magnitude F_{debris}^{input} were left unchanged. Consequently, once the contribution from x_{debris} stops, either due to shrinkage of the surface width or rapid retreat beyond the input location, no additional debris source is released. Hence, only melt out from debris-loaded ice and supraglacial debris advection contribute to the evolution of the supraglacial debris cover. Later on, we ~~have will~~, however, conducted several experiments to determine the impact of potential additional debris sources from the surrounding topography on the future glacier evolution (Sect. 6.27).

All scenarios exhibit a further increase of the temperature, which is most pronounced in the summer season. Projected precipitation, on the other hand, shows slightly decreasing values at annual resolution, but shows a tendency for a drier summer half year (April to September, AMJJAS) and a wetter winter half year (October to March, ONDJFM). By 2071–2100 AD, the mean AMJJAS temperature (total ONDJFM precipitation) anomalies with respect to the 1981–2010 period are +1.4°C (+0.1 %), +2.3°C (+3.7 %), +2.7°C, (+11.2 %) and +4.5°C (+11.7 %) for the RCP 2.6, RCP 4.5, RCP 6.0 and RCP 8.5 scenarios respectively (Figs. 10a and b). Additionally, also a future projection is made under a no change scenario, in which the last observed 10-year climatic interval (2009–2018 AD) is repeated with respect to its mean (corresponding to a AMJJAS mean temperature and a total ONDJFM precipitation amount anomaly of +0.5 °C and -11.0 % mm yr⁻¹ w.e. respectively).

All future scenarios agree to a rapid decline of the glacier length and surface area in the following decade, as a response to the significant warming since the late 1990s AD. ~~The experiments also show that, even for the no change scenario, the glacier will shrink drastically. By 2100 AD, the total length and surface area of the glacier are projected to be 1640 m (-50 %) and 1.275 km² (-53 %), whereas the glacier front will be positioned at an elevation of 3131 m in that scenario. It is thus clear that, at present day, the Djankuat Glacier is not in equilibrium with the current climatic conditions and hence will strive towards a new steady state with a much smaller surface area in the future. For the RCP 2.6, 4.5, 6.0 and 8.5 scenarios, the total glacier length further decreases to 1250 m (-62 %), 1020 m (-69 %), 930 m (-72 %) and 680 m (-79 %) by 2100 AD respectively. Meanwhile, total glacier surface area decreases to 0.760 km² (-72 %), 0.423 km² (-84 %), 0.372 km² (-86 %)~~

620 ~~and 0.139 km² (-95 %) by 2100 AD respectively (Fig. 12).~~ By 2100 AD in the no change scenario, the total length and surface area of the glacier are projected to be 2370 m (-29.3 %) and 2.01 km² (-27.3 %), whereas the glacier front will be positioned at an elevation of 2844 m. It is thus clear that, at present day, the Djankuat Glacier is not in equilibrium with the current climatic conditions and hence will strive towards a new steady state with a much smaller surface area in the future. For the RCP 2.6, 4.5, 6.0 and 8.5 scenarios, the total glacier length further decreases to 1560 m (-52.2 %), 1250 m (-61.7 %), 1070 m (-67.2 %) and 510 m (-84.4 %) by 2100 AD respectively. Meanwhile, total glacier surface area decreases to 1.17 km² (-56.5 %), 0.71 km² (-73.6 %), 0.49 km² (-81.8 %) and 0.20 km² (-92.6 %) by 2100 AD respectively (Fig. 11a and b). As such, for the RCP 6.0 and 8.5 scenarios, the glacier retreats back as far as into the bedrock depression of the Djantugan Plateau.

630 With respect to total runoff volume changes and water resources management, the Djankuat Glacier ~~has already surpassed~~ is close to surpassing its peak water discharge point, as the modelled annual glacier runoff ~~has reached~~ reaches its maximum around ~~2010-2020~~ AD (Fig. ~~13~~11c). Hence, all RCP scenarios exhibit a further decline of the produced runoff volume into the future, which is in accordance with earlier work for this area (Huss ~~&-and~~ Hock, 2018; ~~SROCC~~Hock et al., 2019). The actual course of runoff changes, however, is dependent upon the trade-off between remaining glacier surface area and magnitude of melt. As such, the RCP 8.5 scenario initially produces the highest melt and corresponding runoff volume. Later on, however, the ‘no change’ scenario yields the highest runoff volumes due to the larger remaining glaciated area. It must also be noted that near the end of the modelling period, runoff volume ~~increases again~~ temporarily stabilizes for the RCP 6.0 and RCP 8.5 scenarios. This process is related to the melting of the ice on the Djantugan Plateau, which then reinforces itself due to the mass balance-elevation feedback.

640 However, even under the most extreme RCP 8.5 scenario, the glacier would not completely disappear by the end of the modelling period. Despite accelerated melting of the high-elevation plateau because of the mass balance-elevation feedback, a decreased climate sensitivity due to the steeper laterally averaged slopes in the upper glacier part, as well as the large ice thickness on the Djantugan Plateau (up to 200 m at present-day), prevent a complete disappearance by the end of the modelling period. It must furthermore be noted that the averaging of the future climatic data implies a reduction of spread. When, for example, the model was forced with the highest warming scenario of all CMIP5 models (i.e. the RCP 8.5 scenario of the GFDL-CM3 model, with mean AMJJAS temperature increase of +7.9°C by 2071–2100 AD), the glacier will cease to exist by 2086 AD.

7-6.2 Impact of supraglacial debris cover on glacier evolution

645 Despite present-day areas of visible clean ice on the tongue, a relatively steep slope below the ELA, relatively high ice velocities and a short response time, observations also show that the supraglacial debris cover on the Djankuat Glacier has significantly affected glacier geometry during the last several decades, as evident from the differential retreat of the snout (Figs. 1 and 9a). Its importance for this specific glacier has also been demonstrated by e.g. Rezepkin and Popovnin (2018),

who showed that the debris cover is believed to drastically affect the Djankuat Glacier in terms of its geometry and melting patterns. Debris input onto the Djankuat Glacier's surface due to mass fluxes from surrounding topography are furthermore expected to increase even further in the future (Popovnin et al., 2015; Rezepkin and Popovnin, 2018). To determine the potential effect of these additional debris sources onto the glacier surface, we ~~executed some~~performed additional experiments with varying debris input location, debris input magnitude and time of the release of the debris source from the surrounding topography. We repeated the procedure used in Sect. 2.5, but indicated a 'debris reference scenario', in which a second debris mass flux is initiated from $x_{debris} = x_{ELA} - 1000$ m at $t_{debris} = 2035$ with a magnitude of $F_{debris}^{input} = 1.5$ m yr⁻¹. For x_{ELA} , the average position of the ELA was calculated during a window of ± 15 years surrounding t_{debris} in the 'no additional debris scenario' (Sect. 6.1), which hence varies for each climatic scenario. We therefore choose to not initiate debris fluxes from positions above the ELA, due to the neglect of englacial pathways in our debris model (see Sect. 2.5). We then let one of these three variables change, while keeping the other two at their original value of the 'reference situation'. As such, the debris input location x_{debris} was changed to 1250, 1500 and 1750 m, the time of release t_{debris} to 2050, 2065 and 2080, and at last the magnitude of the debris flux F_{debris}^{input} to 2.0, 2.5 and 3.0 m yr⁻¹ (Fig. 14). As such, the debris input location x_{debris} was changed to 80 %, 60 % and 40 % of the distance between x_{ELA} and x_L (further downstream), the time of release t_{debris} to 2045, 2055 and 2065, and at last the magnitude of the debris flux F_{debris}^{input} to 0.75, 2.25 and 3.0 m yr⁻¹. It must be noted that the values of these parameters are arbitrary, as the exact location, time and magnitude of future debris sources cannot be predicted. By assessing a range of possible values for each of these parameters, we encompass various potential future scenarios in order to account for the high uncertainty regarding these parameters. Figure 12 shows the impact of these variables (rows) on the future length of the Djankuat Glacier under different climatic scenarios (columns). The black lines indicate the scenario where no additional debris source is released in the future. The other lines are for experiments that include an additional future debris source from the surrounding topography for varying values of the earlier mentioned debris-related parameters. It is clear that the addition of an increasingly widespread debris cover dampens glacier retreat. It should however be noted that the effects on glacier length are not immediate, as it takes some time for the debris to be advected to the terminus after its initiation at time t_{debris} .

The effect of the timing of the source release is straightforward: the earlier the debris mass flux is released, the larger the extension of the glacier by the year 2100 AD, as the melt-reducing effect starts earlier in time. The main decisive factor here is the efficient debris advection towards the terminus, because flow velocities are larger in 2035 AD compared to 2050, 2065 and 2080 AD (Fig. 12). The magnitude of the debris input flux F_{debris}^{input} is another crucial parameter determining the length extension of the Djankuat Glacier in the future period. It is, hence, obvious that a higher flux magnitude will contribute more efficiently to a higher debris growth rate. This enhanced effect is a direct consequence of the implementation of Eq. (14), where the debris-related melt reduction depends on the debris thickness (Fig. 12). Concerning the debris input location, results suggest that the closer the input source is located to the terminus, the longer the extension of the glacier will be compared to the situation without an additional debris source. This makes sense, as the time that it takes for the supraglacial

debris to be advected to the front is shorter for down-glacier input locations. Hence, the debris cover will be able to apply its melt-reducing effect much earlier in time, as well as much further down-glacier in space on a still relatively long glacier. Again, the effects on glacier length are not immediate, as it takes some time for the debris to be advected to the terminus.

685 The effect of climatic conditions on debris-related melt reduction and its impact on glacier geometry is twofold. Initially, the melt-reducing effect increases with higher temperature, as can be seen in the case of the no change, RCP 2.6 and RCP 4.5 scenarios. This can be related to the fact that a higher temperature will increase the melt-out of material from debris-loaded ice, whereas also decreased flow velocities prevent sufficient discharge and allow the debris to thicken quickly up-glacier (Fig. 12). Moreover, the distances between the input point and the glacier front at the time of source release decrease with
690 increasing temperature, whereas also retreat rates are relatively larger for higher temperatures. This allows the relatively thick debris to encounter the glacier front much earlier in time. At last, it is important to note that for the same melt reduction factor f_{debris} , the absolute reduction of the ablation amount will be higher when the initial value of the ablation is high. However, for the RCP 6.0 and RCP 8.5 scenarios, the impact of the supraglacial debris cover on the glacier decreases again. Here, a counteracting effect occurs as temperatures rise even further, because the risk of rapid loss of debris-covered area
695 increases. This can be related to either the breaking of the glacier into several fragments where areas of ‘dead ice’ prevent proper connectivity between the main glacier body and the glacier front, or because the front is too close to (or has already passed) the debris source by the time it is released. Finally, the accelerated shrinkage also favors foreland deposition instead of debris accumulation due to frontal retreat, as well as the loss of proper connectivity between the debris source and the main glacier body at the debris input location (Eq. 13, Fig. 12).

700 **8-7 Conclusion**

In this study, a coupled ice flow–mass balance–supraglacial debris cover model was used to simulate the response of the Djankuat Glacier to past, present and future climatic changes between 1752 and 2100 AD. We conducted, for the first time, explicit time-dependent modelling of a Caucasian glacier, including an extended and physically based subroutine related to supraglacial debris cover evolution that was not yet integrated in ~~previous glaciological~~ time-dependent numerical flow line
705 models. As it turns out, the Djankuat Glacier has been retreating almost continuously since the 1850s AD, with some minor steady states or readvances during periods with clusters of colder and/or wetter conditions. The model reconstructed the observed retreat fairly well but required additional mass balance perturbations up to a maximum of $+0.5 \text{ m yr}^{-1}$ w.e., which were applied iteratively via dynamic calibration. However, since the start of the calibration period in the balance year 1967/68 AD, no artificial mass balance perturbations were needed, ensuring proper model calibration and
710 credibility validation.

The future behaviour of the glacier is ~~Future behaviour of the glacier will be~~ determined by corresponding changes in air temperature, precipitation and supraglacial debris cover. A temperature increase of $1 \text{ }^\circ\text{C}$ can only be compensated by a precipitation increase of ca. 35 %, which is not indicated by future climatic projections in the study area. Hence, all scenarios

agree to a rapid decline during the following decade, as a response to the accelerating warming since the 1990s AD. Even
715 after considering constant present- day climatic conditions, the glacier will shrink drastically to ca. ~~50~~30 % of its current
length and surface area by 2100 AD, indicating the imbalance between the current glacier geometry and the present climate.
However, none of the future scenarios cause a total disappearance by the end of the modelling period. Nevertheless, the
glacier will retreat most drastically (ca. ~~80~~93 % of its current surface area) under the RCP 8.5 scenario, as even the thick ice
720 on the high elevations of the Djantugan Plateau will be affected by significant melting. Although the glacier ~~has already~~
~~surpassed~~is close to surpassing its peak water discharge point, the modelled temporal evolution of total runoff volumes
indicates that, in particular the melting of ice on these higher parts of the glacier in higher-temperature scenarios, ~~re-~~
~~intensifies~~temporarily stabilizes runoff near the end of the modelling period due to the mass balance-elevation feedback.

The presence of a supraglacial debris cover is shown to significantly affect glacier geometry during the modelling period.
Hence, the effect of debris-related melt reduction on the eventual glacier length by 2100 AD is dependent upon the trade-off
725 between the growth rate of the total supraglacial debris mass, the efficiency of down-glacier advection of supraglacial debris,
the glacier retreat rate, the connectivity between the debris source and the main glacier, and finally the distance between the
front and the input location at the time of source release. It turns out that debris-related effects are highest when either debris
thickness and area are large, or when melt-reducing effects start earlier in time and/or more down-glacier in space in a
relatively warm climate. However, it must be noted that for some of the conducted experiments, the addition of an extra
730 debris source did not (significantly) influence the glacier's geometry. As such, when temperatures increase even further,
potential inhibiting effects of too rapid shrinkage are to be considered. Hence, accelerated frontal retreat, disrupted debris
discharge and/or connectivity issues at the debris input location may prevent the establishment of a proper melt-reducing
effect.

735
Code availability. The model code was written in MATLAB_R2019a. [A coupled ice flow-supraglacial debris cover model for the Djankuat Glacier, that was used as the basis for this research, can be found and downloaded from: https://github.com/yoniv1/Djankuat_glacier_model.](https://github.com/yoniv1/Djankuat_glacier_model)

740 *Data availability.* The reconstructed historic and future climatic datasets for the Terskol meteo station are available from
Y.V. on request.

Author contribution. Y.V. created the climatic datasets, constructed and calibrated the numerical model, performed the
numerical simulations and wrote the manuscript. P.H. proposed the main conceptual ideas and outlines, helped design and
745 implement the research, provided guidance in interpreting the results and improved the manuscript throughout the entire

process. O.R. and V.V.P. contributed by making glacier field work possible, providing numerous datasets and improving the manuscript with their knowledge and years of experience concerning the Djankuat Glacier.

Competing interests. The authors declare that they have no conflict of interest.

750

Acknowledgements. The contribution of V.V. Popovnin and O. Rybak was supported by the Russian Foundation for Basic Research, grant RFBR No 18-05-00420a: “The latest evolutionary tendencies in water and ice resources of the glaciers in the Caucasus”. The authors furthermore like to thank all researchers [Vladimir M. Fyodorov, Olga Solomina, Dario Martin-Benito, Ekaterina Dolgova, Dimitry A. Petrakov, Iulian H. Holobăcă and Pavel A. Toropov](#), who provided their climate reconstruction data and knowledge, and hence helped to improve the quality of the historic datasets greatly. [We also thank the reviewers Loris Compagno, Ann Rowan and Fabien Maussion for their helpful comments which significantly improved the quality of the manuscript.](#)

755

References

760 Ahouissoussi, N., Neumann, J. E., Srivastava, J. P., Okan, C., and Droogers, P. (Eds.): Reducing the vulnerability of Georgia’s agricultural systems to climate change: impact assessment and adaptation options, World Bank Publications, Georgia, 116 pp., 2014.

Akkemik, Ü, Dagdeviren, N., and Aras, A.: A preliminary reconstruction (A.D. 1635–2000) of spring precipitation using oak tree rings in the western Black Sea region of Turkey, *Int. J. Biometeorol.*, 49(5), 297–302, doi: 10.1007/s00484–004–0249–8, 2005.

765

Akkemik, Ü., and Aras, A.: Reconstruction (1689–1994 AD) of April–August precipitation in the southern part of central Turkey, *Int. J. Climatol.*, 25(4), 537–548, doi: 10.1002/joc.1145, 2005.

Alder, J. R., and Hostetler, S. W.: An interactive web application for visualizing climate data, *Eos Trans. AGU*, 94(22), 197–198, doi: 10.1002/2013EO220001, 2013.

770 Aleynikov, A. A., Zolotarev, E. A., and Popovnin, V. V.: The velocity field of Djankuat Glacier [Поле скоростей ледника Джанкуат], *Data of Glaciological Studies*, 87(1), 169–176, 1999 [in Russian].

[Aleynikov, A. A., Zolotaryov, Ye. A., Voytkovskiy, K. F., and Popovnin, V.V.: Indirect Estimation of the Djankuat Glacier Volume Based on Surface Topography, *Hydrology Research*, 33 \(1\), 95–110, doi: 10.2166/nh.2002.0006, 2002a.](#)

775

Aleynikov, A. A., Popovnin, V. V., Voytkovskiy K. F., and Zolotaryov Y. A.: Indirect estimation of the Djankuat Glacier volume based on surface topography, *Hydrol. Res.*, 33(1), 95–110, doi: 10.2166/nh.2002.0006, 2002b.

- Allen, R. G., Trezza, R., and Tasumi, M.: Analytical integrated functions for daily solar radiation on slopes, *Agric For Meteorol.*, 139 (1–2), 55–73, doi: 10.1016/j.agrformet.2006.05.012, 2006.
- Anderson, L. S., and Anderson, R. S.: Modeling debris-covered glaciers: response to steady debris deposition, *The Cryosphere*, 10(1), 1105–1124, doi: 10.5194/tc–10–1105–2016, 2016.
- 780 [Belozеров, E. Rets, E., Petrakov, D., and Popovnin. V. V.: Modelling glaciers' melting in Central Caucasus \(the Djankuat and Bashkara Glacier case study\), E3S Web Conf., 163, doi: 10.1051/e3sconf/202016301002, 2020.](#)
- [Benn, D. I., Bolch, T., Hands, K., Gulley, J., Luckman, A., Nicholson, L. I., Quincey, D., Thompson, S., Toumi, R., and Wiseman, S.: Response of debris-covered glaciers in the Mount Everest region to recent warming, and implications for outburst flood hazards, Earth Sci. Rev., 114, 156–174, doi:10.1016/j.earscirev.2012.03.008, 2012.](#)
- 785 Boyarsky, I.Y. [et al.](#): The Djankuat Glacier [Ледник Джанкуат] (Ed. by I.Y. Boyarsky), *Gidrometeoizdat, Leningrad, USSR*, 184 p., 1978 [in Russian].
- Bozhinskiy, A. N., Krass, M. S., and Popovnin, V. V.: Role of debris cover in the thermal physics of glaciers, *J. Glaciol.*, 32(111), 255–266, doi: 10.3189/S0022143000015598, 1986.
- Carenzo, M., Pellicciotti, F., Mabillard, J., Reid, T., and Brock, B.W.: An enhanced temperature index model for debris-
790 covered glaciers accounting for thickness effect, *Adv. Water Resour.*, 94(1), 457–469, doi: 10.1016/j.advwatres.2016.05.001, 2016.
- Chernomorets, S. S., Petrakov, D. A., Aleynikov, A. A., Bekkiev, M. Y., Viskhadzhieva, K. S., Dokukin, M. D., Kalov, R. K., Kidyayeva, V. M., Krylenko, V. V., Krylenko, I. V., Krylenko, I. N., Rets, E. P., Savernyuk, E. A., and Smirnov, A. M.:
795 The outburst of Bashkara glacier lake (central Caucasus, Russia) on september 1, 2017 [Прорыв озера Башкара (Центральный Кавказ, Россия) 1 сентября 2017 года], *Earth's Cryosphere*, 22(2), 70–80, doi: 0.21782/EC2541–9994–2018–2(61–70), 2018 [in Russian].
- D'Arrigo, R., and Cullen, H. M.: A 350-year (AD 1628–1980) reconstruction of Turkish precipitation, *Dendrochronologia*, 19(2), 169–177, 2001.
- Dolgova, E.: June–September temperature reconstruction in the Northern Caucasus based on blue intensity data,
800 *Dendrochronologia*, 39(1), 17–23, doi: 10.1016/j.dendro.2016.03.002, 2016.
- Dolgova, E. A., Matkovsky, V. V., Solomina, O. N., Rototaeva, O. V., Nosenko, G. A., and Khmelevskoy, I. F.: Reconstruction of the mass balance of the Garabashi glacier (1800–2005) using dendrochronological data [Реконструкция
баланса массы ледника Гарабаши (1800–2005 гг.) по дендрохронологическим данным], *Ice and Snow*, 1(121), 34–41,
doi: 10.15356/2076–6734–2013–1–34–42, 2013 [in Russian].
- 805 Duffie, J. A., and Beckman, W. A.: *Solar thermal energy processes*, Wiley Interscience, New York, 944 p., 2006.

- Dyurgerov, M. B., and Popovnin, V. V.: Reconstruction of mass balance, spatial position, and liquid discharge of Dzhankuat Glacier since the second half of the 19th century, *Data of glaciological studies*, 40(1), 111–126, 1988 [[Russian Translations Series 67](#)].
- 810 Fyodorov, V. M., and Zalikhanov, A. M.: Analysis of changes in the ice resources of the Central Caucasus [Анализ изменения ледовых ресурсов Центрального Кавказа], *Proc. T.I.Vyazemskiy Karadag Res. Station, RAS nature reserve* [Труды Карадагской научной станции им. Т.И. Вяземского-природного заповедника РАН], 3(7), 68–83, 2018 [in Russian].
- Gantayat, P., Kulkarni, A. V., Srinivasan, J., and Schmeits, M. J.: Numerical modelling of past retreat and future evolution of Chhota Shigri glacier in Western Indian Himalaya, *Ann. Glaciol.*, 58(75~~pt2~~), 136–144, doi: 10.1017/aog.2017.21, 2017.
- 815 Giesen, R. H., and Oerlemans, J.: Response of the ice cap Hardangerjøkulen in southern Norway to the 20th and 21st century climates, *The Cryosphere*, 4(1), 191–213, doi: 10.5194/tc-4-191-2010, 2010.
- Giesen, R. H., and Oerlemans, J.: Calibration of a surface mass balance model for global-scale applications, *The Cryosphere*, 6(6), 1463–1481, doi: 10.5194/tc-6-1463-2012, 2012.
- 820 Griggs, C., De Gaetano, A., Kuniholm, P., and Newton, M.: A regional high-frequency reconstruction of May–June precipitation in the north Aegean from oak tree rings, A.D. 1089–1989, *Int. J. Climatol.*, 27(8), 1075–1089, doi: 10.1002/joc.1459, 2007.
- Hagg, W., Shahgedanova, M., Mayer, C., Lambrecht, A., and Popovnin, V. V.: A sensitivity study for water availability in the Northern Caucasus based on climate projections, *Glob. Planet. Change*, 73(1), 161–171, doi: 10.1016/j.gloplacha.2010.05.005, 2010.
- 825 [Hambrey, M., Quincey, D., Glasser, N. F., Reynolds, J. M., Richardson, S. J., and Clemmens, S.: Sedimentological, geomorphological and dynamic context of debris-mantled glaciers, Mount Everest \(Sagarmatha\) region, Nepal, *Quaternary Sci. Rev.*, 27, 2341–2360, 2008.](#)
- Harris, I., Jones, P., Osborn, T., and Lister, D.: Updated high-resolution grids of monthly climatic observations—The CRU TS3.10 Dataset (updated 2018, v4.02), *Int. J. Climatol.*, 34(3), 623–642, doi: 10.1002/joc.3711, 2014.
- 830 [Hock, R., Rasul, G., Adler, C., Cáceres, B., Gruber, S., Hirabayashi, Y., Jackson, M., Käab, A., Kang, S., Kutuzov, S., Milner, Al., Molau, U., Morin, S., Orlove, B., and Steltzer, H.: High Mountain Areas. In: *IPCC Special Report on the Ocean and Cryosphere in a Changing Climate* \[Pörtner, H.-O., Roberts, DC., Masson-Delmotte, V., Zhai, P., Tignor, M., Poloczanska, E., Mintenbeck, K., Alegria, A., Nicolai, M., Okem, A., Petzold, J., Rama, B., Weyer, N. M. \(eds\)\], 2019.](#)
- 835 Holobăcă, I. H., Pop, O., and Petrea, D.: Dendroclimatic reconstruction of late summer temperatures from upper treeline sites in Greater Caucasus, Russia, *Quat. Int.*, 415(3), 67–73, doi: 10.1016/j.quaint.2015.10.103, 2016.

Huss, M., Bauder, A., and Funk, M.: Homogenization of long-term mass-balance time series, *Ann. Glaciol.*, 50(50), 198–206, doi: 10.3189/172756409787769627, 2009.

Huss, M., and Fischer, M.: Sensitivity of very small glaciers in the Swiss Alps to future climate change, *Front. Earth Sci.*, 40(34), 1–17, doi: 10.3389/feart.2016.00034, 2016.

840 [Huss, M. and Hock, R.: A new model for global glacier change and sea-level rise, *Front. Earth Sci.*, 3, 1–22, doi: 10.3389/feart.2015.00054, 2015.](#)

Huss, M., and Hock, R.: Global-scale hydrological response to future glacier mass loss, *Nat. Clim. Change*, 8(2), 135–140, doi: 10.1038/s41558-017-0049-x, 2018.

[Iqbal, M.: *An introduction to solar radiation*, Academic Press, Toronto, 390 pp., 1983.](#)

845 Jones, P. D., Lister, D. H., Osborn, T. J., Harpham, C., Salmon, M., and Morice C. P.: Hemispheric and largescale land surface air temperature variations: an extensive revision and an update to 2010, (v4.6.0.0, updated 2018), *J. Geophys. Res.*, 117(D05), 1–29, doi: 10.1029/2011JD017139, 2012.

Jouvet, G., Huss, M., Funk, M., and Blatter, H.: Modelling the retreat of Grosser Aletschgletscher, Switzerland, in a changing climate, *J. Glaciol.*, 57(206), 1033–1045, doi: 0.3189/002214311798843359, 2011.

850 Kienholz, C., Hock, R., Truffer, M., Bieniek, P. A., and Lader, R.: Mass balance evolution of Black Rapids glacier, Alaska, 1980–2100, and its implications for surge recurrence, *Front. Earth Sci.*, 5(56), 1–20, doi: 10.3389/feart.2017.00056, 2017.

Kirkbride, M. P.: Ice-marginal geomorphology and Holocene expansion of debris-covered Tasman Glacier, New Zealand. *Debris-Covered Glaciers (Proceedings of a workshop held at Seattle, Washington, USA, September 2000)*, 264(1), 211–217, doi: 10.1007/978-90-481-2642-2_622, 2000.

855 Köse, N., Akkemik, Ü., Dalfes, H.N., and Özeren, M. S.: Tree-ring reconstructions of May–June precipitation for western Anatolia, *Quat. Res.*, 75(3), 438–450, doi: 10.1016/j.yqres.2010.12.005, 2011.

Kotlyakov, V. M., Serebryanny, R. L., and Solomina, O. N: Climate change and glacier fluctuation during the last 1,000 years in the Southern Mountains of the USSR, *Mt. Res. Dev.*, 11(1), 1–12, 1991.

860 Kuzmin, P. P.: *The processes of Snow Cover Melting*, Gidrometeoizdat, Leningrad, USSR. 348 p., 1961 [translated from Russian by E. Vilim].

Lambrecht, A., Mayer, C., Hagg, W., Popovnin, V. V., Rezepkin, A., Lomidze, N., and Svanadze, D.: A comparison of glacier melt on debris-covered glaciers in the northern and southern Caucasus, *The Cryosphere*, 5(1), 525–538, doi: 10.5194/tc-5-525-2011, 2011.

- Lavrentiev, I. I., Kutuzov S. S., Petrakov, D. A., Popov, G. A., and Popovnin, V. V.: Ice thickness, volume and subglacial relief of Djankuat Glacier (Central Caucasus) [Толщина, объём льда и подлёдный рельеф ледника Джанкуат (Центральный Кавказ)], *Ice and Snow*, 4(128), 7–19, doi: 10.15356/2076–6734–2014–4–7–19, 2014 [in Russian].
- 865 Leclercq, P. W., Pitte, P., Giesen, R. H., Masiokas, M. H., and Oerlemans, J.: Modeling and climatic interpretation of the length fluctuations of Glacier Frias (north Patagonian Andes, Argentina) 1639–2009 AD, *Clim. Past.*, 8(1), 1385–1402, doi: 10.5194/cp–8–1385–2012, 2012.
- 870 Makowska, N., Zawierucha, K., Mokracka, J., and Koczura, R.: First report of microorganisms of Caucasus glaciers (Georgia), *Biol.*, 71(6), 620–625, doi: 10.1515/biolog–2016–0086, 2016.
- Martin-Benito, D., Ummenhofer C. C., Köse, N., Güner, H. T., and Pederson, N.: Tree-ring reconstructed May–June precipitation in the Caucasus since 1752 CE, *Clim. Dyn.*, 47(9–10), 3011–3027, doi: 10.1007/s00382–016–3010–1, 2016.
- Nemec, J., Huybrechts, P., Rybak, O., and Oerlemans, J.: Reconstruction of the annual balance of Vadret da Morteratsch, Switzerland, since 1865, *Ann. Glaciol.*, 50(50), 126–134, doi: 10.3189/172756409787769609, 2009.
- 875 Nicholson, L. I., and Benn, D. I.: Calculating ice melt beneath a debris layer using meteorological data, *J. Glaciol.*, 52(178), 463–470, doi: 10.3189/172756506781828584, 2006.
- Oerlemans, J., and Knap, W. H.: A 1-year record of global radiation and albedo in the ablation zone of Morteratschgletscher, Switzerland, *J. Glaciol.*, 44(147), 231–238, doi: 10.3189/S0022143000002574, 1998.
- 880 Oerlemans, J.: Climate sensitivity of glaciers in southern Norway: application of an energy-balance model to Nigardsbreen, Hellstugubreen and Ålfotbreen, *J. Glaciol.*, 38(129), 223–232, doi: 10.3189/S0022143000003634, 1992.
- Oerlemans, J.: A flowline model for Nigardsbreen, Norway: projection of future glacier length based on dynamic calibration with the historic record, *Ann. Glaciol.*, 24(1), 382–389, doi: 10.3189/S0260305500012489, 1997.
- Oerlemans, J.: *Glaciers and climate change*, A. A. Balkema Publishers, Lisse, 160 pp., 2001.
- 885 Oerlemans, J.: *The microclimate of valley glaciers*, Utrecht Publishing and Archiving Services, Utrechtm, 138 pp., 2010.
- Østrem, G.: Ice melting under a thin layer of moraine, and the existence of ice cores in moraine ridges, *Geogr. Ann.*, 41(4), 228–230, 1959.
- Pastukhov, V. G.: *On the mass exchange of the Djankuat Glacier* [Полный массообмен ледника Джанкуат], Graduate work, Moscow State University (Faculty of Geography), 185 pp., 2011 [in Russian].
- 890 Petrakov, D. A., Tutubalina, O. V., Aleynikov, A. A., Chernomorets, S. S., Evans, S. G., Kidyayeva, V. M., Krylenko, I. N., Norin, S. V., Shakhmina, M. S., and Seynova, I. B.: Monitoring of Bashkara Glacier lakes (Central Caucasus, Russia) and modelling of their potential outburst, *Nat. Hazards*, 61(3), 1293–1316, doi: 10.1007/s11069–011–9983–5, 2012.

895 Popovnin, V. V., Rezepkin, A. A., and Tielidze, L. G.: Superficial moraine expansion on the Djankuat glacier snout over the direct glaciological monitoring period [Разрастание поверхностной морены на языке ледника Джанкуат за период прямого гляциологического мониторинга], *Earth's Cryosphere*, 19(1), 79–87, 2015 [in Russian].

Popovnin, V. V., and Naruse, R.: A 34-year long record of mass balance and geometric changes of the Djankuat Glacier, Caucasus, *Bull. Glaciol. Res.*, 22(1), 121–133, 2005.

Popovnin, V. V., and Pylayeva T. V.: Avalanche feeding of Djankuat Glacier [Лавинное питание ледника Джанкуат], *Ice and snow*, 55(2), 21–32, doi: 10.15356/2076–6734–2015–2–21–32, 2015 [in Russian].

900 [Popovnin, V.V. and Rozova, A.: Influence of sub-debris thawing on ablation and runoff of the Djankuat Glacier in the Caucasus. *Nord. Hydrol.*, 33\(1\), 75–94, 2002.](#)

Popovnin, V. V.: Annual mass - balance series of a temperate glacier in the Caucasus, reconstructed from an ice core, *Geogr. Ann. Ser. A-phys. Geogr.*, 81(4), 713–724, doi: 10.1111/1468–0459.00099, 1999.

905 [Rasul, G., and Molden, D.: The global social and economic consequences of mountain cryospheric change, *Front. Environ. Sci.*, 7\(91\), doi: <https://doi.org/10.3389/fenvs.2019.00091>, 2019.](#)

910 Rets, E. P., Popovnin, V. V., Toropov, P. A., Smirnov, A. M., Tokarev, I. V., Chizhova, J.N., Budantseva, N.A., Vasil'chuk, Y.K., Kireeva, M.B., Ekaykin, A.A., Veres, A.N., Aleynikov, A.A., Frolova, N.L., Tsyplenkov, A.S., Poliukhov, A.A., Chalov, S.R., Aleshina, M.A. and Kornilova, E.D.: Djankuat Glacier station in the North Caucasus, Russia: a database of complex glaciological, hydrological, meteorological observations and stable isotopes sampling results during 2007–2017, *Earth Syst. Sci. Data*, 11, 1463–1481, doi: 10.5194/essd-11-1463-2019, 2019.

Rezepkin, A. A., and Popovnin, V. V.: Influence of the surface moraine on the state of Djankuat Glacier (Central Caucasus) by 2025 [О влиянии поверхностной морены на состояние ледника Джанкуат (Центральный Кавказ) к 2025 г.], *Ice and snow*, 58(3), 307–321, doi: 10.15356/2076–6734–2018–3–307–321, 2018 [in Russian].

915 Rototaeva, O. V., Nosenko, G. A., Khmelevskoy, I. F., and Tarasova, L. N.: Balance state of the Garabashi glacier (Elbrus) in 1980-s and 1990-s [Состояние равновесия ледника Гарабаши (Эльбрус) в 1980-х и 1990-х годах], *Data of Glaciological Studies*, 95(1), 111–121, 2003 [in Russian].

Rowan, A. V., Egholm, D. L., Quincey, D. J., and Glasser, N. F.: Modelling the feedbacks between mass balance, ice flow and debris transport to predict the response to climate change of debris covered glaciers in the Himalaya, *Earth Planet. Sci. Lett.*, 430(1), 427–438, doi: 10.1016/j.epsl.2015.09.004, 2015.

920 ~~Rybak, O. O., Rybak, E. A., Korneva, I. A., and Popovnin, V. V.: Mathematical modelling of Djankuat Glacier evolution in present day climatic conditions, *Sustainable Dev. of Mt. Territories*, 10(4), 533–543, doi: 10.21177/1998–4502–2018–10–4–533–543, 2018.~~

- ~~Rybak, O., and Rybak, E. A.: Model-based calculations of surface mass balance of mountain glaciers for the purpose of water consumption planning: focus on Djankuat Glacier (Central Caucasus), IOP Conference Series: Environ. Earth Sci., 107(1), 1–7, doi: 10.1088/1755-1315/107/1/012041, 2018.~~
- 925 Schaefli, B., and Huss, M.: Integrating point glacier mass balance observations into hydrologic model identification, *Hydrol. Earth Syst. Sci.*, 15(1), 1227–1241, doi: 10.5194/hess-15-1227-2011, 2011.
- [Scherler, D., Bookhagen, B., and Strecker, M. R.: Spatially variable response of Himalayan glaciers to climate change affected by debris cover, *Nat. Geosci.*, 4, 156–159, 2011.](#)
- 930 Scherler, D., Wulf, H., and Gorelick, N.: Global Assessment of Supraglacial Debris Cover Extents, *Geophys. Res. Lett.*, 45(21), 11798–11805, doi: 10.1029/2018GL080158, 2018.
- Shahgedanova, M., Nosenko, G., Kutuzov, S., Rototaeva, O., and Khromova, T.: Deglaciation of the Caucasus Mountains, Russia/Georgia, in the 21st century observed with ASTER satellite imagery and aerial photography, *The Cryosphere*, 8(1), 2367–2379, doi: 10.5194/tc-8-2367-2014, 2014.
- 935 Shahgedanova, M., Popovnin, V. V., Aleynikov, A. A., Petrakov, D., and Stokes, C. R.: Long-term change, inter-annual, and intra-seasonal variability in climate and glacier mass balance in the Central Greater Caucasus, Russia, *Ann. Glaciol.*, 46(1), 355–361, doi: 10.3189/172756407782871323, 2007.
- Shahgedanova, M., Stokes, C. R., Gurney, S. D., and Popovnin, V. V.: Interactions between mass balance, atmospheric circulation and recent climate change on the Djankuat Glacier, Caucasus Mountains, Russia, *J. Geophys. Res. Atmos.*
- 940 110(D4), 1–14, doi: 10.1029/2004JD005213, 2005.
- [Shannon, S., Smith, R., Wiltshire, A., Payne, T., Huss, M., Betts, R., Caesar, J., Koutroulis, A., Jones, D., and Harrison, S.: Global glacier volume projections under high-end climate change scenarios, *The Cryosphere*, 13, 325–350, doi: <https://doi.org/10.5194/tc-13-325-2019>, 2019.](#)
- Solomina, O., Bushueva, I., Dolgova, E., Jomelli, V., Alexandrin, M., Mikhalenko, V., and Matskovsky, V.: Glacier variations in the Northern Caucasus compared to climatic reconstructions over the past millennium, *Glob. Planet. Change*, 140(1), 28–58, doi: 10.1016/j.gloplacha.2016.02.008, 2016.
- 945 Stokes, C. R., Popovnin, V. V., Aleynikov, A. A., Gurney, S. D., and Shahgedanova, M.: Recent glacier retreat in the Caucasus Mountains, Russia, and associated increase in supraglacial debris cover and supra-/proglacial lake development, *Ann. Glaciol.*, 46(1), 195–203, doi: 10.3189/172756407782871468, 2007.
- 950 Tailland, J. D.: *Glaciers: the politics of ice*, Oxford University Press, Oxford, 360 pp., 2015.
- [Taylor, K. E., Stouffer, R. J., and Meehl, G. A.: An overview of CMIP5 and the experiment design, *Bull. Am. Meteorol. Soc.*, 93, 485–498, doi: 10.1175/BAMS-D-11-00094.1, 2012.](#)

- Tielidze, L. G.: Glacier change over the last century, Caucasus Mountains, Georgia, observed from old topographical maps, Landsat and ASTER satellite imagery, *The Cryosphere*, 10(1), 713–725, doi: 10.5194/tc-10-713-2016, 2016.
- 955 Tielidze, L., and Wheate, R.: The Greater Caucasus Glacier Inventory (Russia, Georgia and Azerbaijan), *The Cryosphere*, 12(1), 81–94, doi: 10.5194/tc-12-81-2018, 2018.
- [Tielidze, L. G., Bolch, T., Wheate, R. D., Kutuzov, S. S., Lavrentiev, I. I., and Zemp, M.: Supra-glacial debris cover changes in the Greater Caucasus from 1986 to 2014, *The Cryosphere*, 14, 585–598, doi: https://doi.org/10.5194/tc-14-585-2020, 2020.](https://doi.org/10.5194/tc-14-585-2020)
- 960 Toropov P. A., Shestakova, A., and Smirnov, A. M.: Methodological aspects of heat balance components estimation on mountain glaciers, *Russ. J. Earth Sci.*, 17(4), 1–9, doi: 10.2205/2017ES000605, 2017.
- Toropov, P. A., Aleshina, M. A., Kislov, A. V., and Semenov, V. A.: Trends of climate change in the Black sea-Caspian region in the last 30 years [Тенденции изменений климата Черноморско-Каспийского региона за последние 30 лет]. *Moscow University Herald, Geogr. Ser.*, 5(2), 67–77, 2018 [In Russian].
- 965 Toucham, R., Garfin, G. M., Meko, D. M., Funkhouser, G., Erkan, N., Hughes, M. K., and Wallin, B. S.: Preliminary reconstructions of spring precipitation in southwestern Turkey from tree-ring width, *Int. J. Climatol.*, 23(2), 157–171, doi: 10.1002/joc.850, 2003.
- Vacco, D. A., Alley, R. B., and Pollard, D.: Glacier advance and stagnation caused by rock avalanches, *Earth Planet. Sc. Lett.*, 294(1), 123–130, doi: 10.1016/j.epsl.2010.03.019, 2010.
- 970 Vaughan, D. G., Comiso, J., Allison, I., Carrasco, J., Kaser, G., Kwok, R., ... et al.: Observations: Cryosphere. In T. F. Stocker, D. Qin, G. K. Plattner, M. Tignor, S. K. Allen, J. Boschung, A. Nauels, ... et al. (Eds.), *Climate change 2013: The physical science basis. Contribution of working group I to the fifth assessment report of the intergovernmental panel on climate change* Cambridge, United Kingdom and New York, NY, USA: Cambridge University Press, 317–382, 2013.
- Volodicheva, N.: The Caucasus [edited by: Shahgedanova, M.], in: *The Physical Geography of Northern Eurasia*, Oxford University Press, 350–376, 2002.
- 975 Voloshina, A. P.: Meteorology of mountain glaciers [Метеорология горных ледников], *Data of Glaciological Studies*, 92(1), 3–138, 2002 [In Russian].
- [Wirbel, A., Jarosch, A. H., and Nicholson, L.: Modelling debris transport within glaciers by advection in a full-Stokes ice flow model, *The Cryosphere*, 12, 189–204, doi: https://doi.org/10.5194/tc-12-189-2018, 2018.](https://doi.org/10.5194/tc-12-189-2018)
- 980 WGMS: Djankuat, North Caucasus. [World Glacier Monitoring Service ONLINE]. Available at: https://wgms.ch/products_ref_glaciers/djankuat/, last access: 17 December 2018, 2018.

Zekollari, H., Fürst, J., and Huybrechts, P.: Modelling the evolution of Vadret da Morteratsch (Switzerland) since the Little Ice Age and into the future, *J. Glaciol.*, 60(224), 1155–1168, doi: 10.3189/2014JoG14J053, 2014.

985

[Zekollari, H., Huss, M., and Farinotti, D.: Modelling the future evolution of glaciers in the European Alps under the EURO-CORDEX RCM ensemble, *The Cryosphere*, 13, 1125–1146, doi: <https://doi.org/10.5194/tc-13-1125-2019>, 2019.](#)

Zemp, M., Frey, H., Gärtner-Roer, I., Nussbaumer, S., Hoelzle, M., Paul, F., ... et al.: Historically unprecedented global glacier decline in the early 21st century, *J. Glaciol.*, 61(228), 745–762. doi: doi.org/10.3189/2015JoG15J017, 2015.

Zolotarev, E. A.: About the “moraine of the 30s” and the size of the Dzhankuat glacier [О конечной “морене 30-х годов” и размерах ледника Джанкуат], *Data of Glaciological Studies*, 87(1), 177–183, 1998 [in Russian].

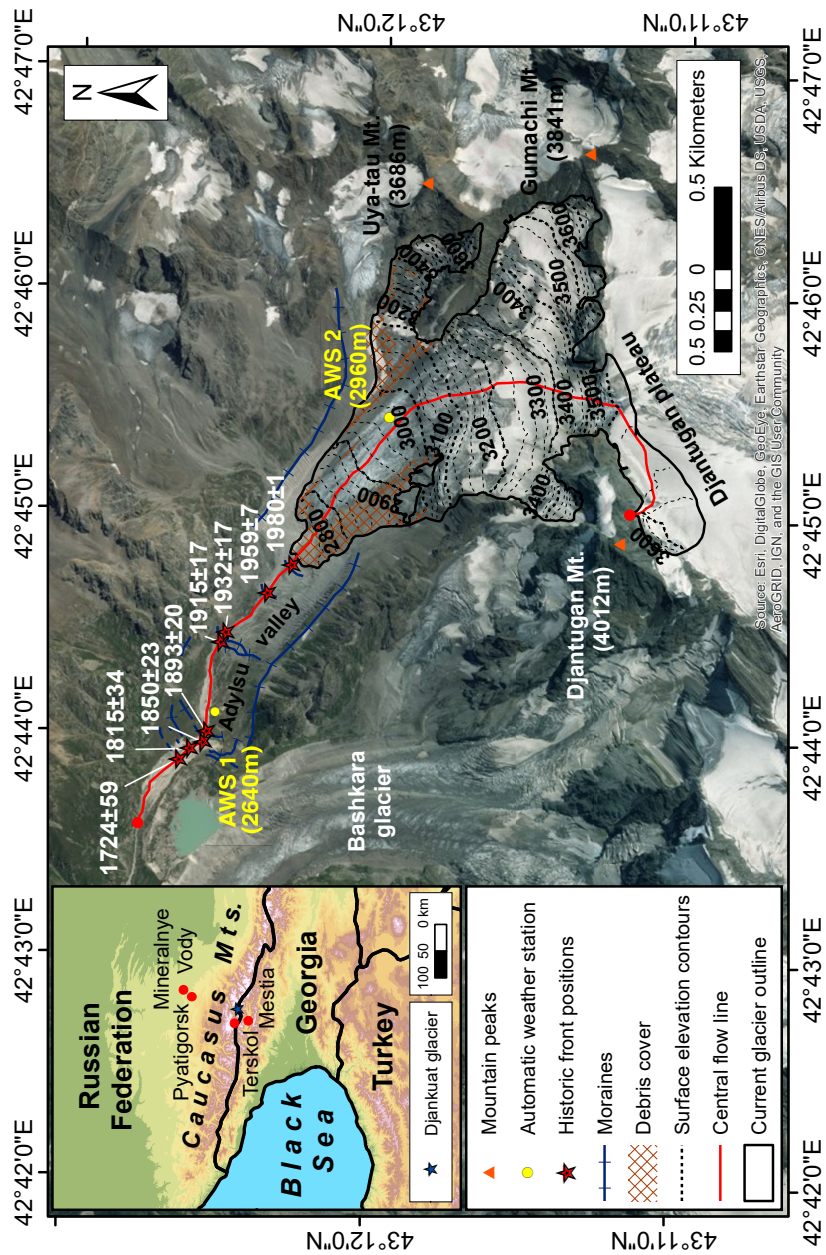
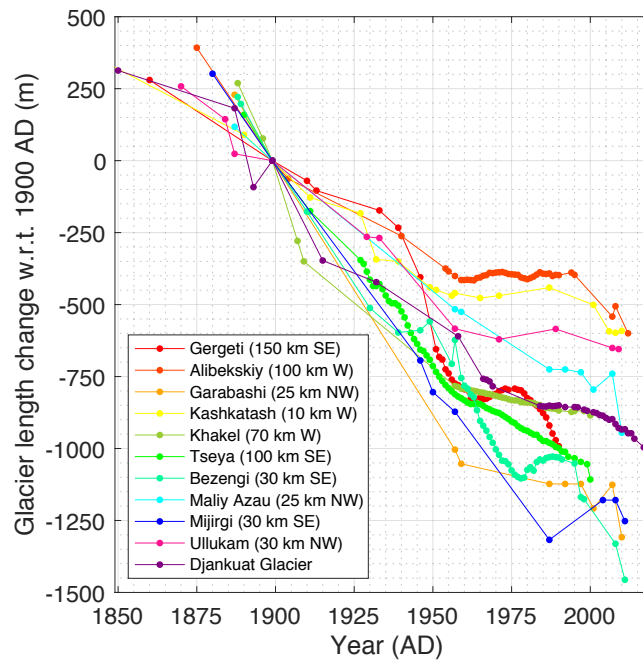


Figure 1. Satellite image of the Djankuat Glacier for the year 2010 AD, showing the most important features in the study area.



995

Figure 2. Comparison of modelled historic length variations of the Djankuat Glacier to other glaciers in the Caucasus area. Observed length variations are derived from Solomina et al. (2016) and WGMS (2018). Approximate distances and direction to the Djankuat Glacier are indicated in the legend. [Historic length variations of the Djankuat Glacier compared to other glaciers in the Caucasus \(Solomina et al., 2016; WGMS, 2018\). Approximate distances and direction to the Djankuat Glacier are indicated.](#)

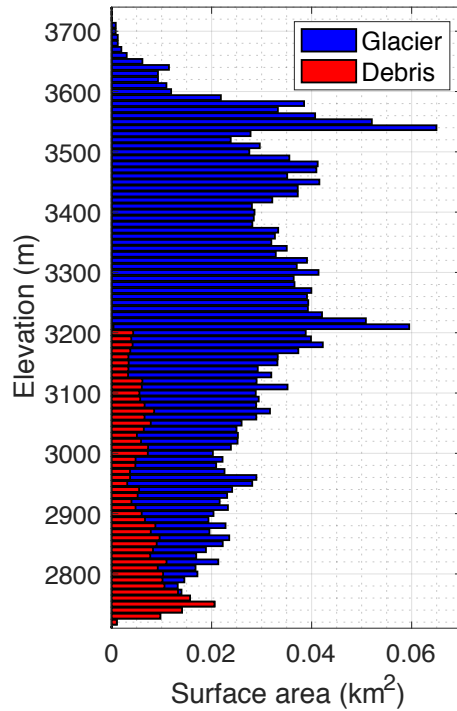


Figure 3. The Djankuat Glacier's surface (blue) and debris covered area (red) for 2010 AD conditions as shown by the area-elevation distribution using 10-m bins. Hypsometric data are derived from the DEM and manual digitalization of the supraglacial debris cover using satellite imagery in Fig. 1.

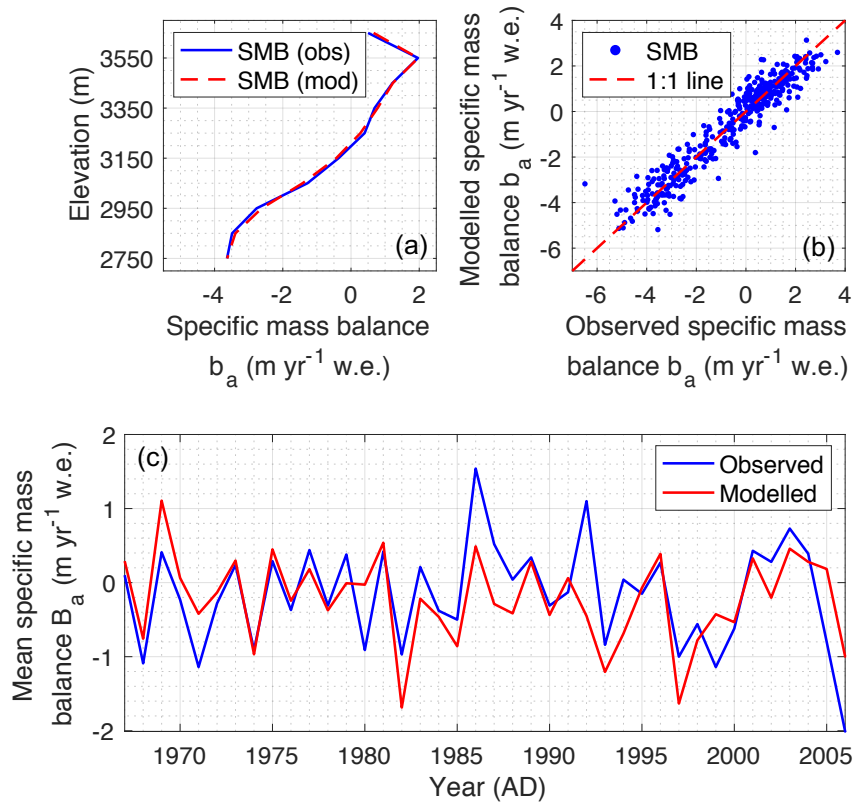


Figure 4. Calibrated mass balance model of the Djankuat Glacier for fixed geometry, showing the observed and modelled (a) mass balance-elevation profile for the 1967/68–2006/07 period, (b) local annual surface mass balances b_a for the 1967/68–2006/07 period and (c) modelled and observed mean specific mass balance B_a since the start of the monitoring period. Observed mass balance data are retrieved from Popovnin and Naruse (2005) and WGMS (2018).

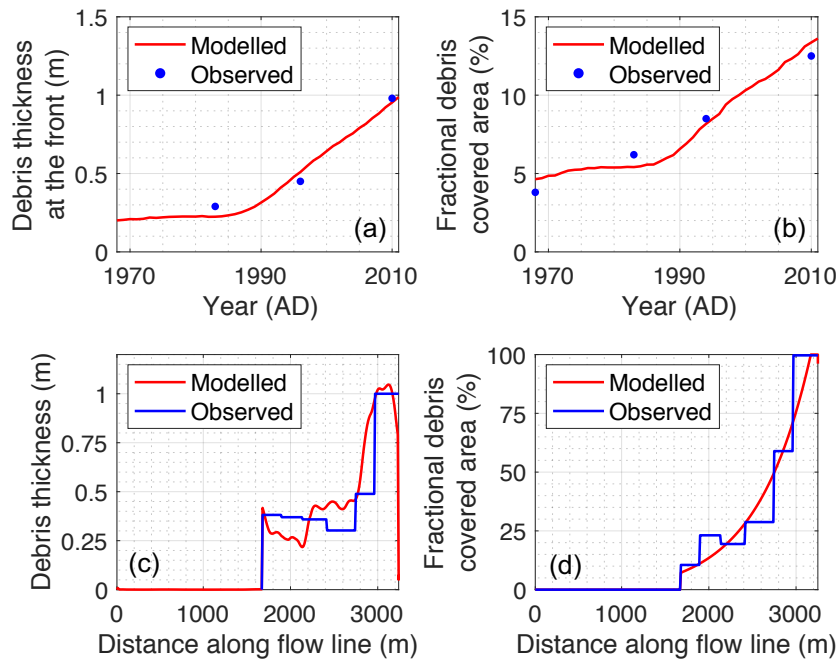


Figure 5. Calibrated supraglacial debris cover model for the Djankuat Glacier, showing the observed and modelled temporal evolution of (a) debris thickness at the front and (b) the glacier-wide fractional debris covered area, as well as observed and modelled (c) debris thickness and (d) debris covered area along the flow line for 2009/10 AD conditions. Observed data from (a), (b) and (c) are from Popovnin et al. (2015), whereas the observed debris covered area in (d) was derived by manually digitizing debris-covered patches along the flow line using 2010 AD satellite imagery in Fig. 1.

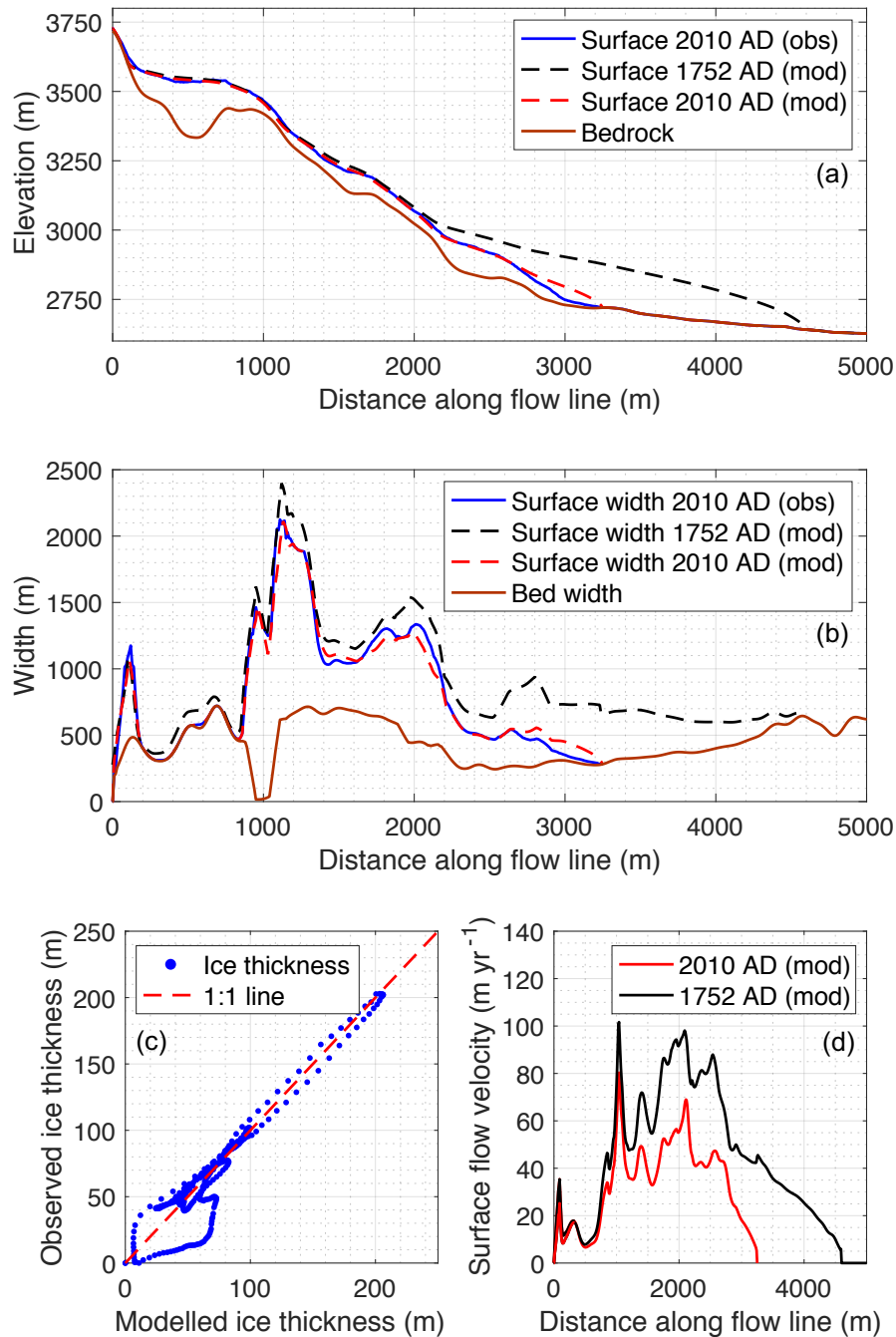


Figure 6. Calibrated flow model, showing (a) the observed and modelled bedrock and surface elevation and (b) bed and surface width for the current (2009/10 AD) and initial state (1752/53 AD), (c) modelled vs. observed ice thickness for 2009/10 AD conditions and (d) current (2009/10 AD) and initial (1752/53 AD) surface flow velocity along the flow line.

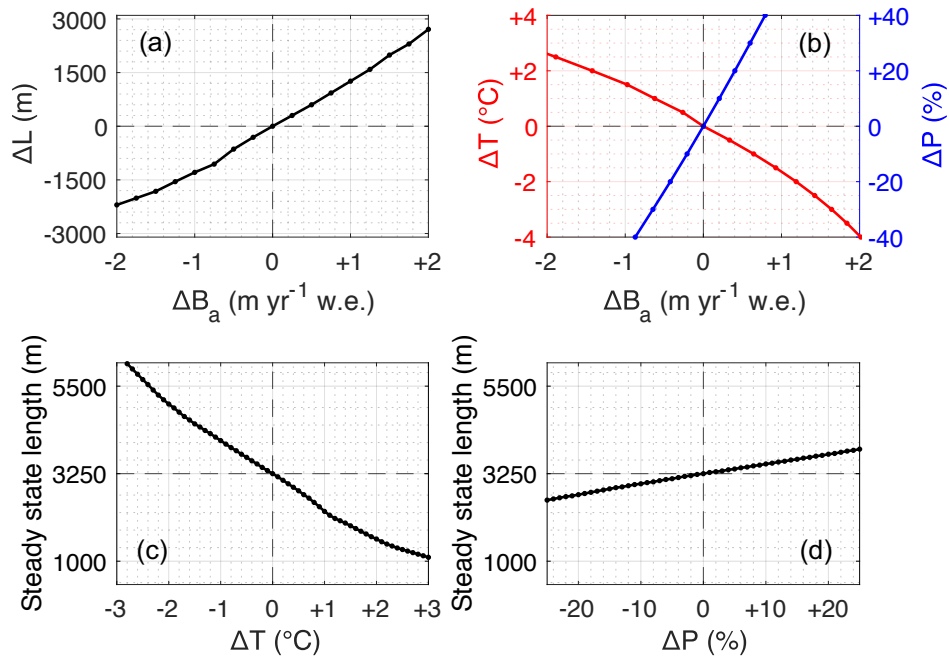


Figure 7. Sensitivity of the Djankuat Glacier showing (a) sensitivity of the glacier steady state length (ΔL) to mass balance perturbations (ΔB_a), (b) sensitivity of the mass balance to temperature (ΔT) and precipitation (ΔP) changes for a fixed present-day glacier geometry, (c) sensitivity of the steady state glacier length to temperature changes, and (d) the same for precipitation changes. All perturbations are with respect to the 1967/68–2006/07 AD reference climate (2.5 $^{\circ}\text{C}$ and 980.7 mm yr^{-1} w.e.), and with respect to a steady state glacier with present-day length (3260 m).

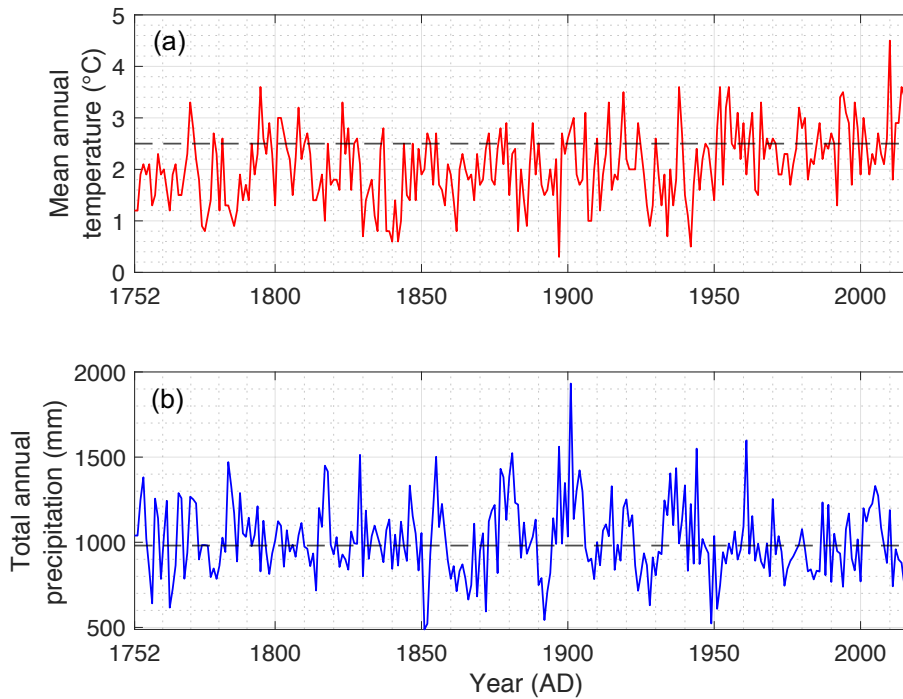


Figure 8. Reconstructed and observed evolution of (a) mean annual temperature and (b) total precipitation amounts for Terskol weather station, based upon proxy data (tree ring reconstructions) and measurements from nearby weather stations (Mestia, Pyatigorsk and Mineralnye Vody). The dashed horizontal line represents the 1981–2010 annual reference values (2.6 °C and 1001.1 mm w.e. yr⁻¹). We refer to the text and Table 2 for more details.

|030

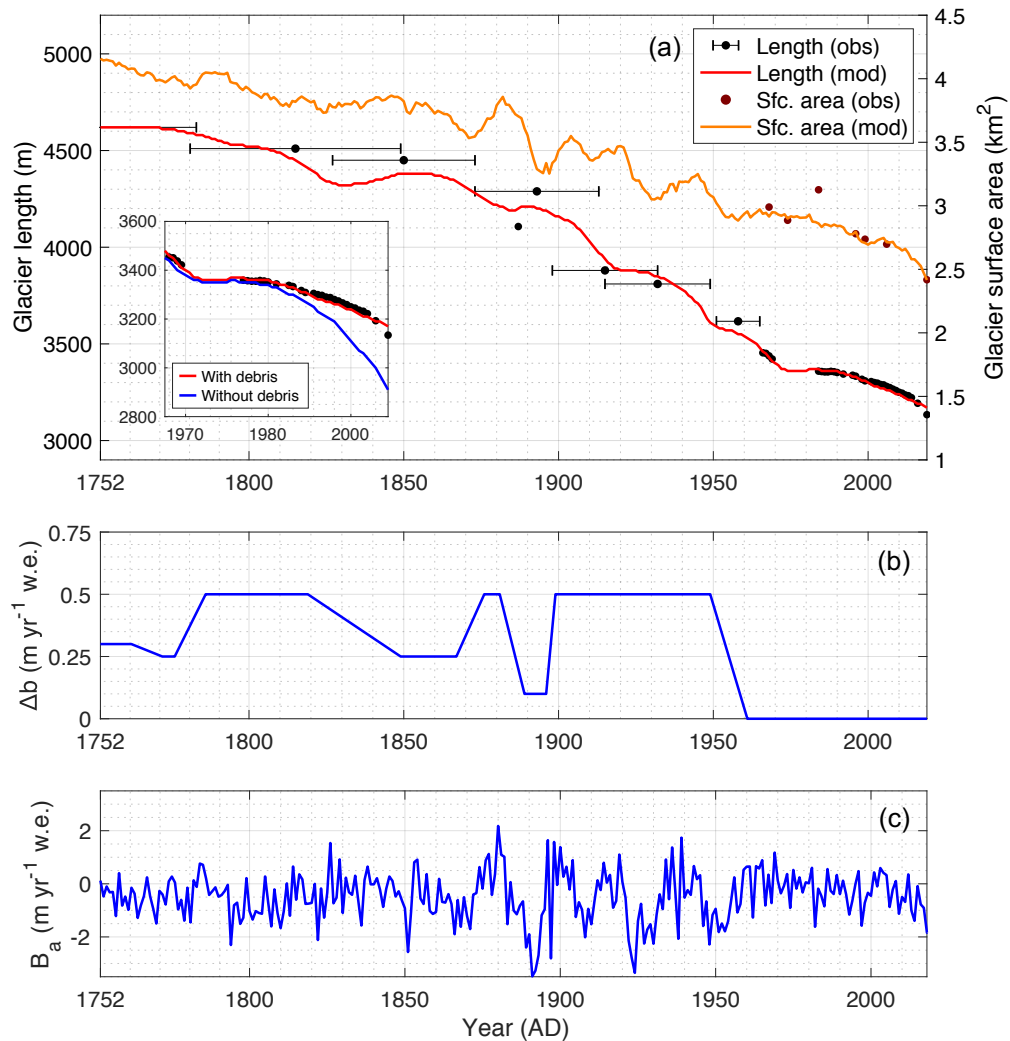


Figure 9. Historic variations of the (a) modelled and observed glacier length of the Djankuat Glacier since 1752/53 AD until 2017 AD, (b) additional mass balance perturbations Δb used in the dynamic calibration procedure and (c) reconstructed time series of the total annual mass balance ΔB_a of the Djankuat Glacier with changing geometry. Observed length variations are derived from lichenometric dating of moraines in the paleovalley, historic documents, and/or field measurements and/or recent satellite imagery (Boyarsky, 1978; Zolotarev, 1998; Petrakov et al., 2012; WGMS, 2018). An additional model run for a 100% clean ice glacier was conducted, which is shown in the box in (a).

035

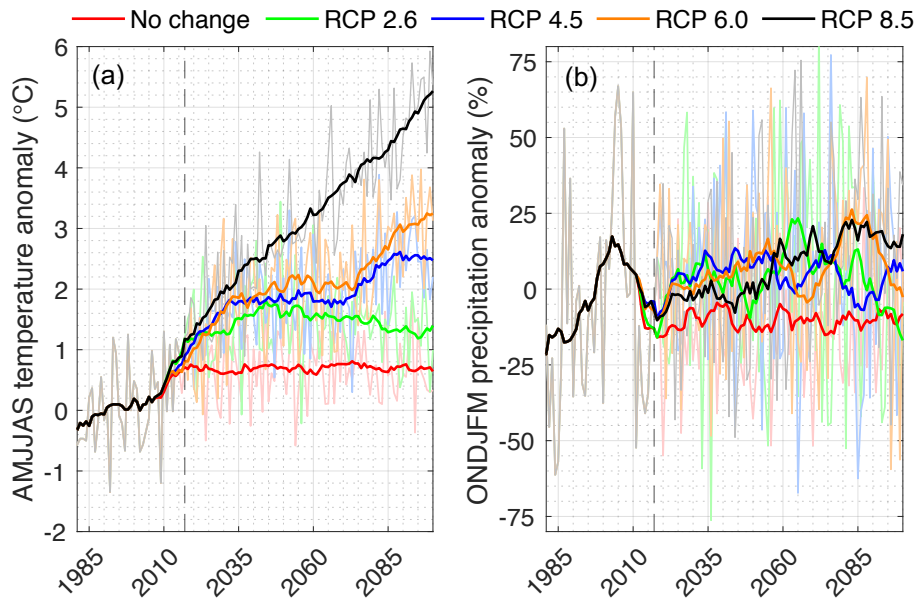
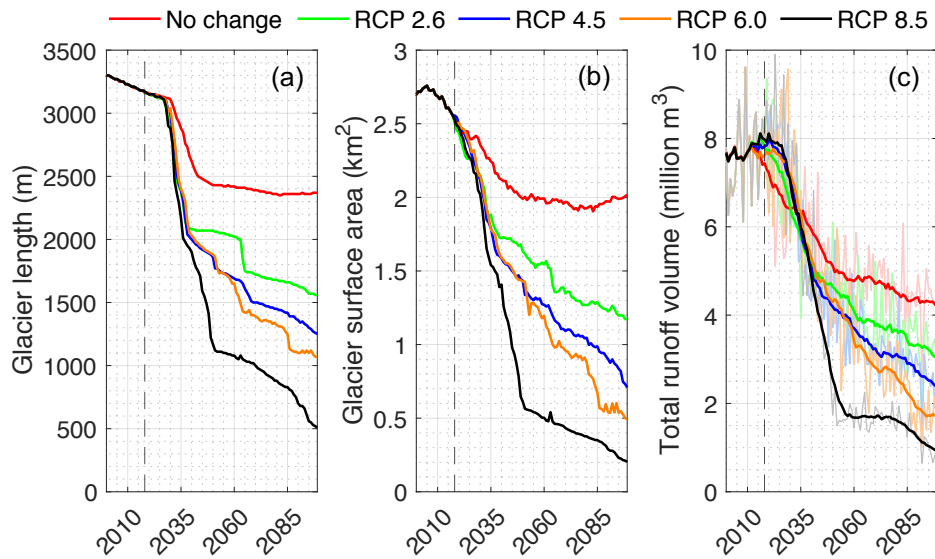


Figure 10. Projected future (a) AMJJAS temperature and (b) ONDJFM precipitation changes for Terskol, as compared to the 1981–2010 reference, for different RCP scenarios until 2100 AD. Thin coloured lines represent annual values, thicker lines represent 15-yr moving means. The dashed vertical line represents the present (i.e. 2017, the most recent year of glaciological observations).



1045

Figure 11. [Modelled \(a\) glacier length, \(b\) glacier surface area, and \(c\) total annual runoff volume of the Djankuat Glacier for different RCP scenarios until 2100 AD. In \(c\), the thin lines represent annual values, while the thicker lines represent 15-yr moving average. The dashed vertical line denotes the present \(i.e. 2017, the most recent year of glaciological observations\).](#)

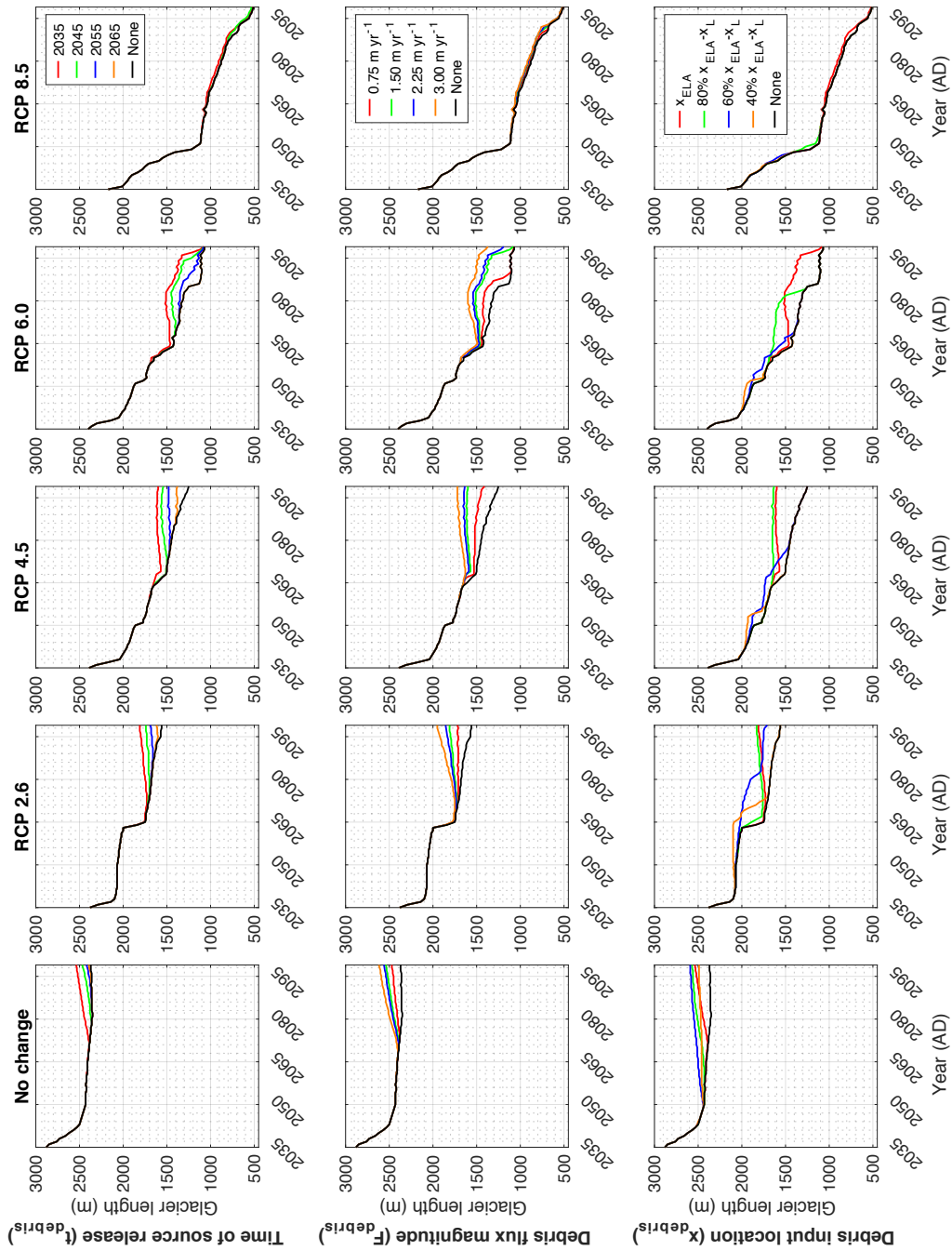


Figure 12. Impact of debris input location x_{debris} , time of release of the debris source t_{debris} and debris flux magnitude F_{debris}^{input} (rows) on the future length ~~extension~~ evolution of the Djankuat Glacier under different climatic scenarios (columns) after 2035 AD.

Table 1. Variables, [constants](#) and their units used in the model. [The – denotes that the value is not a constant.](#)

Variable	Symbol	Value	Unit	Variable	Symbol	Value	Unit
Supraglacial debris cover model							
Timestep debris model	Δt	0.01	yr a	Spatial resolution debris model	Δx	10	m
Characteristic debris thickness	H_{debris}^*	1.15	m	Debris melt-reduction factor	f_{debris}^*	-	-
Debris thickness	H_{debris}	-	m	Growth factor debris area	G_A	-	yr ⁻¹
Debris-covered area	A_{debris}	-	km ²	Englacial debris concentration	C_{debris}	1.05	kg m ⁻³
Debris cover porosity	ϕ_{debris}	0.43	-	Debris rock density	ρ_{debris}	2600	kg m ⁻³
In/output of debris w.r.t. the glacier surface	I_{debris}	-	m yr ⁻¹	Input flux to the glacier surface at input location	F_{debris}^{input}	1.60	m yr ⁻¹
Debris input location	x_{debris}	1680	m	Deposition flux into the foreland	$F_{debris}^{x=L+1}$	-	m yr ⁻¹
Foreland deposition rate of debris at terminus	$F_{debris}^{x=L}$	-	m yr ⁻¹	Distance along flow line	x	-	m
Time of release of debris source	t_{debris}	1958	yr	Constant for strength of debris foreland deposition	c_L	1	m ⁻¹
Distance to the front	D_L	-	m	Average debris thickness of first 30 grid points	H_{debris}^{front}	-	m
Mass balance model							
Timestep mass balance model	Δt	3	hours	Spatial resolution mass balance model	Δx	10	m
Surface elevation	h	-	m	Fraction of diffuse solar radiation	f_{dif}	0.50	-
Elevation of Terskol weather station	$h_{Terskol}$	2141	m	Fraction of direct solar radiation	f_{dir}	0.50	-
Elevation of AWS on Djankuat	h_{AWS}	2960	m	Angle of incidence	θ	-	°
Elevation of AWS in Adylsu Valley	h_{Adylsu}	2640	m	Solar elevation angle	θ_e	-	°
Horizontal precipitation enhancement between Terskol and Adylsu Valley	f_e	1.5	-	Solar zenith angle	θ_z	-	°
Snow redistribution factor	f_{red}	-	-	Fractional cloud cover	f_{cl}	-	-
Precipitation ratio between glacier and Adylsu Valley	$P_{ratioscale}$	-	$\frac{m}{yr^{-1} w. e.}$	Snow depth	d_{snow}	-	m w. e.
Threshold air temperature for rain-snow distinction	T_{resh}	2.0	°C	Incoming extra-terrestrial shortwave radiation at the TOA	$S_{i(TOA)}$	-	W m ²
Temperature lapse rate summer	$\gamma_{T(S)}$	-0.0067	°C m ⁻¹	Characteristic snow depth	d_{snow}^*	0.011	m w. e.
Temperature lapse rate winter	$\gamma_{T(W)}$	-0.0049	°C m ⁻¹	Outflow of retained melt water from snow	W_{snow}	-	$\frac{m}{yr^{-1} w. e.}$
Precipitation lapse rate over glacier	γ_P	0.0023	$\frac{m}{yr^{-1} m^{-1}}$	Liquid snow store	w_{snow}	-	$\frac{m}{yr^{-1} w. e.}$
Net energy flux at glacier surface	Ψ_0	-	W m ²	Snowpack retention capacity	η_s	0.34	-
Albedo for ice	α_{ice}	0.22	-	Latent heat of fusion	L_m	334 000	J kg ⁻¹
Albedo for snow	α_{snow}	0.79	-	Density of water	ρ_w	1 000	kg m ⁻³
Intercept $\Psi_0(T_{air})$	c_0	-39.0	W m ⁻²	Threshold temperature $\Psi_0(T_{air})$	T_{break}	0.0	°C
Slope $\Psi_0(T_{air})$	c_1	13.0	$\frac{W m^{-2}}{°C^{-1}}$	Atmospheric transmissivity	τ	0.53	-
Critical slope for loss due to redistribution	s_{crit}	25	°	Melt production from snow/ice	M	-	$\frac{m}{sy}^{-1} w. e.$
Local annual (or specific) surface mass balance	b_a	-	$\frac{m}{yr^{-1} w. e.}$	Total annual (or mean specific) mass balance	B_a	-	$\frac{m}{yr^{-1} w. e.}$
Ice flow model							
Timestep flow model	Δt	0.0005	yr	Spatial resolution flow model	Δx	10	m
Distance along flowline (x-direction)	x	-	m	Ice thickness	H	-	m
Vertically averaged horizontal velocity	\bar{u}	-	m yr ⁻¹	Surface elevation	h	-	m
Velocity related to internal deformation	\bar{u}_d	-	m yr ⁻¹	Effective slope related to lateral valley wall angles	μ	-	-
Velocity related to basal sliding	u_s	-	m yr ⁻¹	Ice density	ρ_i	917	kg m ⁻³
Surface velocity	u_{sfc}	-	m yr ⁻¹	Gravitational acceleration	g	9.81	m s ⁻²
Ice volume flux	F_{ice}	-	m ³ yr ⁻¹	Flow parameter related to internal deformation	f_d	6.5 * 10 ⁻¹⁷	Pa ⁻³ yr ⁻¹
Width (glacier surface)	W_{sfc}	-	m	Flow parameter related to basal sliding	f_s	3.25 * 10 ⁻¹³	Pa ⁻³ m ² yr ⁻¹
Width (glacier bed)	W_0	-	m	Glacier length	L	-	m

Table 2. Input data used for the Terskol climate reconstruction (1752–2100 AD).

Meteorological parameter	Source	Extent of dataset	Applied correction	
Precipitation	Proxy data (D'Arrigo et al., 2001; Toucham et al., 2003; Akkemik et al., 2005; Akkemik & Aras, 2005; Griggs et al., 2007; Köse et al., 2011; Martin-Benito et al., 2016)	1752– 1997 –present	(1) Average all datasets on a yearly basis (2) Match monthly amount and standard deviation with Terskol data series in the overlapping part of the datasets. (3) Convert to 3-hourly values by using the observed Terskol data sequence as base, but corrected for monthly amounts derived before.	
	CRU TS v4.02 dataset (Harris et al., 2014)	1901–present	(4) Bias correction for additive (temperature) and multiplicative (precipitation) monthly biases and year-to-year variability (a) Use multi-proxy / multi-model mean approach.	
	Pyatigorsk weather station	1934–1997		
	Mestia weather station	1961–2010		
	Terskol weather station	1977– 2018 present (gap 1990–1997)		(b) Bias correction for precipitation (multiplicative) biases and year-to-year variability (standard deviation), see e.g. Huss and Hock (2015) and Zekollari et al. (2019).
	Mineralnye Vody weather station	1938– 2018 present		
	CMP5 simulations (Taylor et al., 2012)	present–2100	(b) Convert to 3-hourly values by using the observed Terskol data sequence as base but corrected for monthly amounts derived before.	
Temperature	Proxy data (Holobaca & Pop, 2015; Dolgova et al., 2017)	1752– 1997 –present	(1) Average all datasets on a yearly basis (2) Match monthly amount and standard deviation with Terskol data series in the overlapping part of the datasets. (3) Convert to 3-hourly values by using the observed Terskol data sequence as base, but corrected for monthly amounts derived before.	
Temperature	CRUTEM4 v4.6.0.0 dataset (Jones et al., 2012)	1850– 2018 present	(4) Bias correction for additive (temperature) and multiplicative (precipitation) monthly biases and year-to-year variability (a) Use multi-proxy / multi-model mean approach.	
Temperature	Mineralnye Vody weather station	1938– 2018 present		
Temperature	Mestia weather station	1961–2010		
Temperature	Terskol weather station	1977– 2018 present (gap 1990–1997)	(b) Bias correction for temperature (additive) biases and year-to-year variability (standard deviation), see e.g. Huss and Hock (2015) and Zekollari et al. (2019).	
Temperature	CMP5 simulations (Taylor et al., 2012)	2019 present–2100	(b) Convert to 3-hourly values by using the observed Terskol data sequence as base but corrected for monthly amounts derived before.	

060

065

070

Table 3. CMIP5 climate models used for the Terskol climate projections (2019–2100 AD).

<u>Model</u>	<u>Spatial resolution</u>	<u>RCP 2.6</u>	<u>RCP 4.5</u>	<u>RCP 6.0</u>	<u>RCP 8.5</u>
<u>BCC-CSM1-1-M</u>	<u>2.81°×2.81°</u>	X	X	X	
<u>INMCM4</u>	<u>1.50°×2.00°</u>		X		X
<u>ACCESS1-3</u>	<u>1.25°×1.88°</u>	X	X		X
<u>CNRM-CM5</u>	<u>1.41°×1.41°</u>	X	X		X
<u>IPSL-CM5A-LR</u>	<u>1.90°×3.75°</u>		X	X	X
<u>IPSL-CM5B-LR</u>	<u>1.90°×3.75°</u>	X	X		X
<u>MPI-ESM-MR</u>	<u>1.88°×1.88°</u>	X	X		X
<u>GFDL-ESM2G</u>	<u>2.00°×2.00°</u>	X	X	X	X
<u>GISS-E2-R</u>	<u>2.00°×2.50°</u>		X	X	X
<u>HadGEM2-CC</u>	<u>1.25°×1.88°</u>		X		X
<u>ACCESS1-0</u>	<u>1.25°×1.88°</u>		X		X
<u>BCC-CSM1-1</u>	<u>2.81°×2.81°</u>	X	X	X	X
<u>BNU-ESM</u>	<u>2.81°×2.81°</u>	X	X		X
<u>IPSL-CM5A-MR</u>	<u>1.25°×2.50°</u>	X	X	X	X
<u>MPI-ESM-LR</u>	<u>1.88°×1.88°</u>	X	X		X
<u>NorESM1-M</u>	<u>1.88°×1.88°</u>	X	X	X	X
<u>CMCC-CMS</u>	<u>3.75°×3.75°</u>		X		X
<u>GFDL-CM3</u>	<u>2.00°×2.50°</u>	X	X		X
<u>GFDL-ESM2M</u>	<u>2.00°×2.50°</u>	X	X	X	X
<u>GISS-E2-R-CC</u>	<u>2.00°×2.50°</u>		X		X
<u>HadGEM2-ES</u>	<u>1.25°×1.88°</u>	X	X	X	